ASSESSING THE IMPACTS OF CLIMATE CHANGE ON COTTON PRODUCTION IN THE TEXAS HIGH PLAINS AND ROLLING PLAINS

A Dissertation

by

NAGA RAGHUVEER MODALA

Submitted to the Office of Graduate and Professional Studies of
Texas A&M University
in partial fulfillment of the requirements for the degree of

DOCTOR OF PHILOSOPHY

Chair of Committee,	Clyde Munster
Co-Chair of Committee,	Srinivasulu Ale
Committee Members,	Nithya Rajan
	Rusty Feagin
Head of Department,	Steve Searcy

December 2014

Major Subject: Biological and Agricultural Engineering

ABSTRACT

The Texas Plains, which include the Texas High Plains and Rolling Plains, is one of the largest cotton growing areas in the world. Cotton cultivation in this region is facing severe challenges from rapidly declining groundwater levels and increasing number of droughts. Projected changes in climate are expected to further add to the uncertainty of cotton production in this region. The overall goal of this research was to study the effects of climate change on cotton yield using the CROPGRO-Cotton Cropping System Model (CSM) within the Decision Support System for Agrotechnology Transfer (DSSAT). The future (2041-2070) climate data generated by three Regional Climate Models (RCMs), namely RCM3-GFDL, RCM3-CGCM3 and CRCM-CCSM was obtained from the North American Regional Climate Change Assessment Program (NARCCAP) and was bias corrected using Distribution mapping techniques..

The CROPGRO-Cotton model was calibrated, validated and further evaluated using the observed data collected from cotton experiments at Chillicothe in the Texas Rolling Plains during the years 2008 and 2012. A GIS-based distributed modeling approach was used to predict cotton yields across major cotton-growing counties in the Texas Plains under historic and future climate scenarios using the calibrated CROPGRO-Cotton CSM. The RCMs predicted an overall decrease in the average rainfall (30 to 127 mm), increase in the intensity of extreme rainfall events (4% to 14% as per RCM3-GFDL), and increase in both minimum (1.9 to 2.9 ºC) and maximum temperatures (2.0 to 3.2 ºC) (as per three RCMs) in the future. Deficit irrigation simulations indicated that the

maximum seed cotton yields under normal and dry weather conditions could be achieved at 100% and 110% ET replacement scenarios, respectively. The cotton yield at Chillicothe was projected to decrease within a range of 2% to 14.9% under the three RCM future climate scenarios. Majority of the counties in the Texas Plains showed a decline in average cotton yield within a range of 2% to 20% under RCM3-GFDL projected future climate scenario, with the counties in the Texas Rolling Plains being the most affected. A combination of early planting and adoption of no-till practices can minimize the climate change-induced yield losses to some extent.

ACKNOWLEDGEMENTS

First a very special thanks to my co-advisor, Dr. Srinivasulu Ale. I offer my sincere gratitude to Dr. Srinivasulu Ale, who has supported me throughout this research and journal writing and thesis writing periods with his patience, enthusiasm in research and immense knowledge. The experience I have gained through this work is invaluable. I would like to thank my co-advisor, Dr. Clyde Munster for introducing me to Dr. Ale and for providing all the support and encouragement throughout this study. I especially thank my graduate committee member, Dr. Nithya Rajan for sharing all the field experimental data that is required for this research and for guiding me through cotton model calibration over Skype. I would like to thank my graduate committee member, Dr. Rusty Feagin for enhancing my interests in the field of Geographic Information Systems through his classes and for referring me to a student GIS Technician position at Map and GIS Library. I would like to thank all my graduate committee members for their encouragement, sound advice and valuable comments.

This research was supported by the Texas A&M AgriLife Research Cropping Systems Initiative and Cotton Incorporated grants.

I would also like to gratefully acknowledge some individuals for their support in completing this research with-out any trouble. Dr. Kelly Thorp, for providing assistance in simulating CSM-CROPGRO-Cotton model and assisting with my questions at any time. Seth McGinnis, Associate Scientist at National Center for Atmospheric Research-

University Cooperation for Atmospheric Research (NCAR-UCAR) for providing assistance related to NARCCAP climate datasets.

A special thanks to Dr. Goldberg, Assistant Professor and the Texas A&M GeoServices for providing the web hosting services and other technical support.

A very special thanks to Miriam Olivares, GIS coordinator for encouraging me to participate in various GIS activities all through my study at Texas A&M University and guiding me through hard-times. I am very grateful to Map and GIS Library staff members: Miriam Olivares, Kathy Weimer, Mark Suter, and Sierra who provided me with lot of opportunities and made my stay more interesting and fun.

I would like to thank my friends Sai Murali Krishna and Pradeep Garigipati for providing valuable contributions in programing.

A special thanks to Sonya Stranges, Administrative Assistant, Texas A&M University for providing all the support and guidance since day one of my doctoral program.

Thanks also go to my friends and colleagues and the department faculty and staff for making my time at Texas A&M University a great experience.

Above all, I thank my parents, who stood beside me and encouraged me constantly, my thanks to my sister and brother in-law for giving me happiness and joy.

Lastly, I offer my regards to all those who supported me in any aspect during the completion of this project.

TABLE OF CONTENTS

Page

LIST OF FIGURES

LIST OF TABLES

CHAPTER I

INTRODUCTION

The Texas Plains region, which includes the Texas High Plains (THP) and the Texas Rolling Plains (TRP) regions, encompasses 67 counties in the north western part of Texas (Figure 1). The THP region is a treeless, windswept, plain surfaced semi-arid region within the Great Plains (Webb, 1931). The High Plains were formed as a result of the alluvial sediment depositions brought by the rivers that originated from the Rocky Mountains (Weeks, 1986; Allen et al., 2008). The Ogallala Aquifer, a major ground water source for the THP region, was formed during the Quaternary or late Tertiary age, which relates to about 10 million years ago (Weeks and Gutentag, 1984; Allen et al., 2008). Water available from this aquifer has led to agricultural revolution in the region and helped in building the economy. As time progressed, water from this aquifer has been used at a faster rate than it is being replenished, resulting in a rapid depletion of the groundwater Table. A similar, but less severe situation exists in the TRP region, which overlies the Seymour Aquifer. The Texas Plains region has witnessed an increasing number of droughts and declining rainfall in the last decade, thus increasing the dependency on the aquifers.

The 2007 agriculture census indicated that about 94% of total irrigated land in Texas was distributed over the THP and TRP (USDA, 2007**;** TWDB, 2007). Irrigation continues to play an important role in agriculture in the THP and TRP with the economic value of crops in the THP amounting to $1.1 billion (TAWC, 2008).

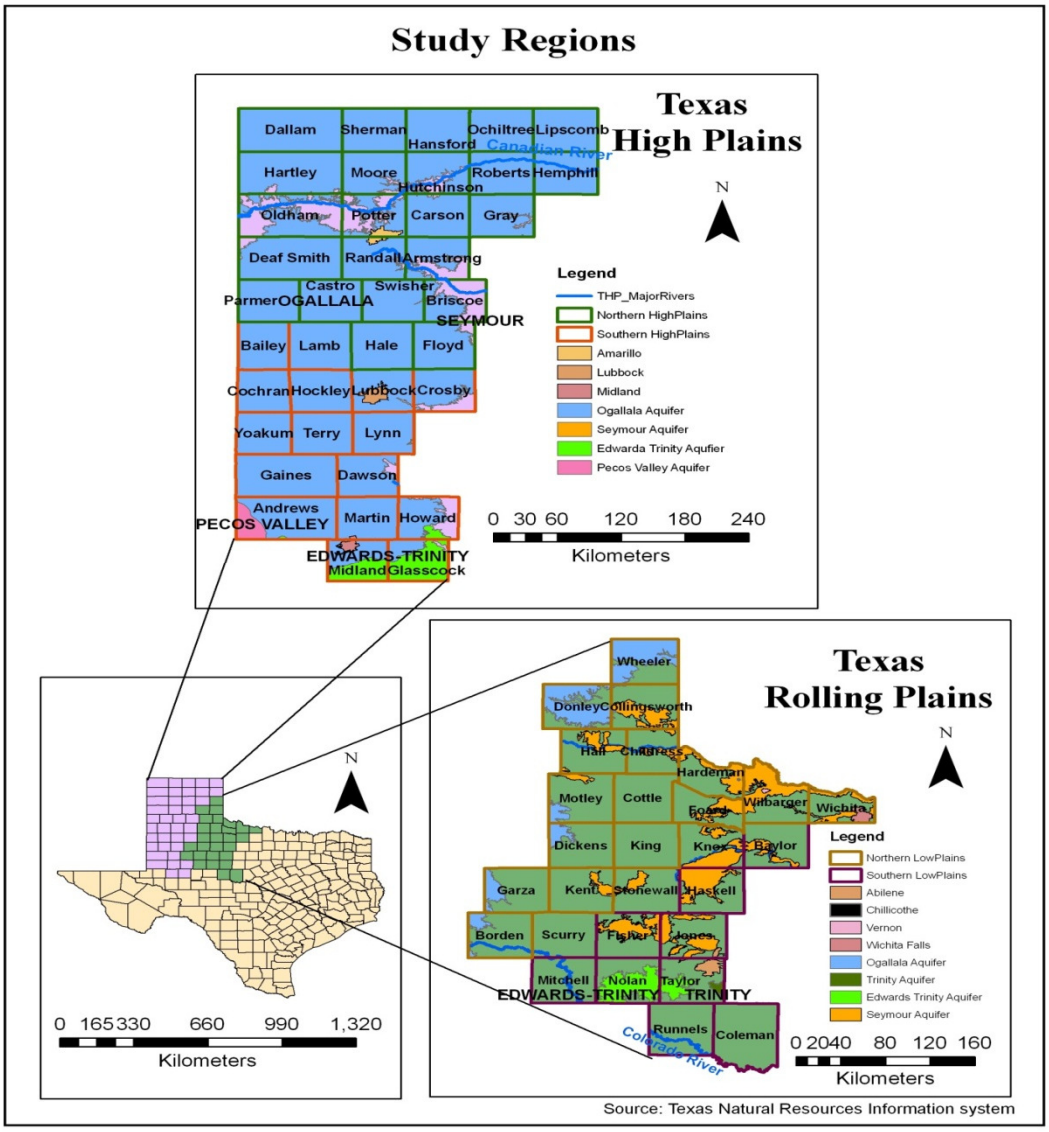

Figure 1. Map showing the study regions: the Texas High Plains and Rolling Plains.

Over 90% and 80% of irrigation in the THP and TRP regions, respectively depends on ground water resources (Figure 2 and 3). The variation in the extent of irrigated cropland area in the THP (Figure 2) and the TRP (Figure 3) over the past 50 years followed the same trend as that of entire Texas. The rural economy of the THP and TRP depends

heavily on ground water supplies from the Ogallala, Dockum, Blaine and Seymour Aquifers that underlay these regions. Irrigated crops in these regions yield 2 to 7 times more than dryland crops (Segarra and Feng, 1994; Colette and Almas, 2005). A recent estimate indicated that a heavily irrigated land in the THP could provide gross returns of $593/ha more than minimally irrigated and $1190/ha more than dryland (Yates et al., 2010). The authors concluded that the rural economy will be drastically affected should the irrigation be completely eliminated.

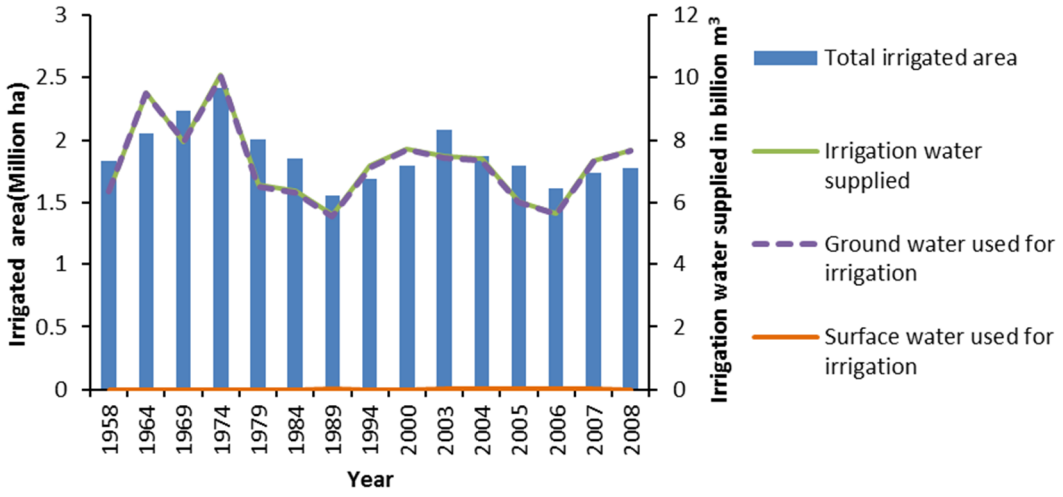

Figure 2. Irrigation water use and cropland statistics for the Texas High Plains (Source: Texas Water Development Board (TWDB). County data provided by Mark Michon, Water Science and Conservation division, TWDB, personnel communication on February 15, 2012).

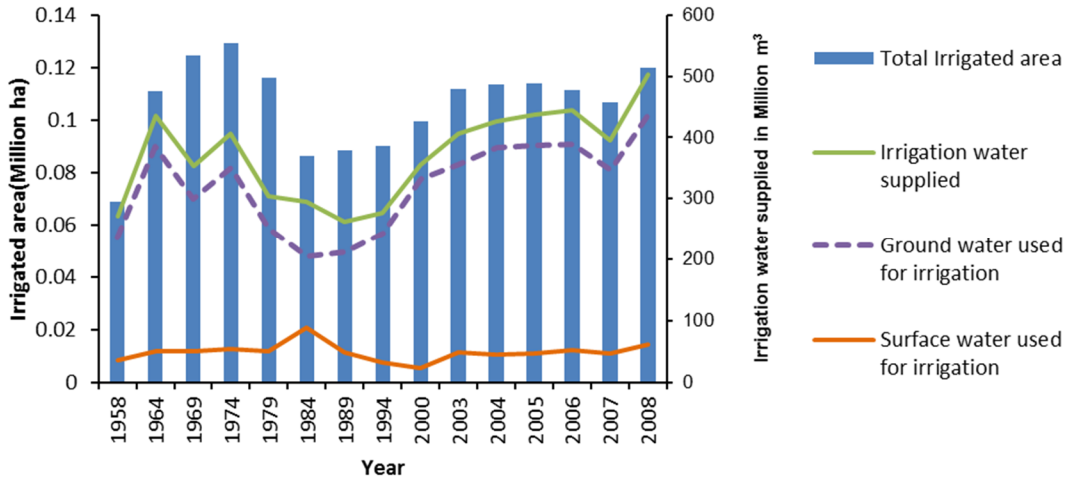

Figure 3. Irrigation water use and cropland statistics for the Texas Rolling Plains (Source: Texas Water Development Board (TWDB). County data provided by Mark Michon, Water Science and Conservation division, TWDB, personnel communication on February 15, 2012).

Major crops that are grown in the Texas Plains are cotton (*Gossypium hirsutum, L*), winter wheat (*Triticum aestivum, L*), corn (*Zea mays, L*) and sorghum (*Sorghum bicolor, L*). Texas is the top cotton producing state in the U.S with a total production of 4.17 million bales of cotton in 2013, about 31.5% of the nation's cotton production (USDA–NASS, 2013; 2014). The cotton production in the northern and western parts of Texas, especially in the panhandle region depends on irrigation from the Ogallala Aquifer (Rajan et al., 2010). Cotton production in the THP and TRP regions has experienced a noticeable decline in recent years due to reduced rainfall amounts and frequent occurrence of severe droughts. Since the Texas Plains region receives inadequate rainfall to meet crop water demands in most years, farmers in this region rely on irrigation for meeting cotton

water requirement. Since this region doesn't have adequate surface water resources, farmers use groundwater for irrigation.

The irrigated agriculture in the THP and TRP regions faces severe challenges due to: i) the decline of groundwater levels in the aquifers in this region, especially in the Ogallala Aquifer (Musick et al., 1988; Colaizzi et al., 2009; Chaudhuri and Ale, 2014a; b), ii) increase in groundwater pumping costs (Nieswiadomy, 1985; Musick et al., 1988; Colaizzi et al., 2009; Adusumilli et al., 2011), iii) impacts of climate change (Nielsen-Gammon, 2011), and iv) increase in the number of dairies in the region, which is promoting farmers to grow more water demanding crops such as corn, which is used as silage. A 45% increase in corn acreage in the THP between 2005 and 2009 was reported by Adusumilli et al. (2011). In addition to the above-mentioned reasons, restrictions imposed on groundwater withdrawals by the Groundwater Conservation Districts (GCDs) (Johnson et al., 2011) have further compounded the problem. The GCDs in the THP region have begun implementing restrictions to pump only 53 cm of ground water during 2012 and 2013, 46 cm during 2014 and 2015, and 38 cm in subsequent years, in order to maintain at least 50% of current saturated thickness of the Ogallala, Edwards-Trinity (High Plains) and Dockum aquifers by 2060 (popularly known as 50/50 water policy) (HPUWCD, 2010). These restrictions pose challenges to local farmers and are forcing them to shift to less-water-demanding crops or completely abandon their farming activities all-together (Rajan et al., 2013). In addition, increasing number of droughts and declining rainfall are further worsening the situation.

In order to sustain agriculture and allied industries, proper planning and management of water resources requires taking climate change into consideration. If these extreme climate events continue to prevail and predictions of climate models prove to be correct, the projected future climate patterns may have significant effects on agriculture and related sectors, food security and water resources, which affect the regional economy. It is therefore essential to assess the potential impacts of climate change at early stages in order to develop adaptation/mitigation strategies and preparedness to promote resilient economies and communities.

The 2012 Texas Water Plan projected a 17% reduction in irrigation demand by the year 2060. One of the reasons cited for the decline in irrigation demand is the possible increased use of efficient irrigation methods. Nielson- Gammon's (2011) future climate projections for Texas showed an increase in temperature, and the number and severity of droughts over the next 50 years. Karl et al. (2009) also projected an increase in the number of warm nights and the number of days with temperatures higher than the normal temperature across the United States. Increase in temperature intensifies soil water evaporation and plant transpiration leading to an increase in soil water deficit (Hatfield et al., 2011). Climate projections across the United States reveal contrasting trends in intensity and frequency of rainfall events over the next decades, with some areas expecting to receive more rainfall while other areas are expected to receive less rainfall (Karl et al., 2009; Hatfield et al., 2011). Climate models predicted an increase in atmospheric CO_2 levels from the current 391 ppm (Mauna Loa CO_2 mean annual value for year 2011) (Tans and Keeling, 2011) to 450 ppm in the next 50 years (Hatfield et al., 2011). The future

climate datasets generated by the North American Regional Climate Change Assessment Program (NARCCAP) (Mearns et al., 2007, 2009) are widely used in various climate change assessment studies (Wang et al., 2009; Takle et al., 2010; Mailhot et al., 2012). In this study, we used the data from three regional climate models (RCMs), namely: Regional Climate Model Version3–Geophysical Fluid Dynamics Laboratory (RCM3-GFDL) (Flato, 2005; Delworth et al., 2006), Regional Climate Model Version3–Third Generation Coupled Global Climate Model (RCM3-CGCM3) (Flato, 2005), and Canadian Regional Climate Model-Community Climate System Model (CRCM-CCSM) (Caya et al., 1995)

Agriculture is very sensitive to climate change, and there are positive as well as negative effects due to climate change (Adams et al., 1990; Hatfield et al., 2011). The projected increase in CO_2 concentration due to climate change could enhance crop growth and yield by increasing photosynthesis (Adams et al., 1990), and increase water use efficiency (WUE) by decreasing stomatal conductance and thereby reducing transpiration per unit leaf area (Kimball, 1982; Cure and Acock, 1986; Allen et al., 1987; Morison, 1993; Sage, 1995). However, this positive effect could potentially be annulled by a projected increase in temperature and variable precipitation (Sage, 1995; Adams et al., 1990; Adams et al., 1998; Hatfield et al., 2011). A critical understanding of the effects of the interactions of the changing climate variables on crop growth and yields in the THP and TRP regions is of utmost importance in order to develop sustainable cropping systems that will better adapt to climate change. Considering these challenges, the science questions that need to be addressed include:

- How the climate will vary in the Texas Plains region in the future?

- How are cotton yields going to be affected due to climate change in this region?
- Which irrigation strategies are beneficial for these regions?
- What changes to crop management practices are needed to adapt to future climate change scenarios?

The Decision Support System for Agrotechnology Transfer (DSSAT) Cropping System model (CSM), CROPGRO-Cotton was used in this study to address the above mentioned science questions. For this study, the DSSAT model has been chosen due to its successful application for different cropping systems under different climatic conditions all over the globe (Paz et al., 2012; Gérardeaux et al., 2013). The DSSAT model, which was developed by the International Benchmark Site for Agrotechnology Transfer (IBSNAT, 1989), is a program that integrates the database management system (soil, climate, and management practices), crop models and various application programs (Tsuji et al., 2002; Jones et al., 2003). It brings together different individually-developed crop models to a single platform. The latest DSSAT 4.5 version is equipped with over 28 crop growth simulation models (Hoogenboom et al., 2010).

Recent advances in geospatial technologies have widened the scope of the DSSAT model to assess regional crop yield predictions. DSSAT requires input data sets on soil, weather, management practices, and crops which can be achieved by integrating DSSAT with the latest geospatial tools. DSSAT provides reliable estimates of crop yields and other crop related outputs for different homogenous soil and weather combinations, while Geographic Information System (GIS) aggregates information from individual units to

make regional predictions. Lal et al. (1993) used this model for developing spatial maps of soybean yield in western Puerto Rico.

The overall goal of this research was to study the impacts of different climate change scenarios on cotton yields in the Texas Plains region and to use geospatial tools and web technologies to develop an interactive online application that would provide easily accessible, bias-corrected, county-based, historic-and future-climate datasets predicted by the GCM's, and cotton yields predicted by the DSSAT CROPGRO-Cotton model. Specific objectives of this study are to:

1) Analyze the spatial and temporal variability of future climate change in the Texas Plains region.
2) Evaluate the CSM-CROPGRO-Cotton model to simulate cotton plant growth and yield, and assess the impacts of current and future climate variability and change on cotton yields.
3) Develop and integrate Geographic Information System (GIS) based methods to aggregate individual field predictions to the regional scale under historic and future climate scenarios.
4) Design and develop the climate database and host it within a relational database management system (Microsoft SQL Server) to provide dynamic access to the data; and to develop an online interface and host the web service for public access.

1.1 Organization of dissertation

This Dissertation consists of five chapters. Chapter 1 is devoted to a general introduction, science questions and the objectives of the research. Chapter 2 addresses the first

objective. It describes the methodology involved in downloading, extracting and, bias correcting climate data for the Texas Plains region as predicted by the three regional climate models. It also provides a detailed analysis of climate predictions. Chapter 3 discusses about the calibration, validation, and evaluation of CSM-CROPGRO- Cotton model based on the observed data from cotton field experiments conducted at Chillicothe Research Station. In addition to identifying appropriate deficit irrigation strategies, this chapter also discusses the effects of various climate model predictions on cotton yields. Chapter 4 is designed to address the objectives 3 and 4. In this chapter, a method to produce regional productivity analysis maps of cotton under RCM3-GFDL predicted future climate scenarios was discussed. This chapter also describes the methodology and technologies involved in developing the interactive web-application. Chapter 5 summarizes the research, draws appropriate conclusions and makes recommendations for future work.

CHAPTER II

SPATIO-TEMPORAL ANALYSIS OF CLIMATE MODEL PREDICTED HISTORIC AND FUTURE CLIMATE DATA FOR THE TEXAS PLAINS REGION

2.1 Introduction

Spatial and temporal uncertainties of climatic conditions have a substantial effect on the spatial distribution of crops and agriculture production. With an increase in the number and severity of droughts in the last decade in the Texas Plains region, the competition for limited irrigation water supplies also increased, thus increasing the dependency on the aquifers. In addition, future climate projections for Texas showed an increase in temperature and the number and severity of droughts over the next 50 years (Nielson-Gammon 2011). This change in climate patterns is posing a serious challenge to local farmers, and is forcing them to shift to less-water-demanding crops or completely abandon their farming activities all-together. In order to sustain agriculture and allied industries, proper planning and management of water resources requires taking climate change into consideration. If these extreme climate events continue to prevail and predictions of climate models prove to be correct, then the projected future climate patterns may have significant effects on agriculture and related sectors, food security and water resources, which affect the regional economy. It is therefore essential to assess the potential impacts of climate change at early stages to plan ahead and be prepared to deal with adverse situations. The scientific question that therefore needs to be addressed is: “How the climate is going to vary in the Texas Plains region in the future”?

Most of the global climate model predictions available in the literature are at coarser resolution (100 km^2 – 250 km^2), and fail to capture the climate variability at the regional scale (Hijmans et al., 2005; Wang et al., 2012). Many downscaling methods were employed to downscale the global climate model predictions to finer resolution (1 km^2 to 50 km^2) (Maurer et al., 2008). During this downscaling process, biases are introduced into the data due to scaling issues and other approximations resulting in in-accurate climate data values (Teutschbein et al., 2012). So, in order to assess the future climate change projections in the Texas Plains region at county level, the bias has to be first removed from the climate data generated by the climate models. In this study, historic and future climate data generated by three Regional Climate Models (RCMs), namely Regional Climate Model Version3–Geophysical Fluid Dynamics Laboratory (RCM3-GFDL) (Flato, 2005; Delworth et al., 2006), Regional Climate Model Version3–Third Generation Coupled Global Climate Model (RCM3-CGCM3) (Flato, 2005), Canadian Regional Climate Model-Community Climate System Model (CRCM-CCSM) (Caya et al., 1995, Collins et al., 2006) was downloaded from the North American Regional Climate Change Assessment Program (NARCCAP) (Mearns et al., 2007; 2009).

The specific objectives of this study were to: 1) download, extract, and pre-process the climate data predicted by three regional climate models (RCMs); 2) bias correct the climate datasets using distribution mapping techniques; and 3) assess the future climate change as predicted by the three RCMs.

2.2 Methodology

A detailed description of the steps followed in climate data downloading, processing and

bias correction is given in the sections below:

2.2.1 Study area

The Texas Plains comprises of both THP and TRP regions. The semi-arid THP region includes 39 counties and it is a major producer of irrigated and dryland crops in Texas (Colaizzi et al. 2009). The major crops grown in the THP region include cotton (*Gossypium hirsutum, L*), winter wheat (*Triticum aestivum, L*), corn (*Zea mays, L*) and sorghum (*Sorghum bicolor, L*). About 90% of irrigation water used in the THP region is pumped from the Ogallala Aquifer (Stewart, 2003; Jensen, 2004; Colaizzi et al., 2009; Adusumilli et al., 2011). In addition to the Ogallala Aquifer, the Edwards-Trinity, the Pecos Valley and the Seymour Aquifers also supply groundwater for irrigation to some areas in this region. The minor aquifers in THP include the Dockum, Lipan and Rita Blanca. The major rivers in the THP region are the Canadian River and the Red River. Major cities in the THP are Amarillo, Lubbock, and Midland. Annual rainfall in this region ranges from 36 cm in the west to 61 cm in the east.

The TRP region, encompassing 28 counties, lies to the east of the THP and borders Oklahoma in the north and the Edwards Plateau in the south. About 85% of the ground water used for irrigation in the TRP region is pumped from the Seymour Aquifer. The Edwards-Trinity, and the Trinity Aquifers are other minor ground water sources in the TRP region. The Colorado River, Brazos River, and Red River are major rivers flowing in the TRP region. Major crops grown in the TRP are winter wheat and cotton. Major urban developments in the TRP include Wichita Falls and Abilene. Annual rainfall in the TRP decreases from 76 cm in the east to 46 cm in the west.

Both THP and TRP regions have the highest number of sunny days in the U.S. The winters in these regions are colder. March, April and May are the windiest months of the year, and peak rainfall occurs during the months of May and September. The months from October to February are generally dry (Allen et al., 2008).

2.2.2 Climate datasets and data processing

The simulated historic (1971-2000) and future (2041-2070) climate datasets were downloaded from the NARCCAP website (Mearns et al., 2007; 2009). The NARCCAP climate datasets were generated by RCMs, which were driven by a set of ocean-atmospheric Global Climate Models (GCMs) that are forced with the A2 Special Report on Emission Scenarios (SRES) (Nakicenvoic et al., 2000). The A2 scenario (IPCC SRES, 2000) was developed based on the assumptions of high population growth, high energy requirements, slow use of efficient technologies and regionally-oriented economic growth. The scenario is oriented towards more fragmented society preserving local identities. The climate data used in this study include daily rainfall, maximum temperature, minimum temperature data and solar radiation simulated by three RCMs namely, Regional Climate Model Version3–Geophysical Fluid Dynamics Laboratory (RCM3-GFDL) (Flato, 2005; Delworth et al., 2006), Regional Climate Model Version3–Third Generation Coupled Global Climate Model (RCM3-CGCM3) (Flato, 2005), Canadian Regional Climate Model-Community Climate System Model (CRCM-CCSM) (Caya et al., 1995; Collins et al., 2006). A detailed description about these climate models can be found at https://www.narccap.ucar.edu/data/model-info.html and the characteristics of these RCMs can be found at https://www.narccap.ucar.edu/data/rcm-characteristics.html .

These climate datasets have a daily temporal resolution and a 50 km^2 spatial resolution. The NARCCAP data was chosen for this study, primarily because of its daily temporal resolution and high spatial resolution compared to other available future climate data sources. Additionally, the NARCCAP data was successfully used in many past studies (e.g. Pryor and Barthelmie, 2011; Chang et al., 2010). An automated program was developed in R (the statistical software package) to extract the climate variables from the downloaded netcdf files into CSV format for all grid points in the study area.

2.2.3 Why bias correction?

In general, RCMs are used to downscale the GCM predictions to a smaller scale (25–50 km^2). In the process of downscaling, systematic biases are incorporated into the data due to scaling issues (spatial averaging at grid level) and errors due to immature/incomplete concepts (Teutschbein and Seibert, 2012). Teutschbein and Seibert (2012) and Ines and Hansen (2006) found that the RCMs have a tendency to predict a high frequency of days with low rainfall in place of dry days. Typical biases in the RCM climate data also include incorrect estimation of extreme temperatures (Ines and Hansen, 2006), and incorrect seasonal variations in rainfall (Teutschbein and Seibert, 2010). There are many bias correction methods available in the literature, ranging from simple to complex statistical methods. For this study, a distribution mapping technique was used to remove the bias from the RCM-predicted climate datasets. This method has been successfully used in previous studies (Hayhoe et al., 2004; Cayan et al., 2008; Li et al., 2010; Teutschbein and Seibert, 2012). Biases in rainfall and temperature were removed using the Gamma and Gaussian distribution mapping techniques, respectively. The removal of these biases is

important for a realistic representation of future rainfall and temperature which can be used in various climate change assessment studies (Wood et al., 2004; Piani et al., 2010).

2.2.4 Bias correction by distribution mapping technique

Distribution mapping technique, which is also referred to as quantile matching (Li et al., 2010) employs a transfer function to correct the RCM-simulated climate data by shifting the distribution of RCM-simulated data to agree with the distribution of observed data. In this approach, it was assumed that the bias is stationary under climate change. The RCM simulated historic climate data of 71 and 94 grid points within the Texas Plains for the RCM3 and CRCM models, respectively, were bias-corrected to match with the observed climate data (Figure 4a, Figure 4b). Each county in the study area has a minimum of one grid point. If a county contains only one grid point, climate data for that grid point was bias -corrected and assigned to that county. If a county has multiple grid points, an average of climate parameter for those grid points was estimated and used in bias correction process. The historic observed climate data for all 67 counties in the Texas Plains were obtained from the Integrated Agricultural Information and Management System (iAIMS) Climatic Data Center, which is maintained by the Texas A&M AgriLife Research Centre at Beaumont (Yang et al., 2010). The iAIMS data center was built based on five weather data sources: the National Climatic Data Center (NCDC), COOP stations, Meteorological Aviation Report (METAR), Crop Weather Program Weather Station Network at Corpus Christi, Texas, and Beaumont Lake research weather stations. The weather station with maximum historic records for each county was selected and any missing data in that weather station was filled with the observed data from other weather stations with in the

county or from the nearby counties. After applying a bias correction transformation to the RCM-predicted historic climate data, the same transformation was applied to remove the bias from the future data.

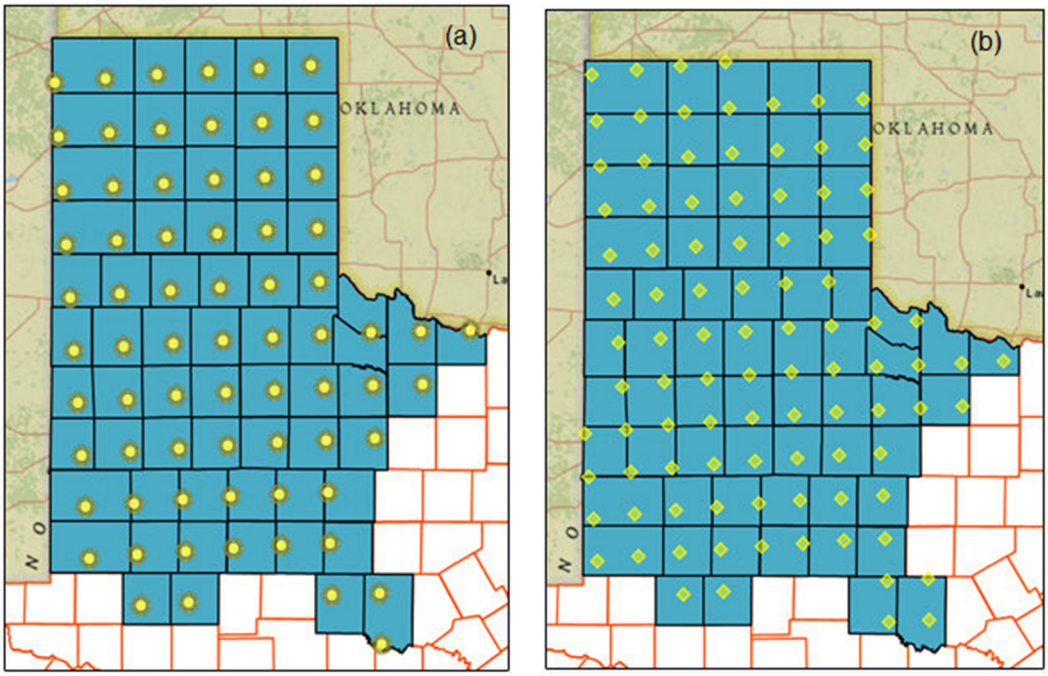

Figure 4. a) Regional Climate Model Version3 (RCM3) grid point locations. b) Canadian Regional Climate Model (CRCM) grid point locations.

2.2.4.1 Bias correction of rainfall

It was observed that the RCM-simulated daily rainfall followed the Gamma distribution pattern, and hence the Gamma distribution mapping technique was employed to remove the bias from the rainfall data. This method was also used effectively to remove bias in past studies (Piani et al. 2010; Teutschbein and Seibert, 2012; Lafon et al., 2013).

The Gamma distribution (Thom, 1958) is expressed as:

$$f_\gamma(x) = \frac{1}{\beta^\gamma \Gamma(\gamma)} x^{\gamma-1} e^{-x/\beta} \quad (1)$$

where: $x = random\ variable$ (Rainfall in this case), $x > 0$

β: $scale\ parameter, \beta > 0$

γ: $shape\ parameter, \gamma > 0$

Γ: $gamma\ function.$

Parameters β and γ were estimated for each grid point and each month, and the methodology used for estimation of these parameters is explained in the following paragraphs.

After closely evaluating the rainfall values simulated by the three RCMs, it was observed that all three models simulated many unrealistic low intensity rainfall events, resulting in an over-prediction of overall frequency of rainfall events (Figure 5). Teutschbein and Seibert (2012) also observed that the RCMs simulated a large number of low rainfall events instead of dry conditions. The error in the estimation of the frequency of daily RCM simulated rainfall events was therefore corrected first, before correcting the bias in rainfall data.

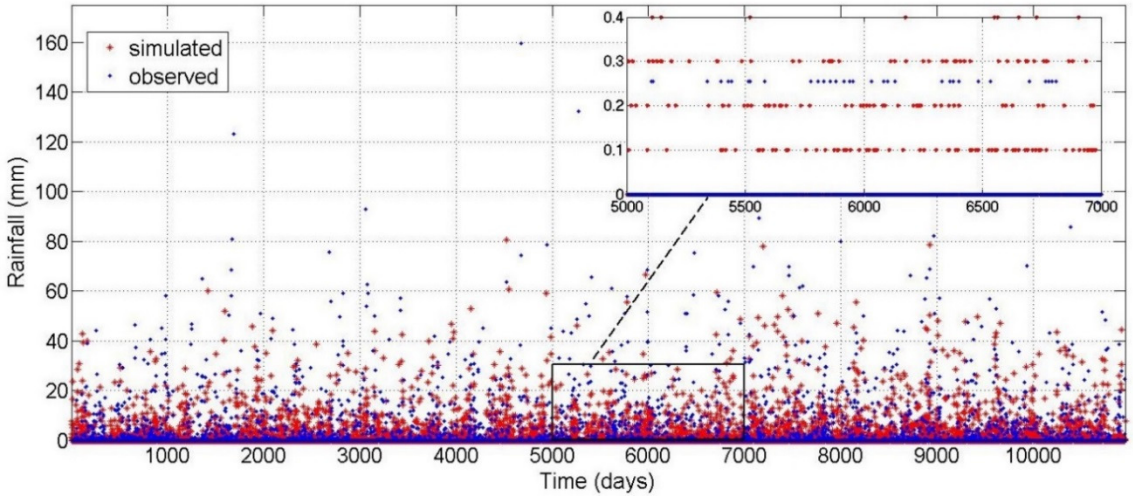

Figure 5. Overestimation of historic (01/01/1971-12/31/2000) rainfall events as simulated by the RCM3-GFDL (Regional Climate Model Version3–Geophysical Fluid Dynamics Laboratory) model in comparison to observed rainfall events for Hardeman County, TX.

In order to address this issue of overestimation in frequency of rainfall events, monthly threshold rainfall amounts for the historic period were estimated and all rainfall events below the threshold values were made zero (Figure 6). After correcting the frequency of rainfall events, the RCM simulated rainfall data for the historic period was bias-corrected with reference to the observed rainfall data for the same period. Cumulative distribution frequency (CDF) curves were developed for both simulated and observed rainfall events for each month. First, the cumulative probability of occurrence of a rainy day within a month was obtained from the generated CDF curve of the RCM simulations. Then, the associated rainfall value for the same cumulative probability on the CDF of the

observed values was identified. This observed rainfall value was used as a final bias-corrected value for the RCM simulations (Figure 7a).

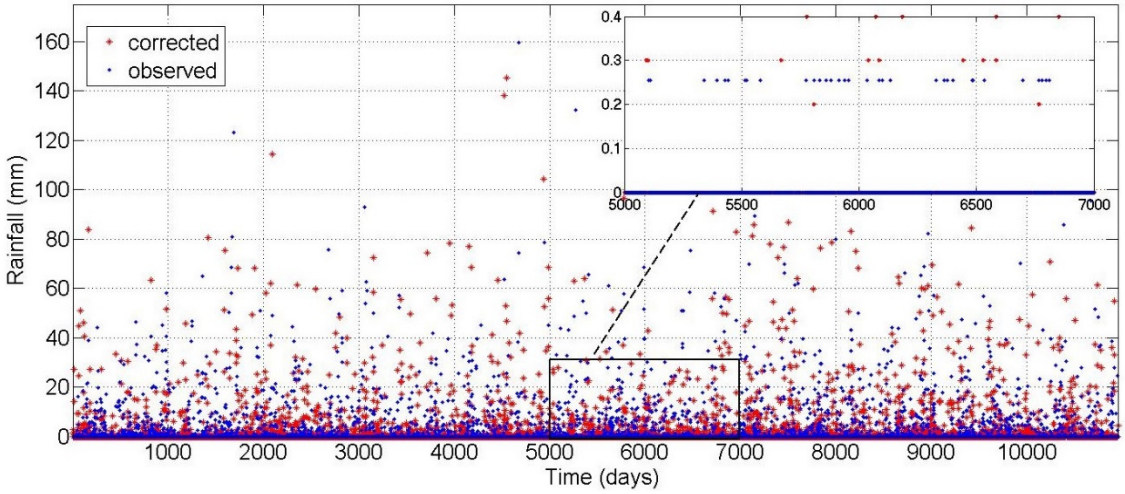

Figure 6. The bias-corrected rainfall events for Hardeman County, TX, over historic period (01/01/1971-12/31/2000) as simulated by the Regional Climate Model Version3–Geophysical Fluid Dynamics Laboratory (RCM3-GFDL) model.

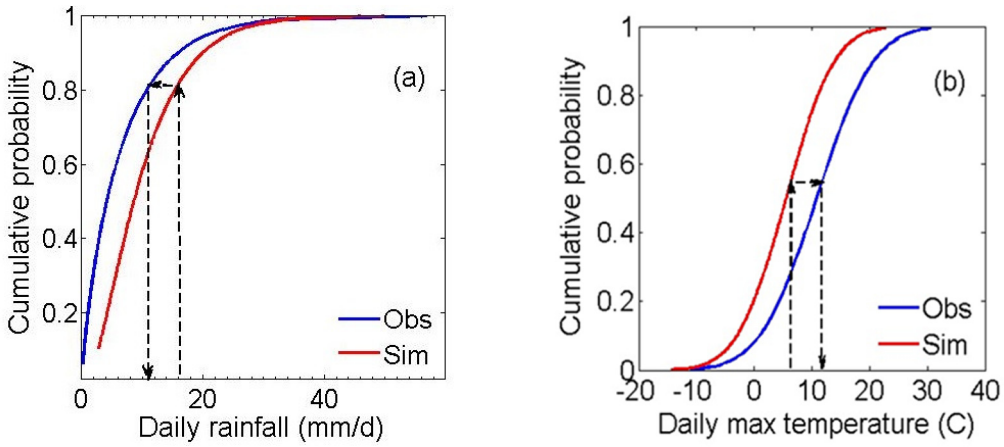

Figure 7. a) Bias correction of rainfall data using the Gamma distribution mapping technique. The Regional Climate Model (RCM) simulated daily rainfall cdf curve (red line) was shifted to align with the observed rainfall cumulative distribution frequency (cdf) curve (blue line). b) Bias correction of maximum temperature data using the Gaussian distribution mapping technique. The RCM simulated daily temperature cdf curve (red line) was shifted to match with the observed temperature cdf curve (blue line).

The process of bias correction of rainfall data can be expressed mathematically in the following five steps (equations 2 to 6):

$$(\gamma_s, \beta_s) = gamafit(x_s) \qquad (2)$$

where: γ_s is a shape parameter for RCM simulated historic rainfall data, β_s is a scale parameter for RCM simulated historic rainfall data, and x_s is RCM simulated historic rainfall.

$$H_{SR} = F_\gamma(x_s, \gamma_s, \beta_s) \qquad (3)$$

where: F_γ is Gamma CDF.

$$(\gamma_o, \beta_o) = gamafit(x_o) \quad (4)$$

where: γ_o is a shape parameter for historic observed rainfall data, β_o is a scale parameter for observed historic rainfall data, and x_o is observed historic rainfall.

$$H_{OR} = F_\gamma(x_o, \gamma_o, \beta_o) \quad (5)$$

$$H_{CR} = F_\gamma^{-1}(H_{SR}, \gamma_o, \beta_o) \quad (6)$$

where: F_γ^{-1} is inverse of Gamma CDF, H_{CR} is historic bias-corrected rainfall.

The following steps (equation 7-9) were then used to bias-correct the RCM simulated future rainfall data.

$$(\gamma_f, \beta_f) = gamafit(x_f) \quad (7)$$

where: γ_f is a shape parameter for RCM simulated future rainfall data, β_f is a scale parameter for RCM simulated future rainfall data, and x_f is RCM simulated future rainfall.

$$F_{SR} = F_\gamma(x_f, \gamma_f, \beta_f) \quad (8)$$

$$F_{CR} = F_\gamma^{-1}(F_{SR}, \gamma_{f.\frac{\gamma_s}{\gamma_o}}, \beta_{f.\frac{\beta_s}{\beta_o}}) \quad (9)$$

where: F_{CR} is future bias corrected rainfall.

2.2.4.2 Bias correction of temperature

The climate model predicted daily minimum and maximum temperatures were bias-corrected using the Gaussian distribution mapping technique as the temperature data followed a Gaussian (normal) distribution. Previous studies (Thom, 1952; Teutschbein et al., 2012) have also reported that Gaussian distribution was the best fit for temperature.

The Gaussian distribution (Cramer, 1999) is expressed mathematically as:

$$f_N(y) = \frac{1}{\sigma.\sqrt{2x}}\, e^{\frac{-(y-\mu)^2}{2\sigma^2}} \qquad (10)$$

where: $y = random\ variable\ (temperature\ in\ this\ case)$

$\mu = mean\ or\ location\ parameter$

$\sigma = standarad\ deviation\ or\ scale\ parameter.$

μ and σ were estimated for each grid point for each month over the thirty year historic and future period. This method follows an approach similar to the Gamma distribution mapping technique (Figure 7b) and each step in the process is expressed mathematically as follows

$$(\mu_s, \sigma_s) = normfit(y_s) \qquad (11)$$

where: μ_s is a location parameter for RCM-simulated historic temperature data, σ_s is a scale parameter for RCM-simulated historic temperature data, and y_s is RCM-simulated historic temperature.

$$H_{ST} = F_N(y_s, \mu_s, \sigma_s) \qquad (12)$$

where: F_N is Gaussian CDF.

$$(\mu_o, \sigma_o) = normfit(y_o) \quad (13)$$

where: μ_o is a location parameter for observed historic temperature, σ_o is a scale parameter for observed historic temperature, and y_s is observed historic temperature data.

$$H_{OT} = F_N(y_o, \mu_o, \sigma_o) \quad (14)$$

$$H_{CT} = F_N^{-1}(H_{ST}, \mu_o, \sigma_o) \quad (15)$$

where: F_N^{-1} is inverse of Gaussian CDF, H_{CT} is historic, bias-corrected temperature.

The above five steps (equation 11-15) were used to bias correct the model simulated historic temperature data in reference to the observed data.

The following steps (equation 16-18) were used to bias correct the RCM simulated future temperature data

$$(\mu_f, \sigma_f) = normfit(y_f) \quad (16)$$

where: μ_f is a location parameter for RCM simulated future temperature data, σ_f is a scale parameter for RCM simulated future temperature data, and y_f is RCM simulated future temperature.

$$F_{ST} = F_N(y_f, \mu_f, \sigma_f) \quad (17)$$

$$F_{CT} = F_N^{-1}(F_{ST}, \mu_f + (\mu_s - \mu_o), \sigma_f \cdot \frac{\sigma_s}{\sigma_o}) \quad (18)$$

where: F_{CT} is future bias corrected temperature.

The above described approach (equations 11-18) was employed to bias correct the minimum and maximum temperature data also.

Bias correction of rainfall and temperatures has been developed and automated for all the grid points using MATLAB program. The MATLAB program is made available to the users through this Dissertation (Appendix I).

2.3 Bias-correction of simulated rainfall and temperature data

The bias correction of simulated rainfall data yielded satisfactory results when compared to historic observed data (Figure 8). This method not only corrected the frequency of rainfall events, but also corrected all moments, i.e., mean, variance, and skew (temporal distribution) (Li et al., 2010). Bias corrected, model predicted daily temperatures also closely matched with observed mean temperatures over the period of 1971-2000 (Figure. 9).

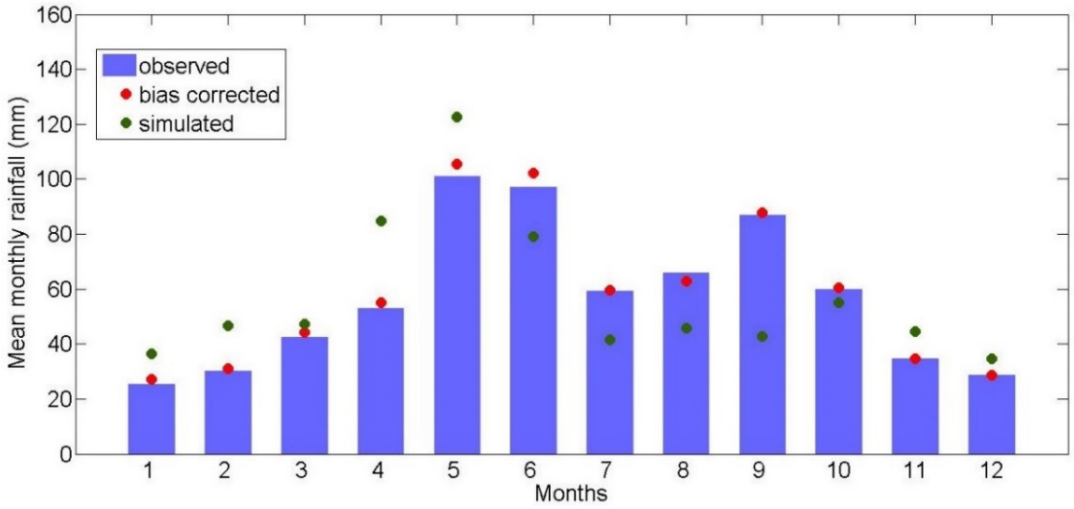

Figure 8. Comparison of bias-corrected RCM3-GFDL (Regional Climate Model Version3–Geophysical Fluid Dynamics Laboratory) model predicted monthly rainfall data with uncorrected and observed monthly mean rainfall for the period 1971-2000 for Hardeman County, TX.

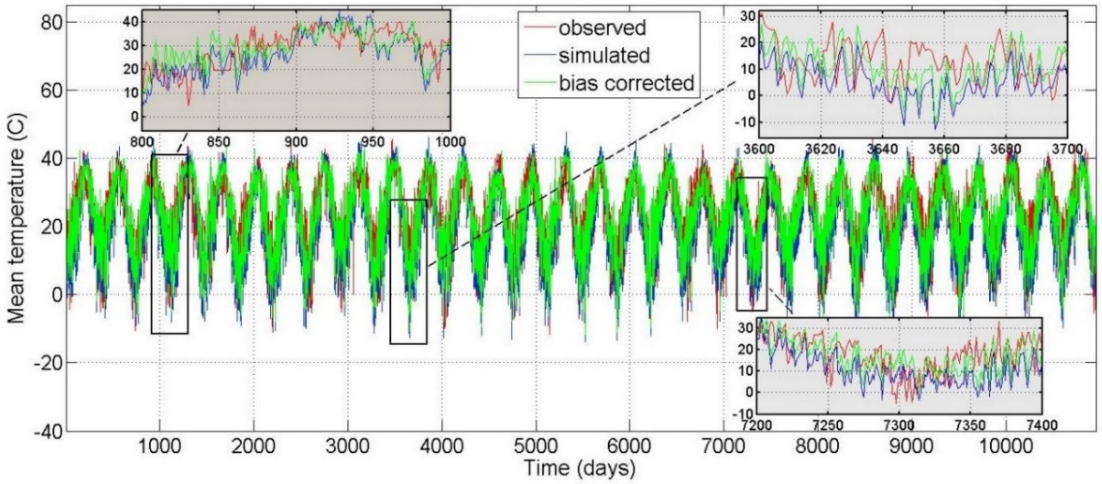

Figure 9. Comparison of RCM3-GFDL (Regional Climate Model Version3–Geophysical Fluid Dynamics Laboratory) model bias corrected daily mean temperature with uncorrected and observed daily mean temperature for the period 01/01/1971-12/31/2000 for Hardeman County, TX.

2.4 Climate change analysis

2.4.1 Future changes in rainfall

After bias correcting, the RCM predicted historic and future climate datasets were used to assess the climate change across the Texas Plains by developing spatial maps. Figure 10 depicts the change in precipitation as predicted by the three RCM's, namely RCM3-GFDL, RCM3-CGCM3 and CRCM-CCSM. All of these three models predicted similar trends in spatial distribution patterns of future rainfall across the region when compared to historic observations (Figure 10). All models predicted a decrease in average annual rainfall in the future (2041-2070) when compared to the historic period (1971-2000) in majority of counties in the Texas Plains (Figure 10). The RCM3–GFDL model predictions of change in average annual rainfall varied from a decrease in average annual rainfall of

61 mm in Taylor and Jones counties (Figure 11) to an increase in average annual rainfall of 32 mm in Lipscomb County (Figure 10a-c). Overall, only 6 out of 67 counties showed an increase in rainfall (Figure 10c) during the future period. According to the RCM3-GFDL model, the counties that are most affected due to climate change are located in the Texas Rolling Plains (TRP) region (Figure 10).

The RCM3-CGCM3 model predictions showed a decline in average annual rainfall in the counties located in the northern High Plains with in a range from 30 mm (Hemphill County) to 127 mm (Hartley County), and a slight increase in average annual rainfall (25.4 mm) in nine counties located in the southern High Plains (Figure 10d-f). The CRCM-CCSM model predicted a decrease in average annual rainfall in all of the counties except for Hartley County (Figure 10g-i). In Hartley County, the model predicted a 25.4 mm increase in rainfall. The county that is mostly affected will be Terry as predicted by CRCM-CCSM (Figure 10g-i). Based on the average of the three climate models, the most affected county is the Oldham County located in the Northern High Plains and the least affected is the Andrew County which is located in the Southern High Plains.

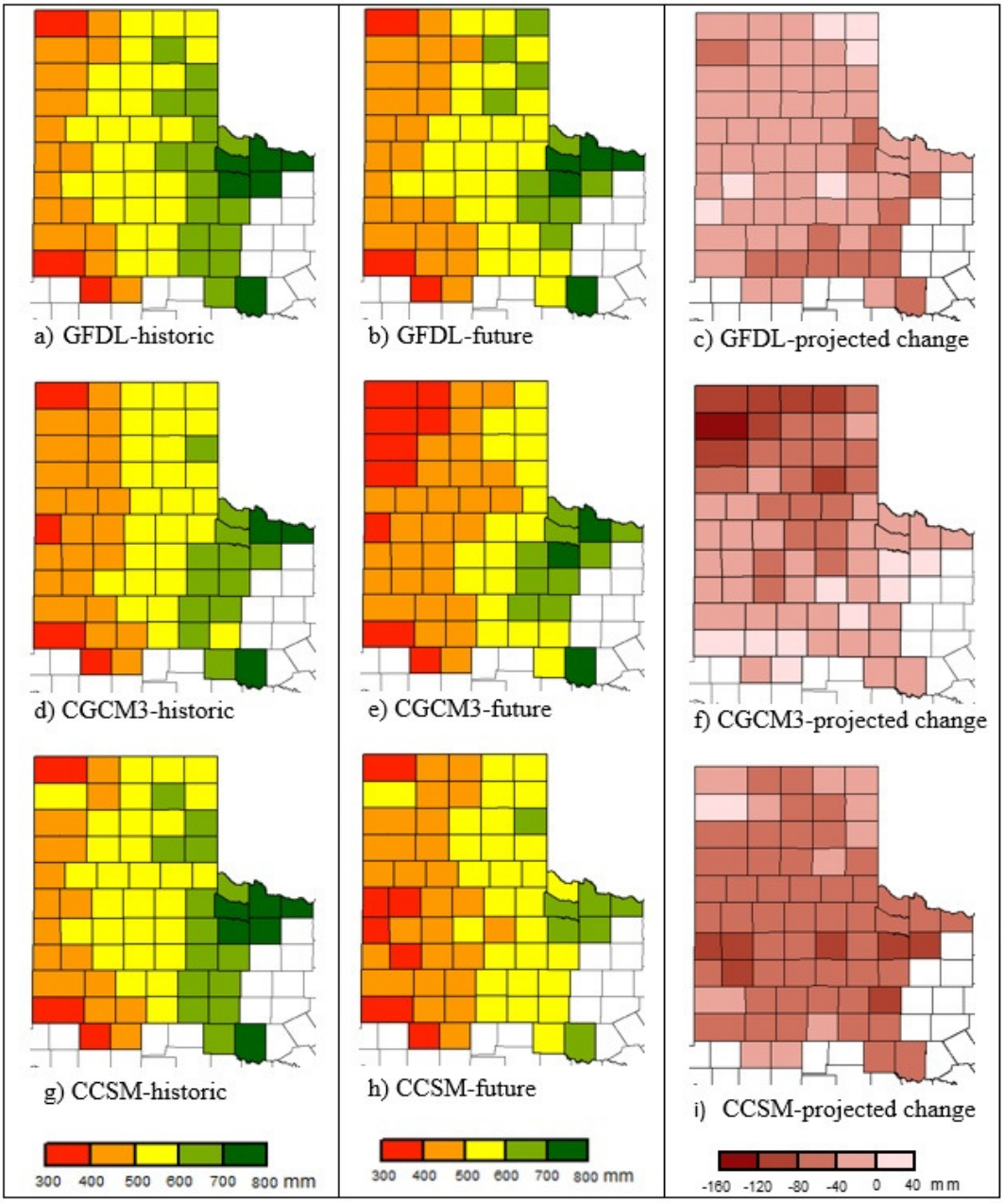

Figure 10. Spatio-temporal variability of average annual historic (1971-2000) and future (2041-2070) rainfall in the Texas Plains region as predicted by three Regional Climate Models: RCM3-GFDL (Regional Climate Model Version3–Geophysical Fluid Dynamics Laboratory), RCM3-CGCM3 (Regional Climate Model Version3–Third Generation Coupled Global Climate Model) and CRCM-CCSM (Canadian Regional Climate Model-Community Climate System Model).

2.4.1.1 Future changes in rainfall frequency and intensity

In order to assess spatial variability in rainfall patterns across the Texas Plains region, 9 and 11 counties were selected in the east-west and north-south directions, respectively (Figure 11). These counties were selected in such a way that they represent latitudinal and longitudinal variation in climate change across the entire region. This detailed analysis of future rainfall data was carried out for RCM3-GFDL model predictions only. Box plot analysis (Figure 12a-d, Table 1) of the predicted historic and future daily rainfall data for the selected counties (Figure 11) indicated an overall decrease in the number of rainfall events by 6% to 10%, and an overall increase in the intensity of rainfall by about 3% to 8% during the 2041-2070 period (Table 2). The third quartile of the daily rainfall events showed an increase when compared to the historic events indicating an increase in the amount of rainfall and in-turn the intensity of moderate to extreme events (Table 1) and this feature can be observed from north to south (Table 1). The percent reduction in the total number of rainfall events varied from 7% in the west to 6% in the east and 6% in the north to 10% in the south.

For the analysis purposes, all outliers in the box plots were (Figure 12a-d) considered as extreme events. There will be an estimated 4% to 7% decrease in the total number of extreme events during 2041-2070 when compared to historic period (1970-2000) according to the RCM3-GFDL model (Figure 13a-d, Table 3). However, further analysis indicated that the intensity of these extreme events will increase by 4% to 17% in the future when compared to the historic trends (Table 3). These observations were in-line with the observations made in the previous studies (Wilby and Wigley, 2002). Figure 13a-

b shows that the total number of rainfall events will increase from the west to east and from figure 13c-d, it can be inferred that the total number of rainfall events will increase from north to the center and then decreases towards the south.

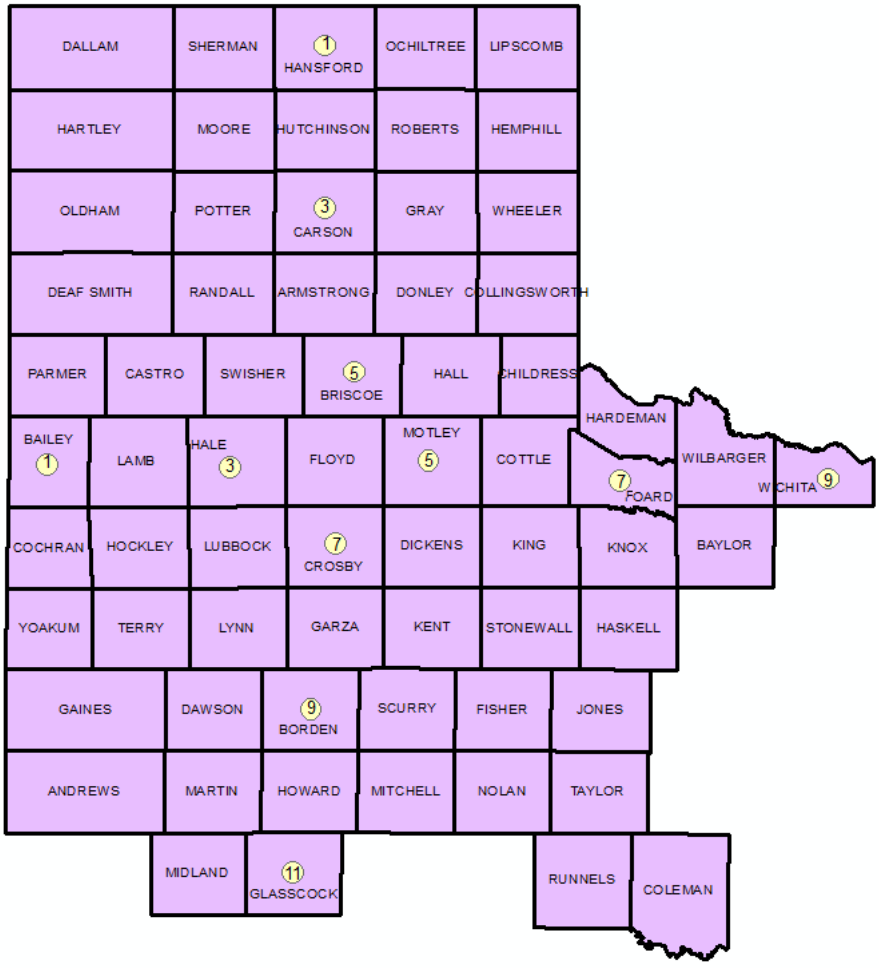

Figure 11. Texas Plains counties selected for the RCM3-GFDL (Regional Climate Model Version3–Geophysical Fluid Dynamics Laboratory) predicted rainfall frequency and intensity analysis study.

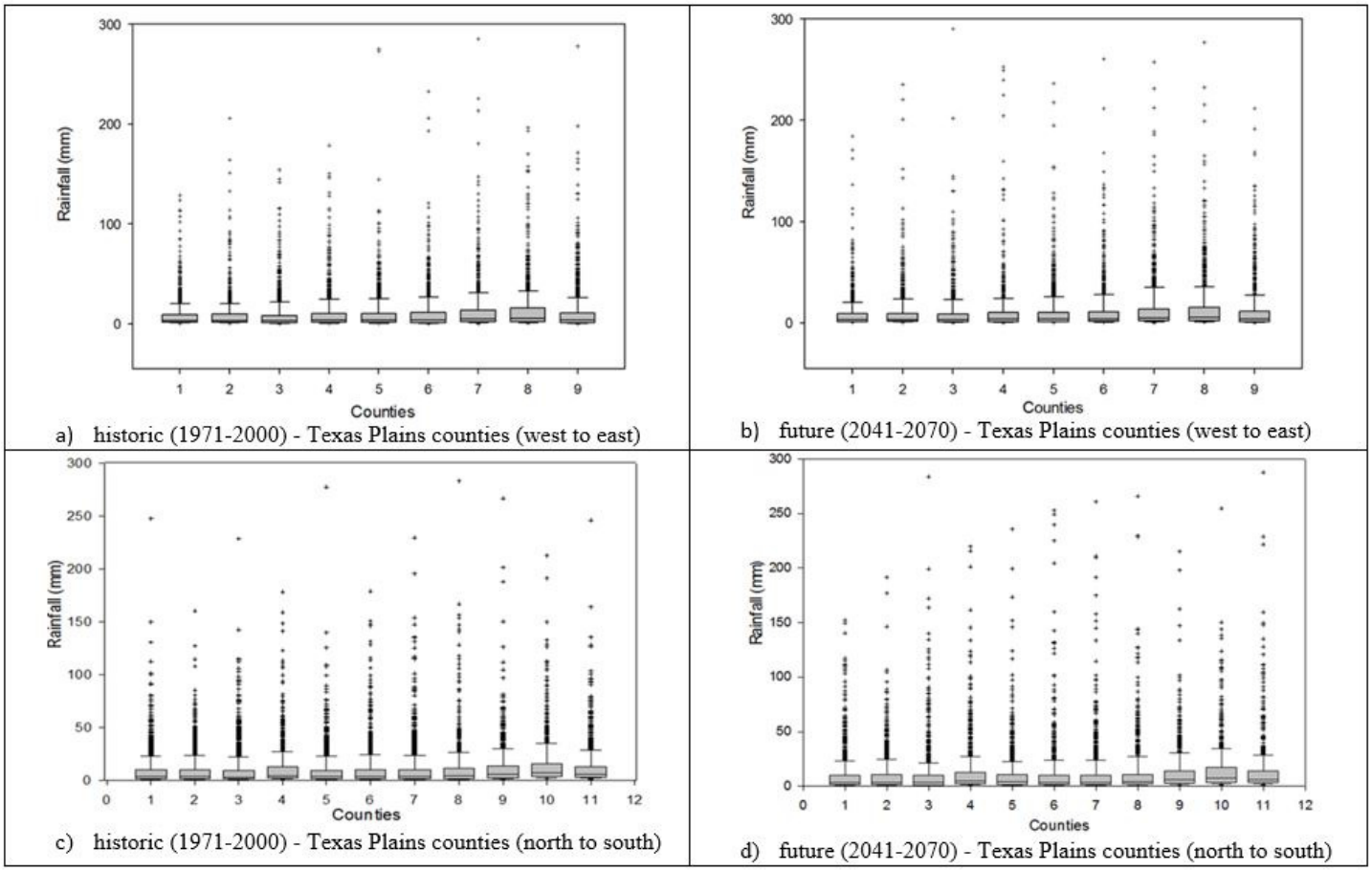

Figure 12. Box plots of RCM3-GFDL (Regional Climate Model Version3–Geophysical Fluid Dynamics Laboratory) predicted historic (1971-2000) and future (2041-2070) daily rainfall distribution for selected counties (Figure 11) in the study region.

Table 1. Distribution of the daily rainfall data from the box-plot analysis (figure 12a-d) of selected counties from figure 11.

Counties (west to east)	First Quartile (mm)			Median (mm)			Third Quartile (mm)		
	Historic	Future	Change	Historic	Future	Change	Historic	Future	Change
1	1.5	1.2	0.3	3.4	3.2	0.2	9.1	9.0	0.1
3	1.2	1.1	0.1	3.1	3.0	0.1	8.2	8.6	-0.4
5	1.4	1.2	0.2	3.7	3.5	0.2	10.5	10.4	0.1
7	1.9	2.0	-0.1	4.8	4.9	-0.1	13.6	13.5	0.1
9	1.2	1.2	0	4.0	3.6	0.4	11.0	11.6	-0.6
Counties (north to south)	First Quartile			Median			Third Quartile		
	Historic	Future	Change	Historic	Future	change	Historic	Future	Change
1	1.6	1.4	0.2	3.5	3.6	-0.1	9.7	10.3	-0.6
3	1.2	1.0	0.2	3.1	3.1	0	9.0	9.7	-0.7
5	1.6	1.6	0	3.8	4.0	-0.2	9.6	10.5	-0.9
7	1.2	1.1	0.1	3.4	3.3	0.1	9.8	9.9	-0.1
9	2.5	2.6	-0.1	5.6	5.7	-0.1	13.3	13.7	-0.4
11	3.1	3.0	0.1	6.0	6.0	0	13.2	14.2	-1.0

Table 2. Analysis of RCM3-GFDL (Regional Climate Model Version3–Geophysical Fluid Dynamics Laboratory) simulated historic (1971-2000) and future (2041-2070) rainfall data for the selected counties across the Texas Plains region.

Counties (west to east)	Total no of rainfall events		Total rainfall (mm)		Over all rainfall intensity (Total rainfall/no of wet days) (Solomon et al., 2007)	
	Historic	Future	Historic	Future	Historic	Future
1	1622	1497	13083	12421	8.1	8.3
3	1917	1722	15636	15111	8.1	8.8
5	1873	1718	18108	17280	9.7	10.0
7	1734	1633	21664	21658	12.5	13.3
9	2183	2050	22609	22528	10.3	11.0
Counties (north to south)	Total no of rainfall events		Total rainfall (mm)		Over all rainfall intensity (Total rainfall/no of wet days)	
	Historic	Future	Historic	Future	Historic	Future
1	1769	1654	15644	15398	8.8	9.3
3	2130	1907	17549	17085	8.2	8.9
5	1970	1757	17273	16391	8.8	9.3
7	1954	1774	18017	17109	9.2	9.6
9	1300	1166	15420	14772	11.9	12.7
11	1090	979	13511	12978	12.4	13.2

Table 3. Analysis of the RCM3-GFDL (Regional Climate Model Version3–Geophysical Fluid Dynamics Laboratory) simulated historic (1971-2000) and future (2041-2070) extreme rainfall events for the selected counties across the Texas Plains region.

Counties (west to east)	No of extreme events		Total rainfall from extreme events (mm)		Rainfall intensity during extreme events (Total rainfall/no of wet days)(Solomon et al., 2007)	
	Historic	Future	Historic	Future	Historic	Future
1	323	289	8626	8416	26.7	29.1
3	394	348	11052	10947	28.0	31.4
5	378	334	12542	12187	33.2	36.5
7	346	327	14458	15113	41.8	46.2
9	427	391	15726	15789	36.8	40.4
Counties (north to south)	No of extreme events		Total rainfall from extreme events (mm)		Rainfall intensity during extreme events (Total rainfall/no of wet days)	
	Historic	Future	Historic	Future	Historic	Future
1	355	339	10473	10536	29.9	31.1
3	420	357	12115	11879	28.8	33.3
5	411	342	9633	9332	23.4	27.3
7	377	349	12372	12181	32.8	34.9
9	270	247	9942	9851	36.8	39.9
11	232	202	8725	8423	37.6	41.7

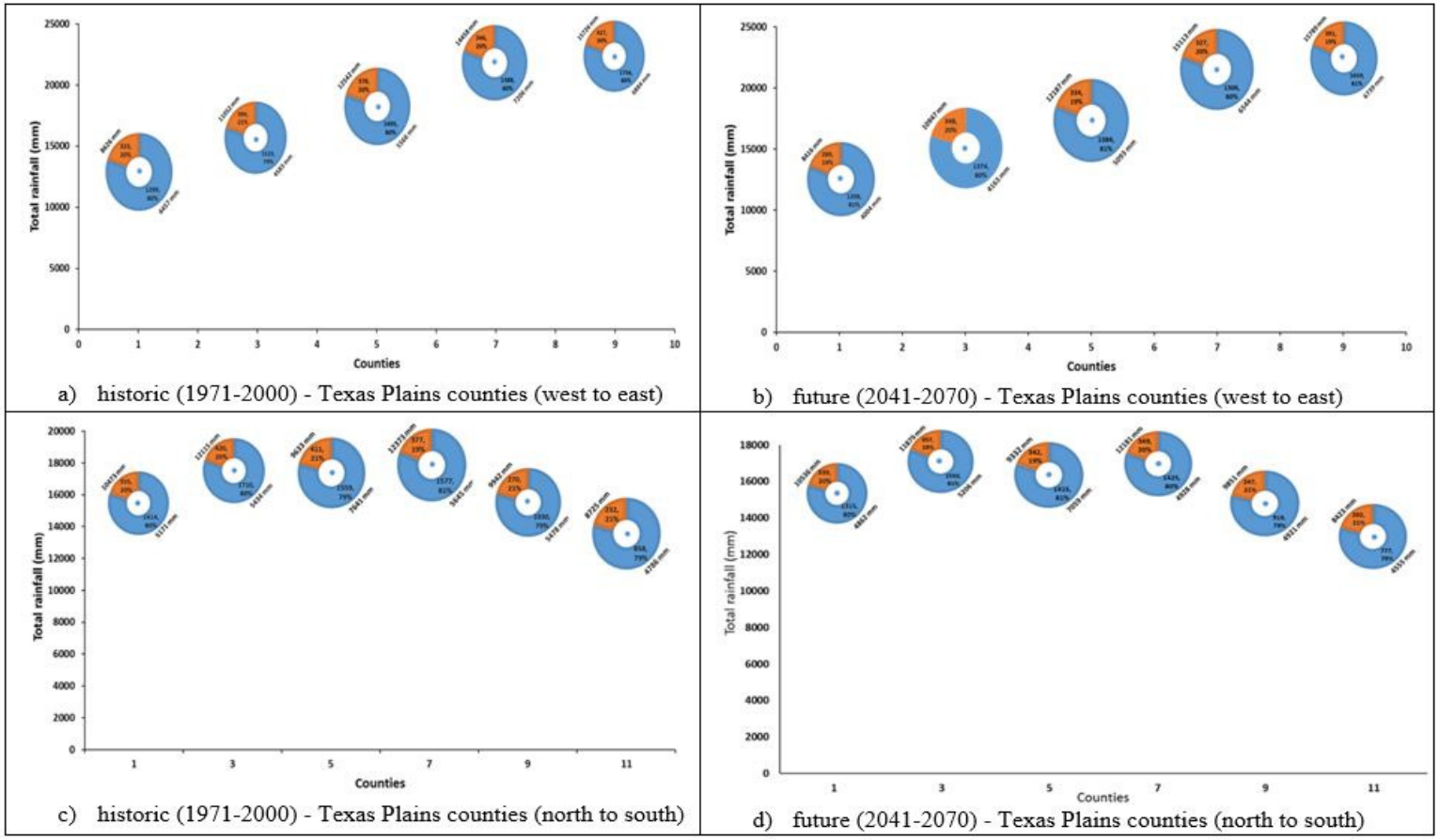

Figure 13. Distribution of rainfall events in selected Texas Plains counties (shown in figure 11) as predicted by RCM3-GFDL (Regional Climate Model Version3–Geophysical Fluid Dynamics Laboratory). The orange portion of the do-nut represents total rainfall received during extreme events and blue portion represents rainfall received during smaller events.

2.4.2 Future changes in air temperature

Both maximum temperature and minimum temperatures under historic (1971-2000) and future climate scenarios across the Texas Plains region, as predicted by three RCMs were analyzed separately. Interestingly, all three models predicted an increase in both maximum and minimum temperature across the region (Figures 14 and 15). The RCM3-GFDL predicted an increase in maximum temperature within a range of 2.0 to 2.6 ºC (Figure 14a-c) and minimum temperature within a range of 1.9 to 2.4 ºC (Figure 15a-c) in the future (Figures 14 and 15). According to the RCM3-CGCM3 model, future increases in maximum temperatures and minimum temperatures ranged between 2.1 to 3.2 ºC (Figure 14d-f) and 2.1 to 2.7 ºC (Figure 15d-f), respectively. The CRCM-CCSM model predicted an increase of 2.1 to 3.2 ºC in maximum temperature (Figure 14g-i) and 1.9 to 2.9 ºC in minimum temperature (Figure 15g-i) under future climate scenarios. The counties in the northern High Plains are predicted to experience greater increases in both maximum temperatures and minimum temperatures when compared to other counties, according to all three models considered in this study.

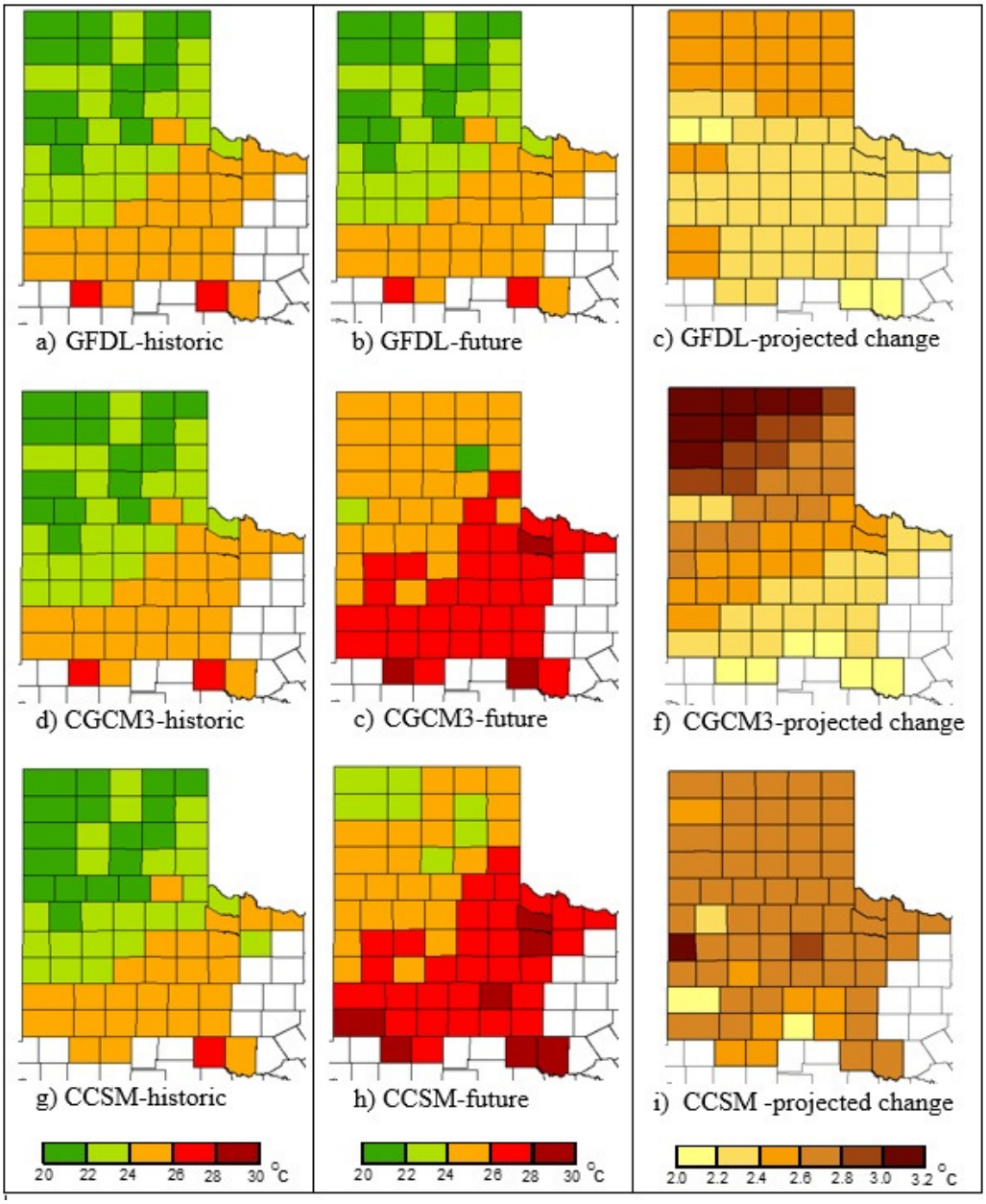

Figure 14. Spatial variability in maximum temperature (TMAX) in the Texas Plains region under historic and future climate scenarios, as predicted by three Regional Climate Models: RCM3-GFDL (Regional Climate Model Version3–Geophysical Fluid Dynamics Laboratory), RCM3-CGCM3 (Regional Climate Model Version3–Third Generation Coupled Global Climate Model) and CRCM-CCSM (Canadian Regional Climate Model-Community Climate System Model).

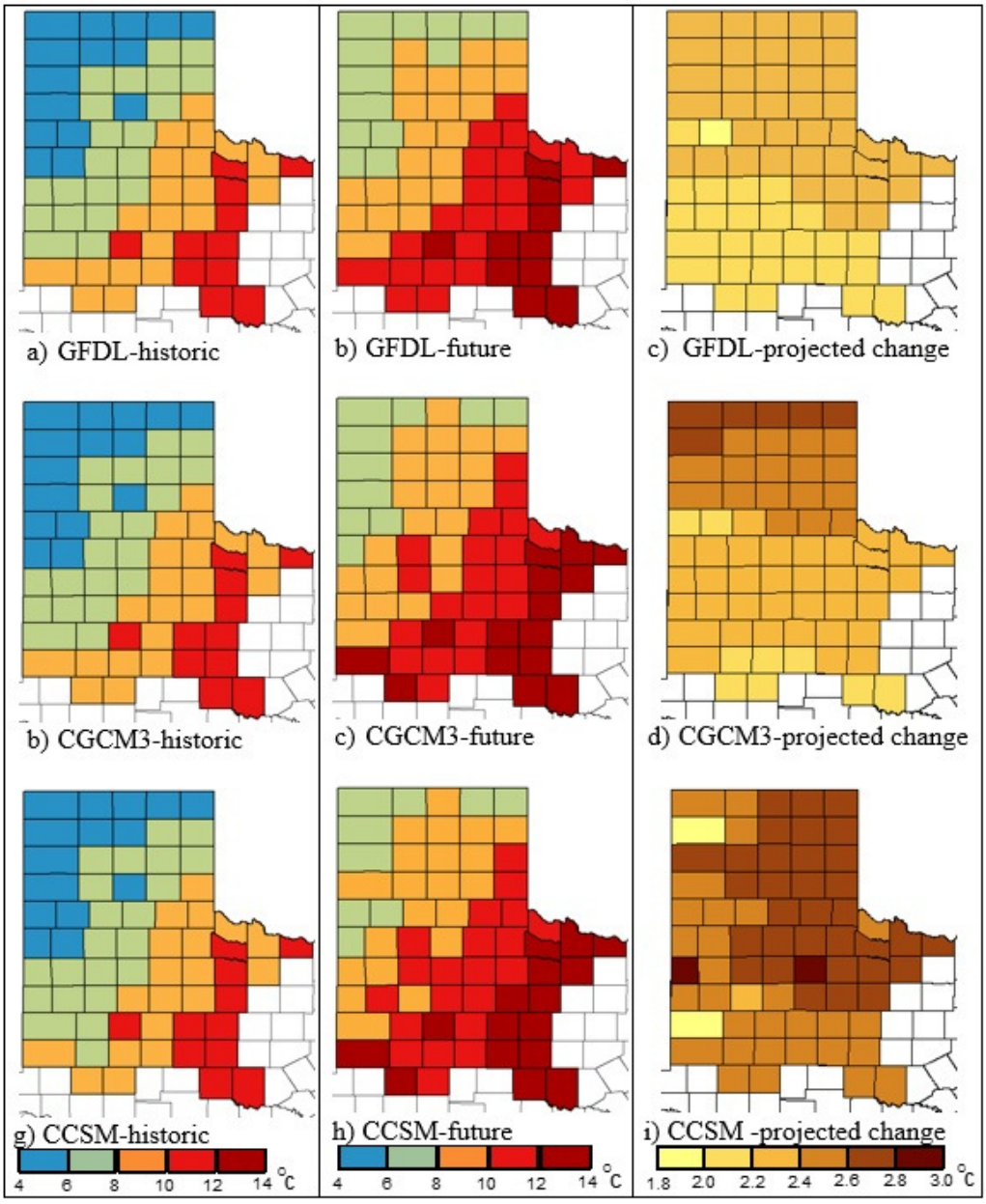

Figure 15. Spatial variability in minimum temperature (TMIN) in the Texas Plains region under historic and future climate scenarios, as predicted by three Regional Climate Models: RCM3-GFDL (Regional Climate Model Version3–Geophysical Fluid Dynamics Laboratory), RCM3-CGCM3 (Regional Climate Model Version3–Third Generation Coupled Global Climate Model) and CRCM-CCSM (Canadian Regional Climate Model-Community Climate System Model).

2.5 Summary and conclusions

The historic (1971-2000) and future (2041-2070) daily rainfall, maximum temperature, and minimum temperature data predicted by three RCMs namely, RCM3-GFDL, RCM3-CGCM3 and CRCM-CCSM were downloaded from the NARCCAP website. The bias associated with the downscaling of climate model projected rainfall and temperature data were successfully removed using the Gamma and Gaussian distribution mapping techniques, respectively. The bias-corrected data was then analysed for studying the spatial and temporal variability of daily rainfall and temperature across the Texas Plains region.

When compared to the historic period (1971-2000), the RCMs predicted i) a decrease in average annual rainfall (30 to 127 mm), ii) a decrease in the number of rainfall events by 6% to 10% and iii) an increase in the intensity of rainfall by about 3% to 8% indicating an increase in the extreme events, in the future (2041-2070). The three RCMs predicted an average increase in the maximum temperature in the range of 2.0 ºC to 3.2 ºC and an average increase in the minimum temperature in the range of 1.9 ºC to 2.9 ºC.

CHAPTER III

EVALUATION OF THE CSM-CROPGRO-COTTON MODEL FOR THE TEXAS ROLLING PLAINS REGION, SIMULATION OF DEFICIT IRRIGATION STRATEGIES FOR INCREASING WATER USE EFFICIENCY, AND ASSESSING FUTURE CLIMATE IMPACTS ON COTTON PRODUCTION

3.1 Introduction

In the agriculture industry across the globe, crop models are being extensively used by researchers and policy makers as important decision making tools for studying the impacts of climate change, management practices and irrigation strategies on crop yields (Thorp et al., 2014). Field experiments in these research areas are resource-intensive and challenging to implement. Under these circumstances, calibrated and validated crop models offer alternative solutions with comparable outcomes. Crop models differ in complexity with some being very simple to use and requiring few input variables and others are complex and require many input variables. The Decision Support System for Agrotechnology Transfer (DSSAT) (Hoogenboom et al., 2012) suite of crop models are complex as they require many input parameters to provide in-depth assessments of crop growth and development and water and nutrient dynamics. DSSAT is a platform which encompasses 28 crop growth models covering fruit crops, vegetable crops, fiber crops, cereals, legumes, oil crops, and root crops. Each crop model simulates crop growth and development in response to weather conditions, soil properties, cultivar characteristics, and crop management data.

The Cropping System Model (CSM), CROPGRO-Cotton distributed with DSSAT can be used to study the impacts of climate change and management practices on crop growth, crop yields, and crop water use. The CSM-CROPGRO-Cotton model has so far been used in very few applications, mostly in the southeastern U.S, Africa, and Australia. Paz et al. (2012) used the CSM-CROPGRO-Cotton model to study the impacts of El Niño/La Niña Southern Oscillation along with different planting dates on cotton yields at various spatial aggregations in 97 cotton-producing counties of Georgia. In another study, CSM-CROPGRO-Cotton model was used to estimate spatial and temporal distribution of water use efficiency of rainfed cotton across cotton growing counties of Alabama, Florida, and Georgia (Garcia y Garcia et al., 2010). In another Georgia study, the CSM-CROPGRO-Cotton model was used in combination with spatial tools to assess the spatial distribution of monthly irrigation water use for cotton (Guerra et al., 2007). The CSM-CROPGRO-Cotton model was also used to study cotton growth and yields under the influence of southern root-knot nematode (*Meloidogyne incognita*) based on the experiments conducted during 2007 at Gibbs farm in Tifton, Georgia (Ortiz et al., 2009).

A limited number of modeling studies in the past have focused on establishing a well-calibrated CSM-CROPGRO-Cotton model for their study regions. Pathak et al. (2012) presented a detailed methodology and described a range of parameters that were needed to be adjusted for CSM-CROPGRO-Cotton calibration based on four experimental studies conducted at Quincy and Citra in Florida, and Griffin in Georgia. A well-calibrated CSM-CROPGRO-Cotton model was also developed based on the experiments conducted at West Florida Research and Education Center Farm located near Jay, FL, by Zamora et

al. (2009), to study the effects of shading on specific leaf area, leaf area index, maximum leaf partitioning, carbon partitioning, and cotton production in a pecan alley cropping system. Gérardeaux et al. (2013) developed a calibrated CROPGRO model to study the effects of an ensemble of six regional climate projections on cotton yields in Cameroon. Their results showed an average increase in cotton yield by 1.3 kg ha^{-1} $year^{-1}$ during the 2005–2050 period due to increase in temperature and CO_2 concentration, and decrease in precipitation. All of the above studies demonstrated the importance of the CSM-CROPGRO-Cotton model calibration in model application and described the methodologies they adopted for successful model implementation.

Texas is the top cotton producing state in the U.S with a total production of 4.17 million bales of cotton in 2013, about 31.5% of the nation's cotton production (USDA–NASS, 2013, 2014). The Texas Rolling Plains (TRP) region in the north central Texas accounts for approximately 13% of the total cotton production in the state (DeLaune et al., 2012). Cotton production in the TRP region has experienced a noticeable decline in recent years due to reduced rainfall amounts and frequent occurrence of severe droughts. Since the TRP region receives inadequate rainfall to meet crop water demands in most years, farmers in this region rely on irrigation for meeting cotton water requirement. Since this region doesn't have adequate surface water resources, farmers use groundwater for irrigation. About 85% of the total water used for irrigation in the TRP region is pumped from the aquifers and the remaining is taken from the surface water sources (County data provided by Mark Michon, Water Science and Conservation division, Texas Water Development Board, personnel communication on February 15th 2012). Nielsen-Gammon

(2011) has predicted warmer summers in the future for this region, which will necessitate larger groundwater withdrawals to meet higher evapotranspiration needs. Studying the effects of various crop and irrigation management practices on cotton yields under current and future climate change scenarios, and development of strategies for water conservation and climate change adaptation is therefore necessary for the TRP region as cotton is one of the major revenue contributors to the local economy. The specific objectives of this study were to: 1) evaluate CSM-CROPGRO-Cotton simulations of cotton growth and yield in the TRP region, 2) identify appropriate deficit irrigation strategies that conserve water while obtaining optimum crop yields, 3) study the impacts of climate change on cotton yields, and 4) evaluate adaptation strategies that can minimize the losses due to climate change. The study emphasizes the establishment of a well-calibrated CSM-CROPGRO-Cotton model for the TRP region, the description of model calibration, validation and evaluation approaches.

3.2 Materials and methods

3.2.1 Study area

The TRP region, encompassing 28 counties, lies in north central Texas and borders Oklahoma to the north (Figure 16). The Seymour aquifer is the major source of irrigation water for this region. The TRP region receives about 46 to 76 cm of annual rainfall with maximum rainfall occurring from May to September. The 30-year average growing season (May–October) precipitation is about 26 cm (DeLaune et al., 2012) and the mean temperature during this period is about 24°C. In general, precipitation decreases from east to west. The most common method of irrigation in the TRP is center pivot sprinkler

irrigation. About 95% of the groundwater pumped from the Seymour aquifer is used for irrigation. Major crops grown in the TRP are cotton (*Gossypium hirsutum, L*), winter wheat (*Triticum aestivum, L*) and sorghum (*Sorghum bicolor, L*) and the dominant soil type in the TRP region is Abilene clay loam.

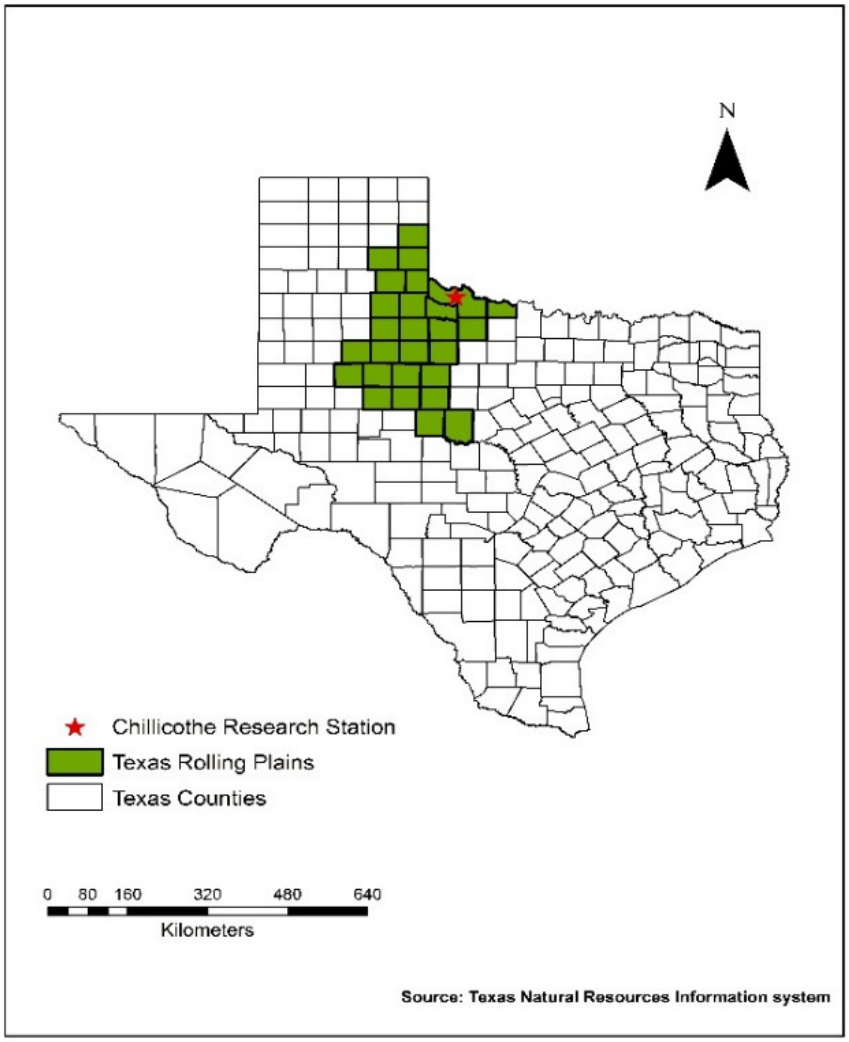

Figure 16. Spatial extent of the Texas Rolling Plains region and location of the Chillicothe Research Station.

3.2.2 Field sites and measured data sets

The observed data for evaluating the CSM-CROPGRO-Cotton model was obtained from the cotton field experiments conducted at Chillicothe Research Station (34.25° N, 99.51° W, 447 m above sea level) in the Hardeman County, Texas (Figure 16) during the period from 2008 to 2012. While data from the 2012 irrigation scheduling experiment (Rajan et al., 2013) were used for model calibration and validation, the data from irrigation and tillage experiments conducted during 2008-2010 period (DeLaune et al., 2012) were used for model evaluation. In 2012, four irrigation scheduling treatments (100% ET replacement, 75% ET replacement, tensiometer based-, and soil moisture based irrigation scheduling) with three blocks were implemented in a randomized complete block design with each plot measuring 23 m by and 4.6 m. The 2008-2010 experiments were also conducted in a randomized block design with each plot measuring 8 m by and 45.7 m to study the combined impacts of different tillage (conventional and conservational till) and irrigation regimes (0%, 33%, 66%, 100%, and 133% ET replacement) on cotton production. Experimental treatments were replicated three times.

In the 2012 irrigation scheduling experiment, soil moisture tension was measured using irrometers and soil moisture was measured using CS 616 time domain reflectometry (TDR) probes. Data related to crop growth, crop development and crop yields were collected during the study. The leaf area index (LAI), canopy height, phenology, and number of main stem nodes were also measured at various crop development stages. LAI was measured destructively using an LI-3100C leaf area meter (LICOR Biosciences, Lincoln, NE). Experimental plots were machine harvested and the lint yields were

estimated after ginning. Details about the 2008-2010 experiments can be found in DeLaune et al. (2012).

3.2.3 Description of CSM CROPGRO Cotton model

For this study, the CSM-CROPGRO-Cotton model was chosen due to its successful application for different cropping systems under different climatic conditions by various researchers across the globe. DSSAT is a platform that integrates the database management system (soil, climate, and management practices), crop models and various application programs including sensitivity analysis and spatial analysis (Tsuji et al., 2002; Jones et al., 2003) by bringing together a diverse array of crop models to a single platform. The latest DSSAT 4.5 (Hoogenboom et al., 2012) version is equipped with over 28 crop growth simulation models. Each crop growth model incorporated in the DSSAT predicts crop growth, development, and yield, and soil water balance, evapotranspiration, and nutrient dynamics models are also available for simulating soil moisture, carbon and nitrogen processes over time based on weather, soils, crop management, and crop cultivar information.

The CSM-CROPGRO-Cotton model, which was developed from the CROPGRO-Soybean model, simulates crop growth and development on a daily timescale. It simulates different crop growth stages such as the emergence, first leaf, first flower, first seed, first cracked boll, and 90% open boll based on the accumulation of heat units or photothermal time (Thorp et al., 2014). The CSM-CROPGRO-Cotton model requires soil, management, environment, and cultivar parameters as inputs (Hunt et al., 2001). Required soil parameters include soil texture, slope, albedo, color, drainage, drained upper limit (DUL),

lower limit (LL), saturated water content (SAT), hydraulic conductivity, organic carbon, bulk density and total soil nitrogen. Management parameters required include: (i) type of irrigation system, irrigation dates, and amounts, (ii) fertilizer application method, amounts, and dates, and (iii) tillage method (conservation tillage), tillage depth and dates. Additionally, cropping system characteristics such as plant population, seeding depth, row spacing, planting dates, planting method, cultivar variety, and harvest dates are required. Environmental variables such as daily maximum temperature, minimum temperature, incoming solar radiation, and precipitation are also required while dew point temperature and wind speed are optional. Cultivar information is input in three data files. More details about the cultivar files are described in the model calibration section. The model is capable of simulating the effects of various management practices, insect damage, disease damage, and climate change. A feature called environmental modification is available in the model, and it allows the user to incorporate changes to the climate variables. The model also allows the user to input ambient CO_2 concentration values which are based on the values measured at Mauna Loa in Hawaii (Thorp et al., 2014).

The CSM-CROPGRO-Cotton model works by calculating various rate variables on a daily time step, integrating the model states over time, and finally updating the state variables (Jones et al., 2003). A warm-up period can be simulated in the model before planting for establishing the soil hydrological conditions. After planting, the model simulates carbon, nitrogen and water dynamics as well as plant processes like photosynthesis, and respiration. The vegetative phase mostly depends on the supply of carbon and nitrogen (Jones et al., 2003). During the vegetative phase, carbon and nitrogen

are partitioned between stems, leaves and roots. These routines estimate the carbon and nitrogen assimilation and their allocation to growing tissues (Jones et al., 2003). Total carbon available for growth in a day is equal to the day's photosynthesis plus mobilized carbon from carbon reserves in leaves, stems, shells, and roots minus maintenance respiration. Maximum carbon available for various plant processes like growth, nitrogen reduction, nitrogen fixation, and growth respiration during the day is calculated as the difference between the sum of carbon synthesized during photosynthesis, and the potential amount of carbon mined in a day; and the maintenance respiration (Jones et al., 2003). During the reproductive phase, the partition mainly depends on the availability of carbohydrates (Jones et al., 2003). If any excess carbohydrates are available after reproductive feature developments, those carbohydrates will be directed for vegetative tissue growth. Photosynthesis is calculated based on the light intercepted by hedgerow canopy (Boote and Pickering, 1994). The model estimates both maintenance respiration and growth respiration losses. All these processes are affected by the amount of water available in the soil. Soil water balance routine in the DSSAT simulates daily soil water processes that affect the availability of soil water (Ritchie, 1985). Daily change in soil water availability is calculated based on the following equation:

$$\Delta S = P + I - ES - EP - R - D \qquad (19)$$

where ΔS = change in storage, P = Precipitation, I = Irrigation, ES = Soil Evaporation, EP = Transpiration, R = Runoff, D = Drainage.

Soil moisture is distributed in several layers with depth increments specified by the user (Ritchie, 1985). Runoff is calculated using the modified Soil Conservation Service

curve number technique (USDA-SCS, 1972) in which the wetness of the soil, calculated from the previous rainfall, replaces antecedent rainfall condition (Williams et al., 1991). This modified procedure is the most conservative method of estimating runoff under known daily precipitation (Ritchie, 1985). This method, however, ignores rainfall intensity and assumes complete infiltration of applied irrigation water.

Drainage in the DSSAT model is estimated based on the "tipping bucket" approach in which the drainage occurs when the water content in the given soil layer is above the drained upper limit (equivalent to field capacity). It is assumed that saturated volumetric water content and drained upper limit of soil water content for each soil layer are fixed. The water content in each layer varies between saturation, the drained upper limit, and the lower limit (equivalent to permanent wilting point) (Ritchie, 1985). Infiltration is estimated as the difference between precipitation plus irrigation and runoff.

DSSAT estimates soil evaporation and plant transpiration separately. DSSAT uses Priestly-Taylor (Priestly and Taylor, 1972) and FAO-56 methods (Allen et al., 1998) to estimate ET. The Priestly-Taylor method does not account adequately for advection (Ritchie**,** 1981). Since the TRP region experiences high wind speeds during some parts of the year, the FAO-56 method, which considers wind speed, was used for estimating evapotranspiration in this study. The amount of solar energy that reaches the soil surface was used to estimate soil evaporation, which was proportional to daytime temperature, LAI, and soil albedo. Potential plant transpiration was calculated as a function of potential evapotranspiration, and light intercepted by canopy.

Root water uptake was calculated using the law of limiting approach, wherein soil resistance, root resistance or atmospheric demand dominates the flow rate of water into roots (Ritchie, 1998). Detailed information about methodologies and processes used in DSSAT can be found in the DSSAT documentation (Hoogenboom et al., 2010).

3.2.4 Model inputs

3.2.4.1 Weather inputs

Daily maximum temperature, minimum temperature, incoming solar radiation, precipitation, wind speed, dew point temperature for the years 2008, 2009, 2010 and 2012 were obtained from the Texas High Plain Evapotranspiration Network (TXHPET) for the Chillicothe station (Porter et al., 2005). Table 4 provides the monthly summary of observed climate data. Average soil temperature parameter (TAV) and the soil temperature amplitude parameter (AMP) were estimated separately for each year. TAV and AMP were set to 25.7 °C and 14.3 °C, respectively for the 2012 irrigation experiments. TAV and AMP, respectively were estimated to be 24 °C and 13.5 °C for 2008, 26.1°C and 14.5 °C for 2009, and 25 °C and 13.5°C for 2010.

Table 4.Monthly summary of climate data for the years 2008-2010 and 2012.

Month	2008						2009					
	SRAD ($MJ\ m^{-2}$)	TMAX (ºC)	TMIN (ºC)	RAIN (mm)	DEW (ºC)	WIND ($km\ d^{-1}$)	SRAD ($MJ\ m^{-2}$)	TMAX (ºC)	TMIN (ºC)	RAIN (mm)	DEW (ºC)	WIND ($km\ d^{-1}$)
May	851	38.1	16.8	79	11.9	287.6	692.7	36.1	7.0	59.1	13.3	256.0
Jun	852.5	40.2	15.4	109.5	17.0	355.9	768.4	40.4	17.7	67.7	13.0	269.7
Jul	827.3	41.6	18.3	39	17.1	268.2	853.0	42.6	17.6	54.6	16.9	260.8
Aug	665.1	40.3	17.6	82.5	18.1	210.8	833.9	40.9	16.1	36.6	16.2	295.1
Sep	596.4	35.2	10	48.2	14.6	164.8	567.9	38.1	8.3	75.6	14.5	227.7
Oct	539.6	34	-0.6	54.6	8.0	249.7	383.0	28.5	0.1	87.3	8.5	243.1
Sum	4332.1	--	--	412.4	--	--	4099.0	--	--	381.0	--	--
Mean	--	32.8	9.5	--	12.3	219.3	--	32.4	8.9	--	12.5	221.8

Month	2010						2012					
	SRAD ($MJ\ m^{-2}$)	TMAX (ºC)	TMIN (ºC)	RAIN (mm)	DEW (ºC)	WIND ($km\ d^{-1}$)	SRAD ($MJ\ m^{-2}$)	TMAX (ºC)	TMIN (ºC)	RAIN (mm)	DEW (ºC)	WIND ($km\ d^{-1}$)
May	820.8	36.8	3.5	63.0	13.3	260.4	861.5	40.9	8.1	20.3	12.2	335.7
Jun	930.6	39.1	18.4	68.0	19.3	298.1	925.4	44.4	14.5	79.1	16.3	289.2
Jul	798.0	38.2	18.7	166.1	21.0	231.4	966.9	44.1	20.2	36.4	15.3	248.0
Aug	900.0	40.2	13.4	34.1	17.8	218.4	714.1	44.2	16.1	80.2	14.6	214.5
Sep	705.1	37.5	6.3	51.0	17.3	251.8	639.4	39.3	12.7	116.1	13.5	202.1
Oct	594.8	32.6	2.4	38.1	6.8	195.4	551.1	35.3	-3.1	8.7	7.0	233.0
Sum	4750.0	--	--	420.3	--	--	4658.4	--	--	340.8	--	--
Mean	--	32.0	8.9	--	13.6	207.3	--	35.4	9.8	--	11.3	217.5

SRAD = incoming solar radiation, TMAX = maximum daily temperature, TMIN = minimum daily temperature, RAIN = precipitation, DEW = dew point temperature, and WIND = wind speed

3.2.4.2 Management inputs

The details of crop, fertilizer and irrigation management practices adopted during different years are outlined in Table 5. The 'Deltapine 0912' cotton variety was planted at a seeding rate of 8 seeds per m of row and a row spacing of 1 m. The pre-plant soil analysis report had shown higher levels of nitrogen residue in the soil and hence no pre plant nitrogen was applied. Nitrogen was knifed in as liquid fertilizer (28-0-0) during square formation at the rate of 35 kg ha^{-1}. Nitrate present in the irrigation water was not accounted for in this study.

In the irrigation and tillage experiments conducted in 2008-2010, the 'Stoneville 4554 B2RF' cotton cultivar was planted with a seeding rate of 13.8 seeds per m of row. The nitrogen fertilizer was knifed on each side of the row three weeks after planting, prior to square formation (Table 5). Seed cotton yields and lint yields were obtained from these experimental studies.

The CSM-CROPGRO-Cotton model does not have a provision to directly select tillage practices. Instead, user can select a tillage implement used in an experiment and specify tillage depth to represent conventional and conservation tillage practices. For conventional tillage, a bedder and row cultivator were used to a depth of 20 cm. For conservation tillage, a tandem disk was used to a depth of 10 cm. The irrigation efficiency of the subsurface drip irrigation system was assumed to be 95%, in view of very small/negligible percentages of losses via evaporation.

Table 5. Management practices implemented in 2008 – 2010, and 2012 experiments.

Management Practice	2012	2008	2009	2010
Planting Date	23 May	15 May	21 May	20 May
Irrigation System	sub surface drip	sub surface drip	sub surface drip	sub surface drip
Irrigation Start date	23 May[a,b,c,d]	22 May[1,2,3,4]	29 May[1,2,3,4]	29 May[1,2,3,4]
Irrigation End date	14 August[a,b,c,d]	3 September[1,2,3,4]	10 September[1,2,3];17 September[4]	7 September[1,2,3,4]
Irrigation amount (mm)	416[a], 317[b], 344[c], 294[d]	64[1], 132[2], 200[3], 265[4]	134[1], 270[2], 380[3], 546[4]	97[1], 191[2], 283[3], 377[4]
Type of Fertilizer	Urea Ammonium nitrate	Ammonium polyphosphate, urea ammonium nitrate	Ammonium polyphosphate, urea ammonium nitrate	Ammonium polyphosphate, urea ammonium nitrate
Amount of Fertilizer	35 kg N ha^{-1}	45 kg N ha^{-1}, 22 kg P ha^{-1}	67 kg N ha^{-1}, 34 kg P ha^{-1}	67 kg N ha^{-1}, 34 kg P ha^{-1}
Tillage	conventional	conventional and conservation	conventional and conservation	conventional and conservation

a = 100% ET replacement, b = 75% ET replacement, c = Tensiometer based scheduling, d = soil moisture based scheduling; 1 = 33% ET replacement, 2 = 66% ET replacement, 3 = 100% ET replacement, 4 = 133% ET replacement.

3.2.4.3 Soil inputs

The dominant soil type at the study site is Abeline clay loam (fine mixed, super active, thermic parchic argiustol), which has good drainage and moderately high saturated hydraulic conductivity (DeLaune et al., 2012). The soil profile was divided into 6 layers, namely, 0-5, 5-12, 12-30, 30-45, 45-60, and 60-160 cm to account for heterogeneity in soil properties. Soil samples to a depth of 60 cm were collected before planting in the year 2012 and were analyzed for common soil properties. Regression equations were developed for each soil property based on the analyzed data. The regression equations were used to estimate the soil properties for the deeper layers (60-160 cm). Soil samples were analyzed for bulk density, pH, organic carbon, and percent silt and clay. The soil hydrological properties like DUL, LL, saturated soil water content, and saturated hydraulic conductivity were estimated using the ROSETTA pedotransfer tool (Table 6) (Schaap et al., 2001). The neural network based ROSETTA tool uses five hierarchical pedotransfer functions to estimate soil hydrological properties based on the soil texture and bulk density. Soil bulk density was estimated based on soil texture within DSSAT. The root growth factor values were estimated using an exponential decay function in DSSAT. The runoff curve number (SLRO) was adjusted to 25.0 to simulate no runoff, as no runoff observed was due to dry weather conditions and subsurface drip irrigation. The same soil composition and hydrological properties were used for all the experiments.

Table 6. Soil composition and hydrological properties used for all simulations

Depth (cm)	SLCL (%)	SLSI (%)	SLOC (%)	SLHW	CEC (cmol kg^{-1})	SLNI (%)	LL (cm cm^{-1})	DUL (cm cm^{-1})	SSAT (cm cm^{-1})	SBDM (g cm^{-3})	SSKS (cm h^{-1})	SRG F
0-5	26	40	1	7.3	20.0	0.1	0.103	0.319	0.440	1.32	0.67	0.950
5-15	26	40	1	7.3	20.0	0.1	0.103	0.319	0.440	1.32	0.67	0.950
15-30	28	32	0.67	7.7	20.3	0.07	0.109	0.301	0.428	1.40	0.46	0.850
30-45	34	27	0.64	7.6	21.4	0.07	0.126	0.311	0.439	1.41	0.45	0.775
45-60	32	34	0.48	7.9	23.5	0.05	0.118	0.314	0.439	1.39	0.44	0.700
60-160	32	34	0.31	7.9	23.5	0.04	0.117	0.311	0.434	1.41	0.39	0.320

SLCL = clay content, SLSI = silt content, SLOC = organic carbon, SLHW = pH in water, CEC = cation exchange capacity, SL NI = Total nitrogen concentration, LL = lower limit, DUL = drained upper limit, SSAT = saturation, SBDM = bulk density, SSKS = saturated hydraulic conductivity, and SRGF = soil root growth factor.

3.3 CSM-CROPGRO-Cotton model calibration, validation and evaluation

The CSM-CROPGRO-Cotton model was calibrated using observed data from the 100% ET replacement treatment, which is expected to represent minimum/no stress conditions, implemented at Chillicothe in the year 2012 (Rajan et al., 2013). Data from the remaining three irrigation scheduling treatments including 75% ET replacement, tensiometer- and soil moisture-based scheduling, were used for validation. The calibrated model was further evaluated using the seed cotton yield data from 30 treatments of a 3-year (2008-2010) cotton irrigation and tillage study at Chillicothe (DeLaune et al., 2012).

Since the DSSAT cultivar database does not include Deltapine 0912 variety, we used the closest cultivar variety, GP 3774, that is already incorporated in the database for calibrating the CSM-CROPGRO-Cotton model for crop growth and development. A manual calibration approach was followed, in which sensitive model parameters were adjusted and their effect on modeled processes were studied by visually comparing simulated versus observed crop growth and yield data and simultaneously assessing the model performance statistics (Table 7). Four different statistical parameters including percent error, root mean square error (RMSE), coefficient of determination (R^2), and coefficient of agreement, were used to assess the performance of CSM-CROPGRO-Cotton model. The model parameters were varied in such a way that the resultant RMSE was low (<0.5), co-efficient of agreement was high (>0.85) and coefficient of determination (R^2) was high (>0.85). Finally, selected model parameter values were compared to the previously published studies (Pathak et al., 2012; Pathak et al., 2007; Ortiz et al., 2009). In this procedure, first the cultivar specific parameters affecting the

crop phenology (Table 8) were adjusted until the simulated crop phenology stages matched reasonably well with observed data. Secondly, the parameters affecting the crop growth (Table 8) were adjusted until a satisfactory match between simulated and observed LAI and canopy height were achieved. Finally, the parameters affecting crop yields (Table 8) have been adjusted until the predicted and observed seed cotton yields matched well. The cultivar specific parameters that were adjusted during calibration are included in cultivar (COGRO046.CUL), ecotype (COGRO046.ECO) and species (COGRO046.SPE) files. Model developers generally recommended to not change the parameters in the COGRO046.SPE file, but in our study, two cultivar parameters XVSHT (number of average observed nodes) and YHWTEM (effect of temperature on the length of each node) in this file had to be adjusted in order to better simulate cotton growth and yield at the study site. The cotton parameters that were adjusted during the model calibration are listed in Table 8.

Table 7. Statistical parameters that were used for evaluating the model efficiency.

Indicators	Equation	Source
Root mean square error	$RMSE = \left[N^{-1} \sum_{i=1}^{N} \left(Yi - \hat{Y}i \right)^2 \right]^{0.5}$	Willmott, 1981;
Co-efficient of determination	$R^2 = \frac{\left(\sum_{i=1}^{N} \left(Yi - \overline{Y} \right) \left(\hat{Y}i - \overline{Y}i \right) \right)^2}{\sum_{i=1}^{N} \left(Yi - \overline{Y} \right)^2 \sum_{i=1}^{N} \left(\hat{Y}i - \overline{Y}i \right)^2}$	Legates and McCabe, 1999
Co-efficient of agreement	$index = 1 - \frac{\sum_{i=1}^{N} (Yi - \hat{Y}i)^2}{\sum_{i=1}^{N} \left(\left\| \hat{Y}i - \overline{Y} \right\| + \left\| Yi - \overline{Y} \right\| \right)^2}$	Willmott,1981;
Percent error	$error = \left[\frac{\hat{Y}i - Yi}{Yi} \right] * 100$	

where $Yi = measured\ value$, $\hat{Y}i = simulated\ value$, $\overline{Y} = \ average\ of\ observed\ values$, $\overline{Y}i = avergae\ of\ simulated\ values$, $N = no\ of\ observations$.

Table 8. CSM-CROPGRO-Cotton model parameters adjusted during the model calibration.

Parameter	Description	Default value	Testing range	Calibrated value
	Crop phenology and development			
PL-EM	Time between planting and emergence	4	3 – 4	3
FL-LF	Time between first flower and end of leaf expansion	75	40 – 75	50
FL-VS	Time from first flower to last leaf on main stem	75	45 – 75	45
	Crop growth			
LFMAX	Maximum leaf photosynthesis rate at 30 ºC, 350 ppm CO_2, and high light (mg CO_2 m^{-2} s^{-1})	1.1	0.4 – 1.8	1.7
RHGHT	Relative height of this ecotype in comparison to the standard height per node (YVSHT) defined in the species file	0.95	0.55 – 0.95	0.6
RWDTH	Relative width of this ecotype in comparison to the standard width per node (YVSWH) defined in the species file	0.85	0.30 – 0.85	0.35
TRIFL	Rate of appearance of leaves on the mainstem	0.2	0.18 – 0.30	0.3
YHWTEM	Effect of temperature on the length of each internode	0.01, 0.01, 0.33, 1.0, 1.0	-	0.01, 0.02, 0.43, 0.85, 0.85
SLAVR	Specific leaf area of cultivar under standard growth conditions (cm^2 g^{-1})	170	120 – 200	130
	Crop yield			
XFRT	Maximum fraction of daily growth that is partitioned to seed + shell	0.55	0.3 - 0.9	0.75
SFDUR	Seed filling duration for pod cohort at standard growth conditions	24	20-35	30
LNGSH	Time required for growth of individual shells	8	7-15	14

3.4 Determination of appropriate deficit irrigation strategies for the Texas Rolling Plains

The calibrated model was used to determine appropriate deficit irrigation strategies for the TRP region that conserve water under different climatic conditions. For the years 2008 to 2010, deficit irrigation strategies with 0%, 33%, 66%, 100% and 133% ET replacement were implemented in the calibrated model to compare the simulated results with observed data for these treatments (DeLaune et al., 2012). For the year 2012, deficit irrigation strategies with 0% to 130% ET replacement with an increment of 10% were simulated and analyzed.

3.5 Assessment of the impacts of future climate change on cotton yields at Chillicothe

The calibrated CSM-CROPGRO-Cotton model was used to study the impacts of future climate change on seed cotton yields. Bias corrected future (2041–2070) daily rainfall, maximum temperature, minimum temperature data as predicted by three regional climate models (RCM3-GFDL, RCM3-CGCM3, CRCM-CCSM) for the Chillicothe region were used as inputs for simulating historic and future climate scenarios in the CSM-CROPGRO-Cotton model. The solar radiation data (not corrected for bias) predicted by three climate models and the weather generator generated wind speed data were also used with the CSM-CROPGRO-Cotton model in the future climate scenarios. All management practices were assumed to be the same as those adopted for the 2012 100% ET replacement experiment at Chillicothe, except for irrigation. Automatic irrigation method was used in the model. Whenever the soil water content was below 50% of the available water

(difference of field capacity and permanent wilting point soil moisture contents), irrigation was triggered until the available soil water content reached 85% level (deficit irrigation strategy). The soil properties that were used in the 2012 experiment were also maintained the same for the CSM-CROPGRO-Cotton model simulations under future climate change scenarios.

For analysis purposes, the climate data for both historic and future periods have been classified into three categories: dry, normal and wet periods based on the growing season rainfall (May to October). The rainfall data was first arranged in ascending order and the top 5 years have been classified as “dry”, the middle five years as “normal” and the last five years as “wet” periods. In addition, the calibrated CSM-CROPGRO-Cotton model was used to evaluate few potential climate change adaptation strategies such as early planting and no-till practice under the RCM3-GFDL predicted future climate scenario.

3.6 Results and discussions

3.6.1 Calibration

With default parameters, the model predicted plant emergence as 8 days after planting (DAP) (results not shown), so the phenology parameter PL-EM in the cultivar file was adjusted to 3 photothermal days to simulate plant emergence as 5 DAP as measured during the experiment. Parameter FL-LF in the cultivar file and parameter FL-VS in the ecotype file were adjusted to simulate end of leaf expansion stage and end of node expansion stage, respectively, according to field observations. After these adjustments, simulated dates of anthesis, first flower, 50% boll open, and physiological maturity fell within the range of

observed dates in the TRP region (Table 9).

Table 9. Comparison of observed and simulated dates of crop phenological stages

Crop phenological stage	Observed (days after planting)	Simulated (days after planting)
Emergence	5	5
Onset of anthesis	46	49
Planting to harvest*	130-160	154

*http://www.cotton.org/tech/ace/growth-and-development.cfm

With default cultivar characteristics, the model underestimated LAI across all growth stages and overestimated canopy height by 45% (figures not shown). Maximum leaf photosynthesis rate (LFMAX) (Table 8) value was adjusted to 1.7 after making sure that model is not simulating any water and nitrogen stresses. A value of 180 was obtained for the specific leaf area (SLAVR) of the cultivar, which is the ratio of leaf area to leaf weight, by averaging the field observed leaf area and leaf weight values. Parameters TRIFL (rate of appearance of leaves on the main stem) and SLAVR were adjusted (Table 8) to improve simulated versus observed LAI (Figure 17a). After adjusting the above mentioned parameters, the model was able to simulate LAI trend satisfactorily, however the model underestimated the LAI values after entering the reproductive phase (Figure 17a, Table 11). CSM-CROPGRO-Cotton model calibration for canopy height prediction required the change of parameters in species file. The number of nodes on main stem (XVSHT) was adjusted based on average observed field data at various growth stages (Table 10).

Table 10. Number of nodes observed at various crop developmental stages.

Plant development stage	No of average observed nodes
Planting	0
Emergence	1
V1 phase	5
End of Juvenile stage	10
Flower induction	10
First flower	16
First peg	18
First pod	20
First seed	24
Last seed	25

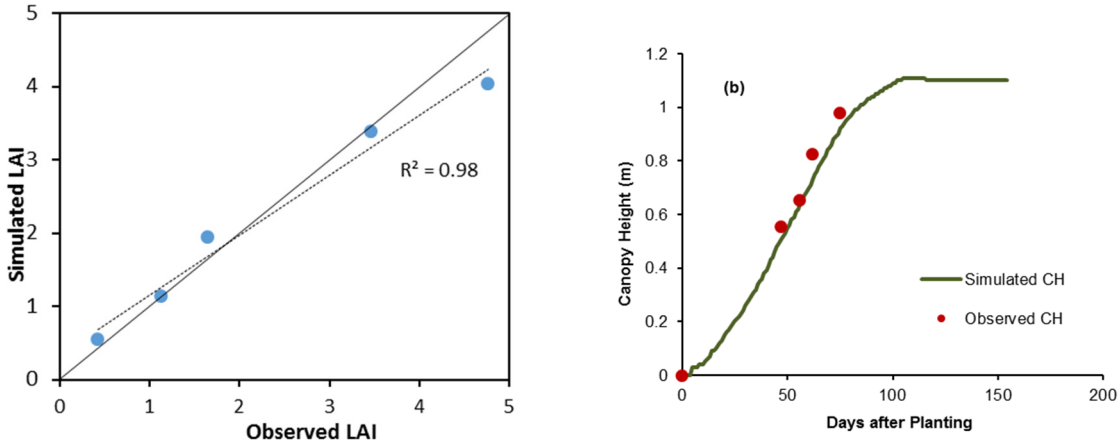

Figure 17. Comparison of simulated and observed a) leaf area index (LAI) and (b) canopy height (CH) of cotton during model calibration.

Table 11. Model performance in leaf area index (LAI) and canopy height prediction during calibration.

Variable	R^2	Root Mean Square Error	Coefficient of agreement
LAI	0.98	0.35	0.98
Canopy height	0.97	0.06	0.96

Since the uncalibrated model under-predicted the canopy height during the early growing season and over-predicted the canopy height during the late growing season, a species file parameter YHWTEM, which defines the effect of temperature on the length of each internode, was increased during the initial vegetative phase and decreased during the beginning of the anthesis phase (Table 8). Parameters RHGHT and RWDTH were also adjusted to get a reasonable canopy height simulation (Figure 17b, Table 8, Table 11). Finally, the cultivar parameters XFRT, SFDUR, LNGSH and TRIFL were adjusted during model calibration for attaining a better match between observed and simulated seed cotton yield (Table 8). The calibrated model simulated a seed cotton yield of 4831 kg ha^{-1} as compared to observed seed cotton yield of 4781 kg ha^{-1} with an error of 1%.

3.6.2 Validation

The calibrated CSM-CROPGRO-Cotton model was validated using the data from three other irrigation scheduling treatments implemented in 2012. These three treatments had the same experimental setup as the 100% ET replacement treatment, except for the method of estimating daily irrigation amounts. The total irrigation amounts applied during the growing season were 329 mm for the 75% ET treatment, 344 mm for the tensiometer based experiment and 295 mm for the soil moisture based scheduling method. The model performance during the validation was satisfactory as indicated by agreement between the observed and simulated LAI (R^2 >0.85) (Figure 18a, Table 12) and canopy height (R^2 = 0.83 – 0.97) (Figure 18b, Table 12). However, the model slightly under predicted canopy height among all treatments. The model simulated crop yields for these three treatments

also matched satisfactorily as indicated by low percent error, which fell within an acceptable range of -1.4 to -9.2 (Table 13).

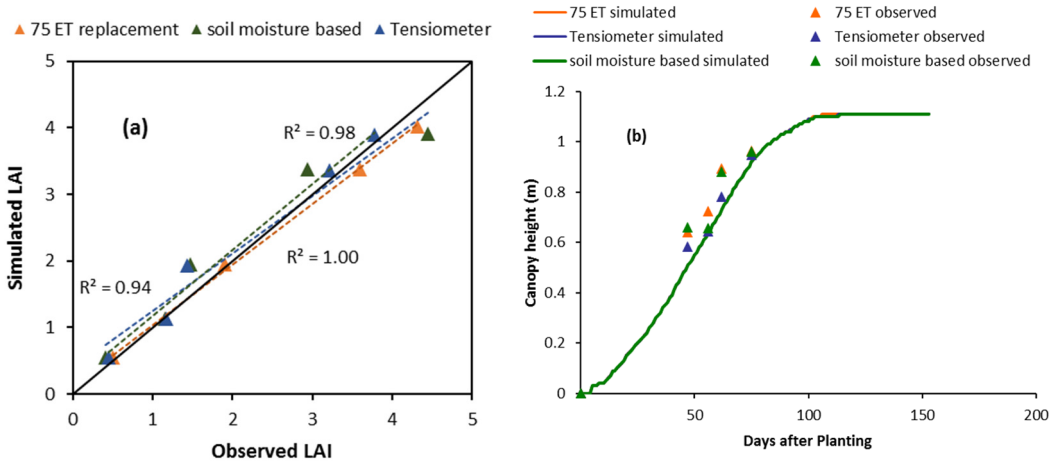

Figure 18. Comparison of simulated and observed a) leaf area index (LAI) and (b) canopy height of cotton during model validation.

Table 12. Model performance statistics for Leaf Area Index (LAI) and canopy height prediction during the validation.

	R^2		Root Mean Square Error		Coefficient of agreement	
Treatments	1	2	1	2	1	2
75% ET replacement	0.99	0.92	0.16	0.12	1.00	0.85
Tensiometer	0.98	0.97	0.25	0.05	0.99	0.97
Soil moisture based	0.94	0.83	0.38	0.11	0.98	0.86

1 = LAI, 2 = Canopy height

Table 13. Comparison of observed and simulated seed cotton yields during the model validation.

Treatments	Observed yield (kg ha^{-1})	Simulated yield (kg ha^{-1})	Percent error
75% ET replacement	4783	4402	-7.9
Tensiometer based	4613	4188	-9.2
Soil moisture based	4279	4217	-1.4

3.6.3 Model evaluation

The CSM-CROPGRO-Cotton model was further evaluated using the data from a 3-year study on cotton irrigation and tillage management conducted on an adjacent subsurface drip irrigated field between 2008 and 2010 (DeLaune et al., 2012). The CSM-CROPGRO-Cotton model simulated seed cotton yields for all irrigated treatments, were in error range of -24% to 13%, except for 0% (rainfed) and 33% ET replacement treatments (Table 14). For the dry (0% and 33% ET) replacements, the model mostly overestimated cotton seed yield for conservation tillage experiments in all the years except for the 2008 rainfed treatment and 33% ET replacement in 2010; and underestimated for conventional tillage except for the 33% ET replacement in 2008 and rainfed treatment in 2010 (Table 14). The model predictions for conservation tillage were slightly better than those for the conventional tillage (Table 14). Overall, the model predicted seed cotton yield reasonably well ($R^2 \approx 0.90$) for 15 conventional (Figure 19a) and 15 conservational tillage (Figure 19b) treatments during the 2008-2010 cropping seasons.

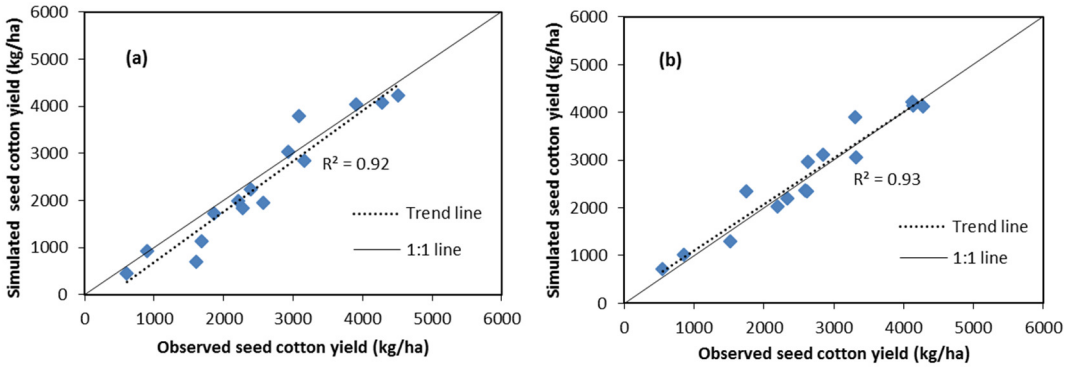

Figure 19. Comparison of simulated and observed crop yields from various irrigation treatments under (a) conventional tillage (b) conservational tillage during model evaluation.

Table 14. Measured and simulated seed cotton yields for various treatments from year 2008 – 2010 during model evaluation.

		Conventional Tillage			Conservational Tillage		
	Treatments (ET replacement)	Observed	Simulated	% error	Observed	Simulated	% error
2008	0	1603	691	-56.9	2189	2028	-7.3
	33	3082	3788	22.9	3310	3893	17.6
	66	3912	4044	3.4	4284	4130	-3.6
	100	4279	4080	-4.6	4123	4224	2.4
	133	4507	4231	-6.1	4139	4153	0.3
2009	0	607	455	-25	548	723	31.9
	33	1859	1733	-6.8	1752	2348	34.0
	66	2391	2239	-6.4	2624	2971	13.2
	100	3156	2838	-10.1	3319	3053	-8.0
	133	2936	3035	3.4	2845	3119	9.6
2010	0	901	934	3.7	854	1010	18.3
	33	1678	1137	-32.2	1515	1307	-13.7
	66	2269	1845	-18.7	2329	2201	-5.5
	100	2215	1998	-9.8	2593	2362	-8.9
	133	2573	1959	-23.9	2616	2351	-10.1

The Irrigation Water Use Efficiency (IWUE), a ratio of difference between irrigated seed cotton yield and dryland seed cotton yield divided by the total amount of irrigation water applied (Howell, 2003; DeLaune et al., 2012), was also estimated for these experiments and compared with the observed efficiencies (Table 15). The IWUE values calculated from the model simulated seed cotton yields were in close agreement with the observed values, except for the deficit irrigation treatments. The simulated IWUE values for 33% ET replacement treatments were higher when compared to observed values (Table 15) as the model under-predicted seed cotton yields (Table 14). However, simulated IWUE decreased with increased irrigation amounts, a trend that was also observed in other field studies (DeLaune et al., 2012; Bordovsky et al., 1992).

Table 15. Comparison of estimated Irrigation water use efficiency (IWUE) values with reported IWUE values.

ET replacement %	Irrigation water use efficiency values estimated from DSSAT simulations (mean)(kg m^{-3})	Irrigation water use efficiency values reported in DeLaune et al., 2012 (mean) (kg m^{-3})
33	1.42	1.25
66	0.98	1.01
100	0.74	0.80
133	0.55	0.58

3.7 Model application

The calibrated model was used to determine suitable deficit irrigation strategies for the

TRP region for the weather conditions during the 2008 and 2012 period. Simulated average (2008-2010) seed cotton yield under different ET replacement strategies (0% to 133% ET replacement) for both conventional and conservation tillage scenarios followed a similar trend that was observed by DeLaune et al. (2012) in their field experiments (Figure 20). The maximum simulated yields were obtained for the 133% ET replacement under conventional tillage and for the 100% ET replacement scenario under conservational tillage. When the irrigation strategy was switched from 100% ET replacement to 133% ET replacement, the simulated seed cotton yield increased by 3.5% under conventional tillage and slightly decreased by 0.2% under conservational tillage (Figure 20). When the irrigation strategy was changed from 66% ET replacement to 100% ET replacement (a 31% increase in the amount of irrigation water applied), the simulated seed cotton yield increased by only 9.7% and 3.6% under conventional and conservation tillage practices, respectively.

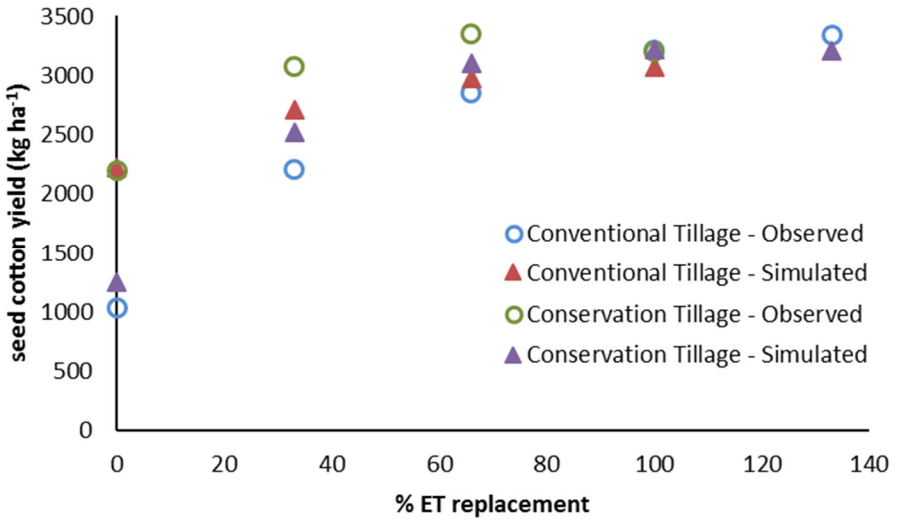

Figure 20. Seed cotton yields in response to deficit irrigation amounts using 2008-2010 irrigation and tillage management experiments.

In 2012, the CSM-CROPGRO-Cotton model simulated the maximum seed cotton yield of 5217 kg ha^{-1} with the 110% ET replacement scenario, and the simulated yield for the 100% ET replacement case was 4831 kg ha^{-1}. The crop yields started declining from 120% ET replacement scenario (Figure 21). For achieving a 6% increase in seed cotton yield, about 20% of additional irrigation water (100% ET replacement to 120% ET replacement) was therefore needed. Similarly, for achieving a 21% increase in seed cotton yield from the 70% ET replacement scenario to 100% ET replacement scenario, about 43% of additional irrigation water was needed (Figure 21). The yield productivity was therefore higher between the 70% ET replacement and the 100% ET replacement, when compared to the treatments with greater than 100% ET replacement.

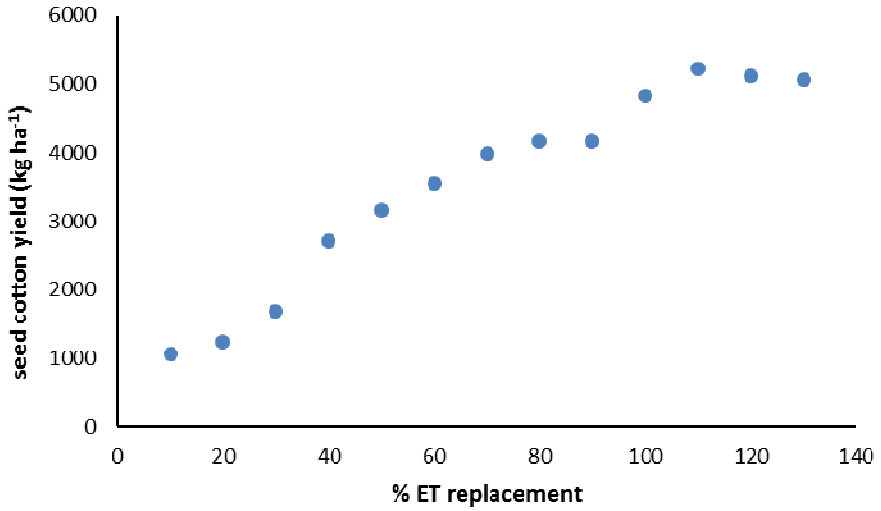

Figure 21. Seed cotton yields in response to deficit irrigation amounts using 2012 Cotton experiment.

From the above two simulated experiments, it can be noted that the relationship between seed cotton yield and various % ET replacements was very different among the years studied (Figures 20 and 21), mainly because of the differences in weather conditions. The weather conditions in the TRP region during the 2008-2010 period were normal (Table 4), but the year 2012 was substantially drier with a 16% decrease in rainfall and an increase in mean temperature by 1.85°C during the growing season as compared to 2008-2010. The results indicated that the application of any additional amount of irrigation water above the 100% ET replacement would not be advantageous under both normal and drier weather conditions. A substantial savings in irrigation water can be achieved without adversely impacting cotton yields in a normal year by adopting deficit (<100% ET

replacement) irrigation strategies. However, in a drier (less than normal rainfall) year, adoption of deficit irrigation strategies could substantially affect cotton yields and hence 100% ET replacement would be necessary to maintain crop yields (Figure 21). From figures 20 and 21 we can say that some of the allowed deficit will be removed at random times due to rainfall, lessening the impact of a deficit irrigation strategy on yield. However, there is a risk of increased yield loss in years where no rainfall occurs and producers should consider that risks when adopting deficit irrigation strategies. The simulated trends obtained in this study are comparable to the findings of Bronson et al. (2001) for the nearby Southern High Plains region, who reported that the optimum cotton yields under surface drip irrigation method could be achieved by adopting deficit irrigation strategies with 71% to 97% ET replacement.

3.8 Effects of future climate change on cotton yields at Chillicothe

On an average, the CSM-CROPGRO-Cotton model simulated a decrease in seed cotton yield ranging from 2.0% to 14.9% (Table 16) under future climate scenarios predicted by all three climate models when compared to the simulated historic average seed cotton yield. The reduction in seed cotton yield under the RCM3-GFDL model scenarios was the highest (14.9%) when compared to other two climate models (Table 16). The reduction in seed cotton yields under three future climate model simulated scenarios can be attributed to the combined effect of increase in both average annual minimum (2.2 to 2.5°C) and maximum temperature (2.3 to 2.7°C) as well as decrease in average annual rainfall (11.4 to 67 mm). The simulated minimum seed cotton yield under future climate projections ranged from 2163 kg/ha (RCM3-GFDL model) to 2866 kg/ha (RCM3-CGCM3 model),

and the simulated future maximum cotton yields ranged from 3699 kg/ha (CRCM-CCSM model) to 4070 kg/ha (RCM3-CGCM3 model), respectively (Table 16). On an average, simulated future seed cotton yield under the three climate model projections was reduced by 9.8% when compared to historic cotton yield.

Table 16. Comparison of CSM-CROPGRO-Cotton model simulated seed cotton yields under three climate model predicted historic and future climate scenarios.

Climate Models	RCM3-GFDL seed cotton yields (kg/ha)			RCM3-CGCM3 seed cotton yields (kg/ha)			CRCM-CCSM seed cotton yields (kg/ha)		
	Historic	Future	Decrease (%)	Historic	Future	Decrease (%)	Historic	Future	Decrease (%)
Minimum	3148	2163	31.2	3101	2866	7.6	3378	2621	22.4
Mean	3769	3207	14.9	3603	3530	2.0	3900	3341	14.3
Maximum	4255	3714	12.7	4462	4070	8.9	4398	3699	15.9

A separate analysis of average seed cotton yields for three 5-year (dry, normal and wet) periods under future climate scenarios showed that the simulated seed cotton yields in all three periods (dry, normal and wet) were higher under the RCM3-CGCM3 model projected future climate scenarios when compared to other two climate models (Figure 22). Under wet conditions, the simulated seed cotton yields were the highest under the RCM3-CGCM3 projected future climate scenario followed by the RCM3-GFDL model (Figure 22). Interestingly, higher yields were achieved in dry period under two RCM scenarios, mainly because of enabling the auto irrigation feature. The amount of irrigation water applied to achieve reasonable yields was substantially higher under dry conditions when compared to normal and wet periods (Table 17).

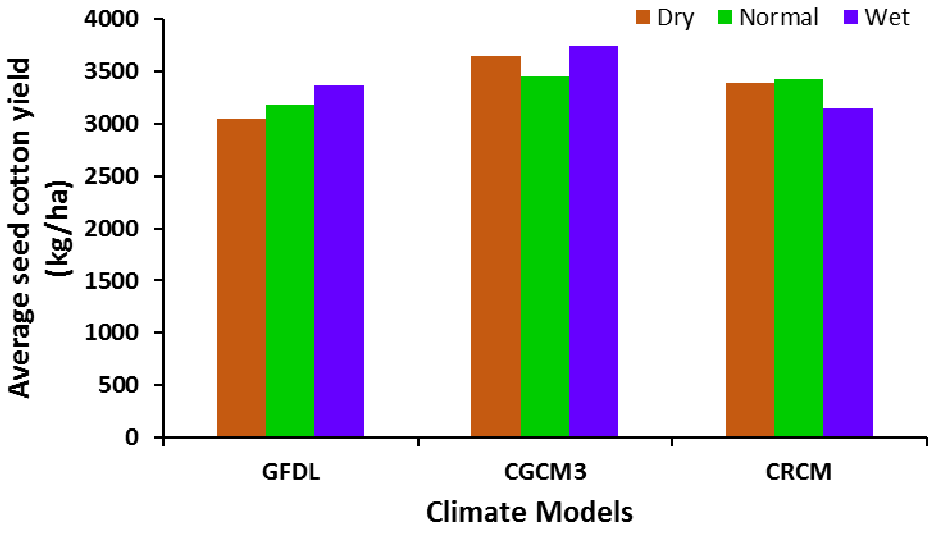

Figure 22. Comparison of simulated average seed cotton yield under dry, average and wet year periods as predicted by three climate models.

Table 17. Comparison of simulated average (2041-2070) seasonal irrigation water applied under dry, normal and wet periods.

	Dry period (mm)	Normal period (mm)	Wet period (mm)
RCM3-GFDL	369	243	132
RCM3-CGCM3	339	295	219
CRCM-CCSM	366	297	190

3.9 Climate change adaptation strategies

3.9.1 Changing planting date

CSM-CROPGRO-Cotton model simulations under A2 future climate scenario simulated by RCM3–GFDL showed an average (2041-2070) increase of 0.8%, 0.8% and 0.6% in

the seed cotton yield with the preponement of planting dates by 15, 10, and 5 days, respectively, with reference to the 2009 planting date of May 23 (Baseline scenario) (Figure 23, Table 18). Early planting of cotton in the future can therefore help to some extent to compensate for some of the potential yield losses that could occur due to increase in temperature (Figure 14-c and 15-c) and decrease in rainfall (Figure 10-c). A further analysis of the effects of changing planting date on cotton yield in dry, wet and normal years indicated interesting results (Table 18). In dry years, the predicted cotton yields increased by 8.0%, 8.4% and 11.9% (with reference to base line scenario) when planting was done early by 15, 10 and 5 days, respectively. In wet years, predicted cotton yields were increased between 2.8% and 5.3% (with reference to base line scenario) when planting date was preponed by 5 to 15%. The effect of changing planting date on cotton yield in normal years was inconsistent, however. These results need further assessment.

Table 18. Effect of planting date on seed cotton yield (with reference to simulated average (2041-2070) cotton yield under baseline scenario – planting date of May 23) in dry, normal and wet years (5-years each).

	Percent change in comparison to the baseline scenario (planting on May 23)		
	Planting 15 days early	Planting 10 days early	Planting 5 days early
Dry years	8.0	8.4	11.9
Normal years	1.0	-3.0	-6.0
Wet years	2.8	5.3	5.3
Average (2041-2070)	0.8	0.8	0.6

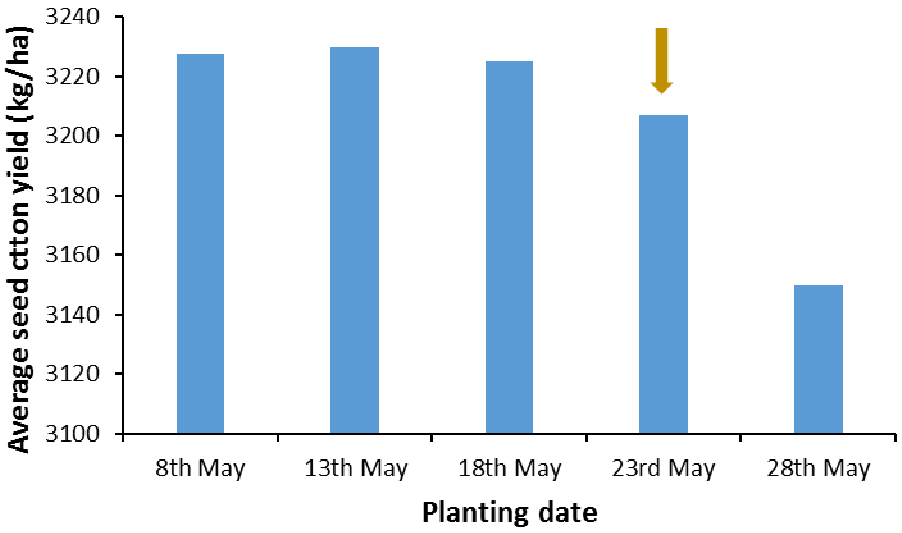

Figure 23. Effect of planting date on cotton lint yield under RCM3-GFDL (Regional Climate Model Version3–Geophysical Fluid Dynamics Laboratory) predicted A2 future climate scenario for the period 2041-2070. Analysis is conducted for Chillicothe (Hardeman County). Arrow represents the baseline scenario (planting date of May 23).

3.9.2 Adoption of no-tillage

The simulated seed cotton yields under no-till conditions and RCM3–GFDL projected future climate scenarios showed an average (2041-2070) increase of 0.4% in seed cotton yields (Table 19). Evapotranspiration by plants is expected to increase in the future due to predicted increase in temperatures (Figure 14-c and 15-c). Under no-till conditions, the water losses due to evapotranspiration are reduced, thus making more water available for the crop.

Table 19. Average simulated seed cotton yields under no-till and combined effect of no-till and early planting (the RCM3-GFDL (Regional Climate Model Version3– Geophysical Fluid Dynamics Laboratory) climate model predictions.

Management practice	Average simulated seed cotton yields (2041-2070) (kg/ha)	Percent increase from the base line scenario (%)
Conventional tillage (base line scenario)	3207	-
No-Till	3218	0.4
No-Till+ Early Planting (10days)	3240	1.1

A combination of both no-till and early planting gave slightly better results. The combined effect resulted in an average increase of 1.1% of seed cotton yields when compared to the average simulated yields under conventional tillage and planting date of May 23rd (Table 19).

3.10 Summary and conclusions

A well-calibrated CSM-CROPGRO-Cotton model was successfully established for Chillicothe in the TRP region after its extensive testing on two different experiments that were conducted during 2008 to 2012. The model predicted crop phenology stages, LAI (R^2 = 0.98), canopy height (R^2 = 0.97), and crop yield (% error= 1.0) adequately for the 100% ET replacement treatment during model calibration. The model responded well to the changes in the irrigation amounts during validation as indicated by a close match between the simulated and observed LAI, canopy height, and crop yields on three other (75% ET replacement, tensiometer-based and soil moisture based) irrigation scheduling treatments. The model was further evaluated on a three-year (2008-2010) tillage and

irrigation experiment, and the simulated seed cotton yields were within the acceptable error range (-24% to 13%), except for dry treatments (rainfed and 33% ET replacement). Overall, the evaluated CSM-CROPGRO-Cotton model demonstrated the potential to simulate cotton growth and development in the TRP region, and predicted seed cotton yields in response to different management practices and climatic conditions reasonably well.

The calibrated model was used to evaluate deficit irrigation strategies for this region. It was found that significant water savings could be achieved without severely affecting crop yields by adopting deficit irrigation strategies under normal weather conditions such as those during 2008 to 2010. However, during drier conditions such as in 2012, practicing deficit irrigation can significantly reduce crop yields. Even in a dry year, deficit will probably be an optimum strategy, especially if applied at critical growth stages.

The seed cotton yield predictions by CSM-CROPGRO-Cotton model over the future climate period (2041-2070) showed an average decline in the range of 2% (RCM3-CGCM3) to 14.9% (RCM3-GFDL). A combination of no-till and early planting date could potentially minimize the yield losses due to climate change by about 1.1% according to climate projections made by the RCM3-GFDL model.

CHAPTER IV

TEXAS PLAINS CLIMATE CHANGE INTERACTIVE GIS WEB APPLICATION: A GEOSPATIAL DECISION SUPPORT TOOL TO REACH WIDER USER BASE

4.1 Introduction

Multi-billion dollar decisions in several sectors are dependent on climate data predictions. Hence, it is essential to make climate predictions with minimal uncertainty and share them freely (Overpeck et al., 2011). Accessing, processing and understanding future climate change from current available sources is quite challenging. Previously, Global Climate Models (GCMs) predictions were used mostly by research scientists, but recently resource managers, policy makers, farmers, public health officials, etc. have begun increasingly seeking access to these climate datasets to make informed decisions and plan for potential climate change in the future (Overpeck et al., 2011). Climate scientists should make sure that their research findings are not only shared within their community, but also made available to the public, so that maximum benefits can be reaped (Overpeck et al., 2011). The recent developments in web based geospatial technology have made it possible to spatially and temporally view and share the climate datasets in usable formats. GIS technology provides tools to not only visualize the data, but also enable users to analyse the spatially explicit data (Takow et al., 2013).

One of the main objectives of this work was to enable users in the Texas Plains region a new way of interacting with the climate data, which were not available before. Previously, the data formats prevented all but domain experts from being able to visualize

or utilize the data. This meant that important climate data which can potentially impact billions of dollars was being underutilized. Most of the climate datasets were available in netcdf or raster grid formats. The development of netcdf tools that were compatible with GIS software has enabled users to view the climate data spatially. However, much of development in processing of the netcdf files in GIS has to be done before using the tools effectively. The existing statistical tools in MATLAB and R enabled users to extract and process the netcdf files in a more efficient manner than the tools available in GIS.

Until recently, the GCM climate predictions were provided at monthly temporal resolution over a spatial resolution of 200-250 km^2. At this coarser spatial resolution, it was difficult to capture the variability of climate change within a region (Wang et al., 2012, Hijmans et al., 2005). With the development of new statistical downscaling methods and weather generators, it became possible to downscale the GCM data to a smaller spatial resolution of 25-50 km^2 (Maurer et al., 2008). Several data sources that provide climate data in finer resolution grid formats such as PRISM (Daly et al., 2008) and WorldClim (Hijmans et al., 2005) already exist. These climate data sources have been traditionally utilized by the domain experts. In order to make this data easily accessible to a wider range of users, the data from these sources have to be converted to a meaningful scale and into a readily usable format (Wang et al., 2012). Some users who conduct research on ecology or hydrology require finer spatial resolution datasets, while others who perform research related to agricultural applications require datasets with increased temporal resolution. Even at 25-50 km^2 resolution, some systematic biases are

incorporated in to these datasets (Teutschbein et al., 2012), and this study presented an approach that minimizes bias in climate datasets (see Chapter 2).

This study addresses the need to provide a comprehensive historical climate data and future climate change projections at a scale suitable for the use of researchers, resource managers, and policy makers in the Texas Plains. The web application is also designed to provide projected cotton yields under future climate change scenarios. This work was built on existing climate datasets that were generated by the North American Regional Climate Change Assessment Program (NARCCAP) (Mearns et al., 2007; 2009). The overall goal of this research was to use geospatial tools and web technologies to develop an interactive online application that would provide easily accessible, bias-corrected, county-based, historic-and future-climate datasets predicted by the GCM's, and the projected cotton yields predicted by DSSAT-CROPGRO-Cotton model under future climate change scenarios. The specific objectives of this research were to: 1) design and develop the climate database and host it within a relational database management system (Microsoft SQL Server) to provide dynamic access to the data; and 2) develop an online interface and host the web service for public access.

This chapter is divided into two sections, which address the objectives 3 and 4. In order to incorporate the projected cotton yields into web-application, the regional productivity study has been conducted first to predict cotton yield for each county. In the first section, a methodology is proposed to generate the regional productivity analysis maps of cotton for the Texas Plains region and then to analyze the results. This methodology integrates Geographic Information System (GIS) with the CSM-

CROPGRO-Cotton model to expand the scope of site-specific simulations to a regional scale. GIS was also used to generate the regional productivity maps which are useful for regional planning. In the second section, methodology and technologies used to create the Texas Plains Climate Change (TPCC) web application are discussed.

4.2 Methodology

4.2.1 Regional cotton productivity analysis

All major cotton growing counties in the Texas Plains with at least 400 ha of cotton acreage were included in the regional productivity analysis. A total of 32 counties in the Texas Plains met the above criteria. In this analysis, each county was considered as a mapping unit. A GIS based distributed modeling approach was used to aggregate predictions from all mapping units to make regional predictions of cotton yields. Each mapping unit consisted of one or more NARCCAP climate grids. For the 32 counties included in the analysis, a total of 1920 DSSAT cotton projects ((32 counties * 30 historic years) + (32 counties * 30 future years)) were created. The bias-corrected, RCM3-GFDL model predicted historic (1971-2000) and future (2041-2070) climate data (precipitation, minimum and maximum temperature, and solar radiation) for the selected counties was input as weather data for the DSSAT cotton projects. The genotype and phenotype characteristics that were established for Chillicothe experimental site in the Texas Rolling Plains (Modala et al., 2014), were used in the regional productivity analysis.

The management practices (such as fertilizer application, cropping window, tillage practices, etc.) were assumed to be the same as those followed in Chillicothe experiments. Automatic irrigation method was used in the model. Whenever the soil water content was

below 50% of the available water (difference of field capacity and permanent wilting point soil moisture contents), irrigation was triggered until the available soil water content reached 85% level (deficit irrigation strategy). The soil properties in the selected TRP counties were assumed to be the same as those found at Chillicothe (Modala et al., 2014). Using the results of recent analysis of soil samples collected at Bushland and Halfway (Table 20a-b), soil input files were created for the selected counties in the THP region. The effects of spatial and temporal variability of climate and soil properties on crop yields across the two regions were analysed. The following assumptions were therefore made while conducting the regional productivity analysis:

- All of the selected counties were assumed to follow similar crop and fertilizer management practices for cotton production.
- There is no spatial variability in weather patterns within each mapping unit (selected county).
- Soil properties in nearby counties surrounding mapping units where soil samples were collected (Table 20), were assumed to be similar to those at the sampling sites.

Table 20. Soil composition and hydrological properties used in Regional Productivity Analysis

a. Analysis results of soil samples collected at Bushland in the Texas High Plains

Depth (cm)	SLCL (%)	SLSI (%)	SLOC (%)	SLHW	CEC (cmol kg^{-1})	SLNI (%)	LL (cm cm^{-1})	DUL (cm cm^{-1})	SSAT (cm cm^{-1})	SSKS (cm h^{-1})	SRGF
0-5	33	46	0.94	7.7	22.4	0.1	0.119	0.342	0.464	0.62	0.950
5-15	33	46	0.94	7.7	22.4	0.1	0.119	0.342	0.464	0.62	0.950
15-30	39	40	0.75	7.7	29.3	0.09	0.133	0.333	0.454	0.39	0.850
30-45	35	46	0.68	8.1	33.9	0.08	0.122	0.330	0.446	0.36	0.775
45-60	37	42	0.68	8.2	36.5	0.07	0.128	0.333	0.453	0.41	0.700
60-75	37	40	0.61	8.3	37.1	0.06	0.127	0.327	0.447	0.37	0.600
60-160	37	40	0.54	8.3	55.5	0.06	0.127	0.327	0.447	0.37	0.320

b. Analysis results of soil samples collected at Halfway in the Texas High Plains

Depth (cm)	SLCL (%)	SLSI (%)	SLOC (%)	SLHW	CEC (cmol kg^{-1})	SLNI (%)	LL (cm cm^{-1})	DUL (cm cm^{-1})	SSAT (cm cm^{-1})	SSKS (cm h^{-1})	SRGF
0-5	17	19	0.76	8.3	19.5	0.07	0.083	0.235	0.402	1.38	0.950
5-15	17	19	0.76	8.3	19.5	0.07	0.083	0.235	0.402	1.38	0.950
15-30	25	27	0.66	8.1	23.4	0.07	0.104	0.281	0.415	0.58	0.850
30-45	31	27	0.56	7.9	25.4	0.07	0.119	0.299	0.426	0.42	0.775
45-60	36	24	0.54	7.8	28.3	0.07	0.134	0.311	0.435	0.43	0.700
60-75	34	24	0.50	7.9	32.9	0.06	0.129	0.305	0.429	0.42	0.600
60-160	34	24	0.50	7.9	32.9	0.06	0.129	0.305	0.429	0.42	0.320

SLCL = clay content, SLSI = silt content, SLOC = organic carbon, SLHW = pH in water, CEC = cation exchange capacity, SLNI = Total nitrogen concentration, LL = lower limit, DUL = drained upper limit, SSAT = saturation, SBDM = bulk density, SSKS = saturated hydraulic conductivity, and SRGF = soil root growth factor.

For analysis purposes, the cotton yield simulation results have been divided into dry, normal and wet periods. The growing season (May - October) rainfall data was first arranged in ascending order and the top 5 years have been classified as “dry”, the middle five years as “normal” and the last five years as “wet” periods.

4.2.2 Development of the Texas Plains Climate Change web application

The first step in the creation of the TPCC web application was designing a database that included county polygon geographic information, county general information (e.g., population, area), and the county-wise bias-corrected climate datasets for all three RCMs. The entire database was hosted on a Microsoft SQL Server 2012 (Figure 24). The county polygon geographic information was extracted from Google fusion Tables. The polygon geographic information was converted to the required Well-Known Text (WKT) format for storing on the SQL server. The WKT format was defined by the Open Geospatial Consortium (OGC). A JavaScript Object Notation (JSON) page containing WKT, general information, and climate datasets for all three climate models was created for each county using JQuery as the scripting language to retrieve data and create the output visualizations. The data from the JSON page was used to generate the county polygons and HighChart graphs that overlay the Google map. The entire web service was hosted on Microsoft Internet Information System (IIS) (Figure 24). The page was designed using the Hypertext mark-up language (HTML5), cascading style sheets (CSS3) and Google Map API JavaScript.

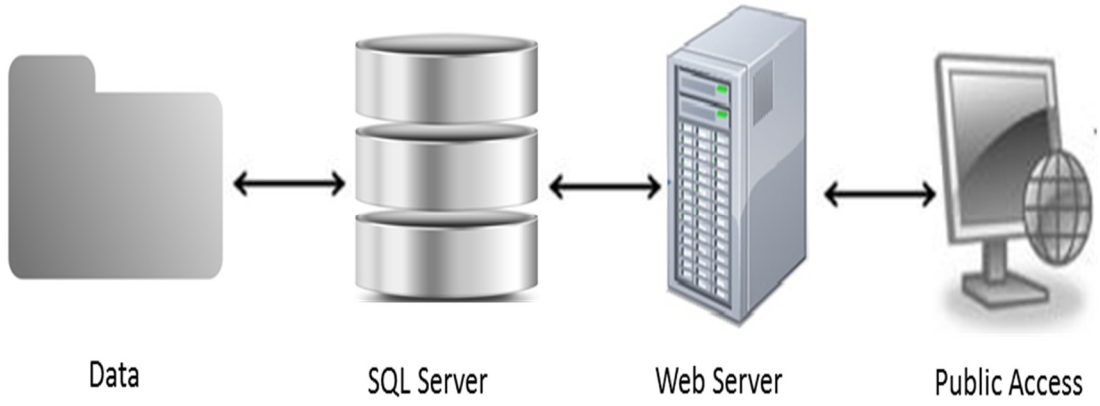

Figure 24. Diagrammatic representation of the architecture involved in creating the Texas Plains Climate Change (TPCC) web application.

4.3 Results and discussions

4.3.1 Regional productivity analysis

Under the RCM3-GFDL model projected future climate scenario, the CSM-CROPGRO-Cotton model simulated a decrease in seed cotton yield, ranging from 0.7% to 20.0% in many counties across the Texas Plains (Figure 25). The counties with the maximum reduction is seed cotton yields are located in the TRP region. This is due to the decrease in the rainfall (Figure 10-c from Climate Change Analysis in Chapter 2). According to the CSM-CROPGRO-Cotton model simulations, a slight increase in seed cotton yield (0.1% to 3.3%) was predicted in only five counties (Deaf Smith, Lamb, Briscoe, Crosby, and Dickens), which are located in the Southern High Plains.

In the TRP region, it was observed that the decrease in seed cotton yields in the counties located to the east (Foard, Wilbarger, Wichita, etc.) is more when compared to the counties located to the west (Hall, Childress, Taylor, etc.) (Figure 25). The percent decrease in rainfall (Figure 10-c from Climate Change Analysis) and percent increase in temperatures had substantial effect (Figure 14-c and Figure 15-c from Climate Change Analysis) on the reduction of seed cotton yields in this region. It has to be noted that same soil properties have been applied across the TRP region.

The cotton yield in the THP region increased under dry conditions; slightly decreased under normal conditions, and decreased further under wet conditions in the future as simulated by the CSM-CROPGRO-Cotton model (Figure 26). During the same period, the cotton yields in the TRP were predicted to be declined by up to 40% under dry conditions, and 20% under normal and wet conditions when compared to the historic simulations (Figure. 26).

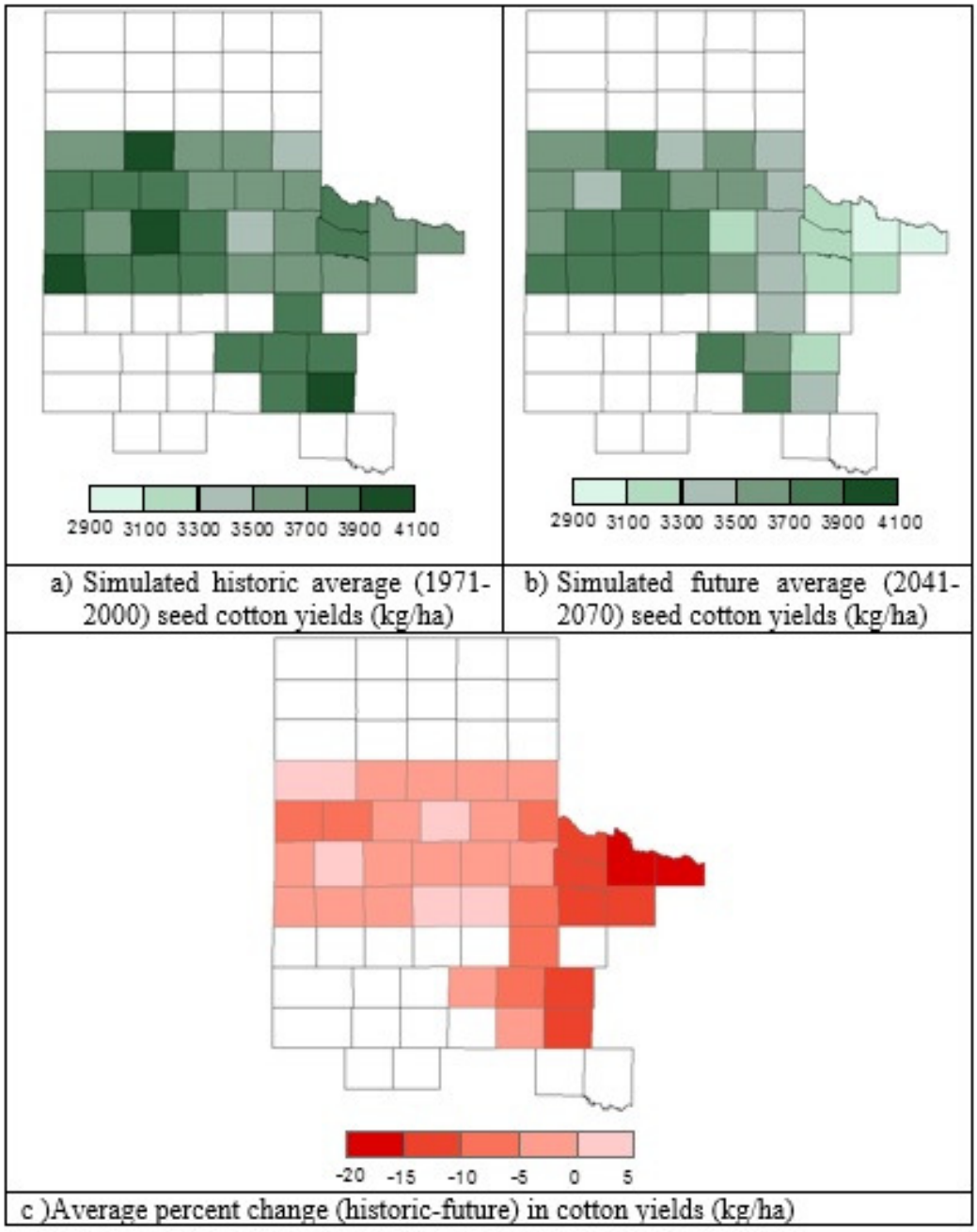

Figure 25. DSSAT-CROPGRO-Cotton model simulated seed cotton yields under historic and future climate scenarios projected by the RCM3-GFDL (Regional Climate Model Version3–Geophysical Fluid Dynamics Laboratory) climate model (Please note that this analysis was carried for only those counties that have more than 400 ha of cotton). Negative sign indicates decrease in cotton yields.

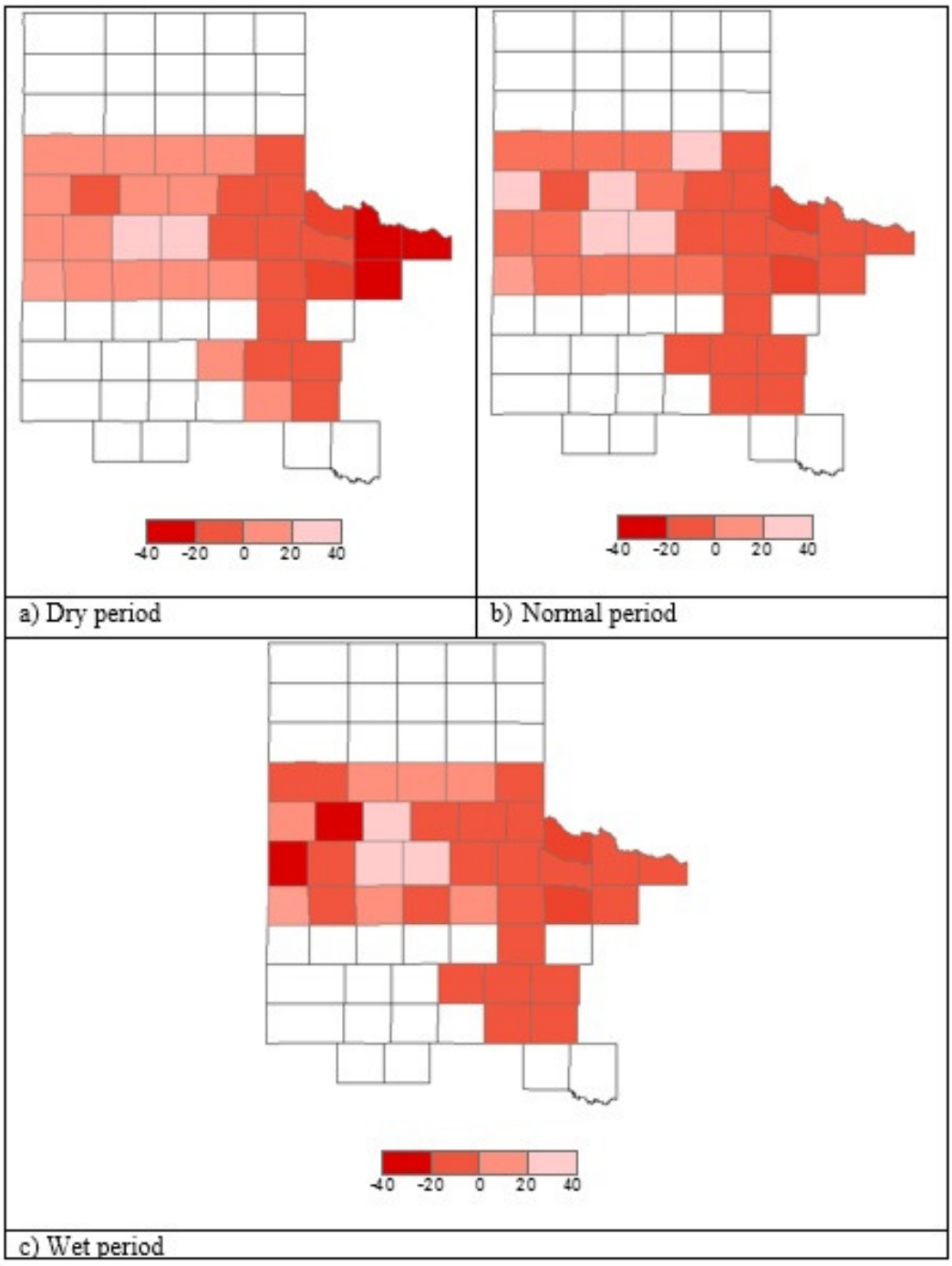

Figure 26. Maps showing spatial varibility of average percent change (historic-future) in cotton yields (kg/ha) under dry, normal and wet periods.

4.3.2 TPCC web application

After ensuring that the bias-corrected climate data matched reasonably well with the observed data, the bias-corrected climate datasets for each county were used in developing the database required for the TPCC web application. The TPCC interactive online web application was designed to provide the user with the ability to view temporal and spatial variability of historic and future climate change as predicted by three climate models across the Texas Plains region. Figure 27 shows the home page of the TPCC web application and the navigation bar from which users can select their choice of climate model by clicking on the CLIMATE MODELS tab. The ABOUT DATA tab provides the users with a brief description about the climate models, climate datasets and methodology employed in correcting the datasets and references. Users can request extractions of monthly and daily bias corrected climate datasets for all the three models. Users can access the mean monthly rainfall (Figure 28), mean monthly maximum temperature (Figure 29), and mean minimum temperature predicted by each climate model for each county. Users can also access the bias corrected ensemble average of mean temperature and rainfall predicted by the three climate models (Figure 30).

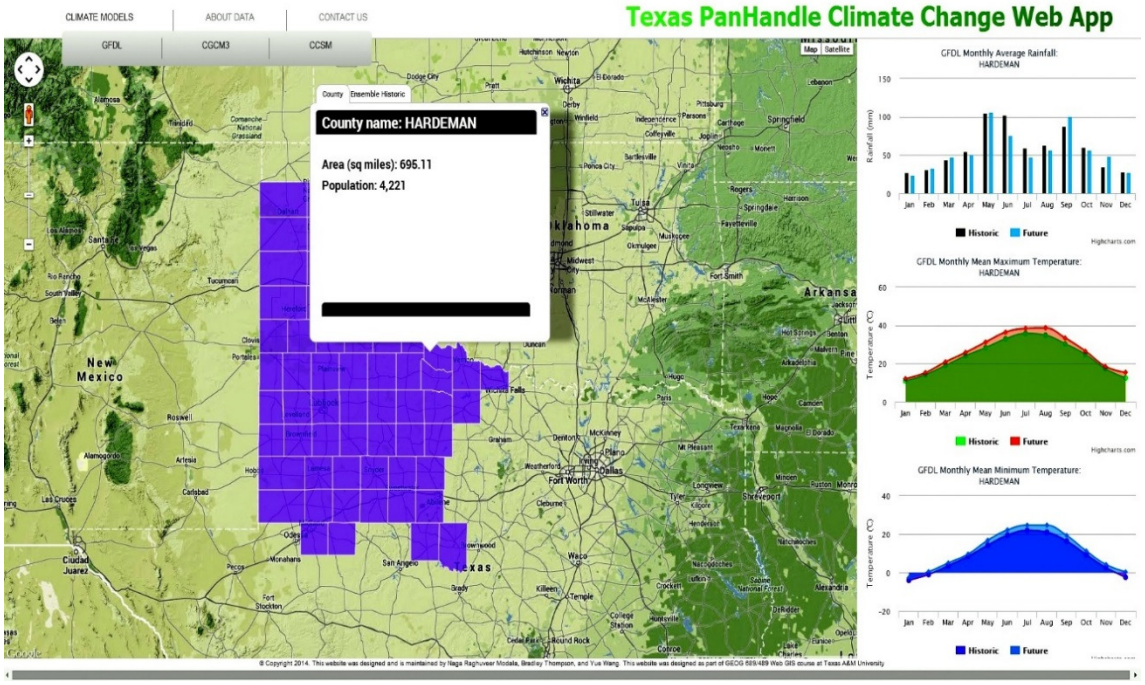

Figure 27. Homepage of the Texas Plains Climate Change (TPCC) web application displaying the RCM3-GFDL (Regional Climate Model Version3–Geophysical Fluid Dynamics Laboratory) climate predictions for Hardeman County, TX.

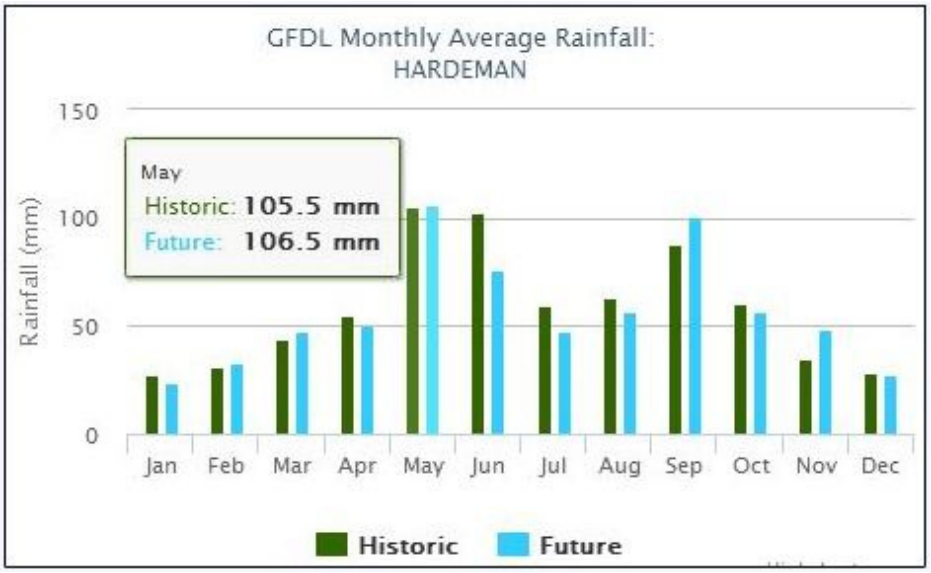

Figure 28. Comparison of bias corrected, RCM3-GFDL (Regional Climate Model Version3–Geophysical Fluid Dynamics Laboratory) predicted mean monthly historic and future rainfall for the Hardeman County, TX.

Figure 29. Comparison of bias corrected, RCM3-GFDL (Regional Climate Model Version3–Geophysical Fluid Dynamics Laboratory) predicted monthly mean historic and future maximum temperature for the Hardeman County, TX.

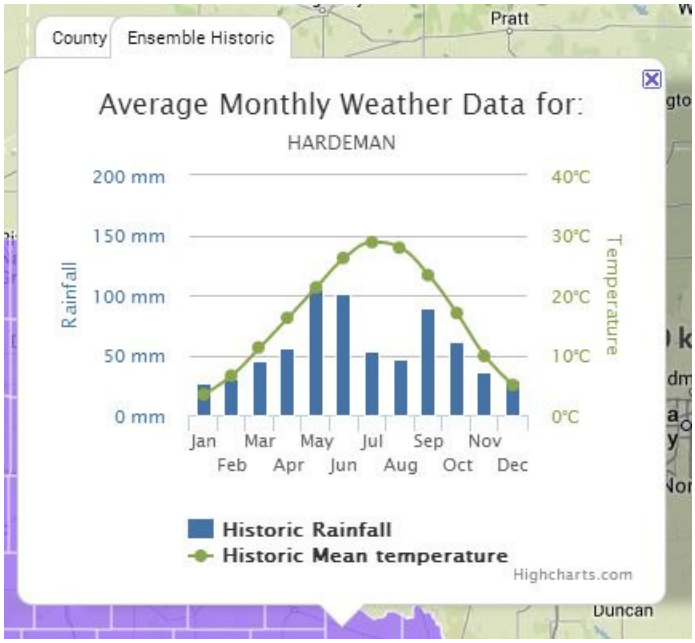

Figure 30. Ensemble average of historic rainfall and mean temperature for the Hardeman County, TX.

A feature called “Info Bubble” has been added to the TPCC webpage. When a user clicks on any county polygon, the info bubble will pop up with two different tabs (Figure 30): “County” and “Ensemble Historic”. The “County” tab (Figure 30) provides general information about the county such as geographic area, population, and the ”Ensemble Historic” tab (Figure 30) provides the ensemble averages of historic mean temperature and rainfall.

In the graphs located to the right of the webpage (Figure 27), the user is provided with the options to view only historic, only future, or both climate datasets by clicking the legend at the base of each chart. When a user hovers the mouse cursor on a marker in the chart, the month and the associated quantitative value (rainfall/temperature) pop up

(Figure 28, Figure 29). The default base map used in the application is a Google terrain map, but the users can also select a satellite base map if they wish. The use of Google Maps API and HighCharts is expected to enhance the users' experience as they are provided with additional tools to interact with the website, like built-in "zoom in" and "zoom out" functionality, and the ability to pan across the region.

The web-GIS based application developed in this study will expand the reach, utility, and the impact of the climate data by making it available in forms and formats that are familiar to a wide range of user groups in the region. There are several potential ways in which users can use this application tool in several sectors including agriculture, which is likely to be vulnerable to climate change. For example, Viticulture is an important agricultural activity in the region. Texas Plains is home to approximately 60 vineyards totalling 440 ha, and six wineries including the second-largest producer in the state, the Liano Estacado Winery (Hellman and Takow, 2011). Climate is one of the key controlling factors in grape and wine production as it affects the suitability of grape varieties to a particular region as well as the type and quality of the wine produced. Previous studies emphasized the importance of the availability of bias corrected climate variables for climate change analyses of wine grape suitability (Diffenbaugh and Scherer, 2013). The availability of future climate data can help develop and evaluate strategies for mitigating the effects of climate change so that consistent yields of particular wine varieties can be maintained under future climatic conditions. Another example of potential use of this application tool relates to production of cotton, which is a major crop in the Texas Plains region that could be at risk due to projected climate change. The cotton dependent

industries can access this readily available bias-corrected daily climate data for studying the impacts of future climate change on cotton production using crop growth models and be prepared for the future. Other potential key users include the policy makers who devise management strategies (e.g. 50/50 Management plan in the Southern High Plains for prolonging the availability of groundwater from the Ogallala aquifer) for projected climate change scenarios, and the stakeholders who adopt those management strategies.

4.4 Summary and conclusions

An interactive TPCC web application was developed to display and to provide access to the bias corrected historic and future rainfall and temperature data for 67 counties in the Texas High Plains and Rolling Plains regions as well as the predicted cotton yields for 32 counties. The datasets required for creating this web application were obtained from the NARCCAP website. The historic (1971-2000) and future (2041-2070) climate data predicted by three RCMs, namely RCM3-GFDL, RCM3-CGCM3, and CRCM-CCS were used in this application. However, these datasets contained systematic biases and hence Gamma and Gaussian distribution mapping techniques were effectively used for bias correcting the rainfall and temperature datasets, respectively.

The TPCC web application was developed using a combination of database, server, and web based geospatial technologies to store and access the data dynamically. Through the TPCC web application, users with a limited technical background can easily access bias corrected mean monthly rainfall, maximum temperature, minimum temperature predicted by each RCM and also an ensemble average of rainfall and mean temperature predicted by the three RCMs. Web based geospatial tools used for creation of

this online application enable the users to interact with the application effectively. In addition to viewing the spatio-temporal variation in climate data, users can request for the datasets for their own analysis and planning purposes. The TPCC web application was designed to meet the needs of a wide range of users in the Texas Plains. The application will eventually be expanded to include all counties in Texas and climate datasets from all of the 11 RCMs that are currently available on the NARCCAP website.

The regional productivity analysis study under RCM3-GFDL climate predictions showed a decline in cotton yields ranging from 0.7% to 20.0% across the cotton-growing counties in the Texas Plains. The crop modeling simulation results indicated that the counties located in the Texas Rolling Plains are expected to be affected the most.

CHAPTER V

SUMMARY AND CONCLUSIONS

5.1 Summary

Cotton is one of the major crops cultivated in the Texas Plains region (which includes the Texas High Plains and Rolling Plains) and it is a major contributor to the regional economy. Changing climate, declining groundwater levels, and regulatory restrictions on groundwater pumping are some of the serious challenges being faced by the cotton producers in the Texas Plains region. The overall goal of this research was to assess the impacts of climate change on cotton growth and yield in the Texas Plains region using the CROPGRO-Cotton Cropping System Model (CSM) within the Decision Support System for Agrotechnology Transfer (DSSAT; version 4.5), and to suggest climate change adaptation strategies.

As the first step, the future (2041-2070) and historic (1971-2000) climate data generated by three Regional Climate Models (RCMs), namely RCM3-GFDL, RCM3-CGCM3, and CRCM-CCSM, for the Texas Plains region was obtained from the North American Regional Climate Change Assessment Program (NARCCAP) and used in this study. Gamma and Gaussian distribution mapping techniques were employed for removing the bias associated with the downscaling of climate model projected rainfall and temperature (maximum and minimum) data, respectively. The spatial variability of projected climate change across the Texas Plains region was then assessed.

The CSM-CROPGRO-Cotton model was initially calibrated, validated and evaluated based on observed cotton yield and phenology data obtained from the cotton experiments conducted between the years 2008-2010 and 2012 at Chillicothe Research Station near Vernon in the Texas Rolling Plains. The calibrated model was first used to evaluate various deficit irrigation strategies for the Rolling Plains region. The calibrated model was later used to study the impacts of projected climate change on cotton growth and yield over the period from 2041 to 2070 at Chillicothe and across 32 cotton-growing counties in the Texas Plains. Early planting and no-till management strategies were evaluated as potential climate change adaptation strategies using the RCM3-GFDL predicted future climate data.

Using the Chillicothe-calibrated CSM-CROPGRO-Cotton model and GIS-based methods, regional productivity maps of cotton for the Texas Plains region were developed based on the assumptions of uniform crop and fertilizer management practices across the region, and spatial uniformity of climate variables within the county. An interactive TPCC web application was finally developed to display and to provide access to the bias corrected historic and future rainfall and temperature data for 67 counties in the Texas Plains region, and predicted cotton yields for 32 counties.

5.2 Conclusions

The following conclusions were drawn from this research:

1. The RCMs predicted a decrease in average annual rainfall in the range of 30 to 127 mm in the future (2041-2070) when compared to the historic period (1971-2000) across the Texas Plains region. The future (2041-2070) rainfall projections by the

RCM3-GFDL model indicated an overall decrease in the number of rainfall events by 6% to 10%, and an overall increase in the intensity of rainfall by about 3% to 8%.

2. The RCMs predicted an average increase in the maximum temperature in the range of 2.0 ºC to 3.2 ºC and an average increase in the minimum temperatures in the range of 1.9 ºC to 2.9 ºC in the future (2041-2070).
3. The CSM-CROPGRO-Cotton model demonstrated the potential to simulate the effects of various crop, tillage and irrigation management strategies on cotton production in the Texas Plains, and also to assess the effects of future climate change on cotton yields.
4. The CSM-CROPGRO-Cotton model simulated crop phenology stages, LAI (R^2 = 0.98), canopy height (R^2 = 0.97), and crop yield (% error= 1.0) accurately during the model calibration. The model predictions of LAI, canopy height, and crop yield during model validation and evaluation have also matched closely with observed data, except under dry conditions (0% ET replacement and 33% ET replacement).
5. Under normal rainfall conditions, the simulated percentage reduction in seed cotton yield was marginal (3.5 to 8.8%) when the amount of irrigation water applied was decreased from 100% to 66% ET replacement. A significant water savings could therefore be achieved without severely affecting crop yields by adopting deficit irrigation strategies under normal weather conditions.
6. Under drier conditions, percent decrease in seed cotton yield was substantial (about 21.2%) when irrigation strategy was switched from 100% to 70% ET replacement.

Adopting deficit irrigation strategies during drier conditions could substantially reduce crop yields.

7. Under the future climate scenarios predicted by three RCMs, a decline in seed cotton yield ranging from 2% to 14.9% was predicted at Chillicothe. A combination of no-till practice and early planting of cotton can potentially minimize the yield losses due to climate change to some extent.
8. Majority of the counties in the Texas Plains showed a decline in average seed cotton yield (2% to 20%) under RCM3-GFDL predicted future climate scenarios, with the counties in the Texas Rolling Plains being the most affected.
9. The Texas Plains Climate Change (TPCC) web application was successfully developed and it demonstrated the potential of using web-based geo-spatial technology for effectively displaying and sharing the results of high end scientific research to a wide range of users.

REFERENCES

Adams, R. M., Hurd, B. H., Lenhart, S., & Leary, N. (1998). Effects of global climate change on agriculture: an interpretative review. *Climate Research,* 11(1), 19-30.

Adams, R.M., Rosenzweig, C., Peart, R. M., Ritchie, J. T., McCarl, B. A., Glyer, J. D., Curry, R. B., Jones, J. W., Boote, K. J., & Allen, L. H. (1990). Global climate change and US agriculture. *Nature,* 345, 219-224.

Adusumilli, N. C., Rister, M. E., & Lacewell, R. D. (2011). Estimation of irrigation water demand: A case study for the Texas High Plains. In *Selected Paper presented at the Southern Agricultural Economics Association Annual Meeting*, Corpus Christi, Texas.

Allen Jr, L. H., Boote, K. J., Jones, J.W., Jones, P. H., Valle, R. R., Acock, B., & Dahlman, R. C. (1987). Response of vegetation to rising carbon dioxide: Photosynthesis, biomass, and seed yield of soybean. *Global Biogeochemical Cycles*. 1(1), 1-14.

Allen, R. G., Pereira, L. S., Raes, D., & Smith, M. (1998). Crop evapotranspiration-Guidelines for computing crop water requirements-FAO Irrigation and drainage paper 56. FAO, Rome, 300, 6541.

Allen, V. G., Brown, C. P., Segarra, E., Green, C. J., Wheeler, T. A., Acosta-Martinez, V., & Zobeck, T. M. (2008). In search of sustainable agricultural systems for the Llano Estacado of the U.S. Southern High Plains. *Agriculture, Ecosystems and Environment*, 124(1), 3-12.

Boote, K., & Pickering, N. (1994). Modeling photosynthesis of row crop canopies. *HortScience: A Publication of the American Society for Horticultural Science (USA),* 29(12), 1423-1434.

Bronson, K., Onken, A., Keeling, J., Booker, J., & Torbert, H. (2001). Nitrogen response in cotton as affected by tillage system and irrigation level. *Soil Science Society of America Journal*, 65(4), 1153-1163

Caya, D., Laprise, R., Giguère, M., Bergeron, G., Blanchet, J.P., Stocks, B. J., Boer, G. J., & Mcfarlane, N.A. (1995). Description of the Canadian regional climate model. *Boreal Forests and Global Change*, Springer Netherlands, 477-482.

Cayan, D. R., Maurer, E. P., Dettinger, M. D., Tyree, M., & Hayhoe, K. (2008). Climate change scenarios for the California region. *Climatic Change*, *87*(1), 21-42.

Chang, H. H., Zhou, J., & Fuentes, M. (2010). Impact of climate change on ambient ozone level and mortality in South-eastern United States. *International Journal of Environmental Research and Public Health*, 7(7), 2866-2880.

Chaudhuri, S., & Ale, S. (2014a). Long-term (1930-2010) Trends in Groundwater Levels in Texas: Influences of Soils, Landcover and Water Use. *Science of the Total Environment,* 490, 379-390.

Chaudhuri, S., & Ale, S. (2014b). Lon-term (1960-2010) trends in groundwater contamination and salinization in the Ogallala aquifer in Texas, USA. *Journal of Hydrology,* 513, 376-390.

Colaizzi, P. D., Gowda, P. H., Marek, T. H., & Porter, D. O. (2009). Irrigation in the Texas High Plains: A brief history and potential reductions in demand. *Irrigation and Drainage,* 58(3), 257-74.

Colette, A.W., & Almas, L. K. (2005). Comparing production optimization strategies for Texas panhandle producers in response to declining water availability due to decline in the Ogallala Aquifer. *In 2005 Southern Agricultural Economics Association Annual Meeting*, 35601, Little Rock, Arkansas.

Collins, W. D., Bitz, C. M., Blackmon, M. L., Bonan, G. B., Bretherton, C. S., Carton, J. A., & Smith, R. D. (2006). The Community Climate System Model version 3 (CCSM3). *Journal of Climate*, 19(11).

Cramér, H. (1999). *Mathematical methods of statistics*, 9, Princeton University press.

Cure, J. D., & Acock, B. (1986). Crop responses to carbon dioxide doubling: a literature survey. *Agricultural and Forest Meteorology*, 38, 127-145.

Daly, M. Halbleib, Smith, J. I., Gibson, W. P., Doggett, M. K., Taylor, G. H., & Curtis, J. (2008). Physiographically sensitive mapping of temperature and precipitation across the conterminous United States. *International Journal of Climatology*, 28(15), 2031-2064.

DeLaune, P., Sij, J., Park, S., & Krutz, L. (2012). Cotton production as affected by irrigation level and transitioning tillage systems. *Agronomy Journal,* 104(4), 991-995.

Delworth, T. (2006). GFDL's CM2 global coupled climate models. Part I: Formulation and simulation characteristics. *Journal of Climate*, 19(5).

Diffenbaugh, N. S., & Scherer, M. (2013). Using climate impacts indicators to evaluate climate model ensembles: Temperature suitability of premium wine grape cultivation in the United States. *Climate dynamics*, 40(3-4), 709-729.

Flato, G. M. (2005). The third generation coupled global climate model (CGCM3). *Available on-line at http://www. cccma.bc.ec.gc.ca/models/cgcm3.Shtml* [Accessed 3 March 2014].

Garcia y Garcia, A., Persson, T., Paz, J. O., Fraisse, C., & Hoogenboom, G. (2010). ENSO-based climate variability affects water use efficiency of rainfed cotton grown in the southeastern USA. *Agriculture, Ecosystems & Environment,* 139(4), 629-635.

Gérardeaux, E., Sultan, B., Palaï, O., Guiziou, C., Oettli, P., & Naudin, K. (2013). Positive effect of climate change on cotton in 2050 by CO2 enrichment and conservation agriculture in Cameroon. *Agronomy for Sustainable Development,* 33(3), 485-495.

Guerra, L., Garcia y Garcia, A., Hook, J., Harrison, K., Thomas, D., Stooksbury, D., & Hoogenboom, G. (2007). Irrigation water use estimates based on crop simulation models and kriging. *Agricultural Water Management,* 89(3), 199-207.

Hatfield, J. L., Boote, K. J., Kimball, B. A., Ziska, L. H., Izaurralde, R. C., Ort, D., & Wolfe, D. (2011). Climate impacts on agriculture: Implications for crop production. *Agronomy Journal*, 103(2), 351-370.

Hayhoe, K., Cayan, D., Field, C. B., Frumhoff, P. C., Maurer, E. P., Miller, N. L., & Verville, J. H. (2004). Emissions pathways, climate change, and impacts on California. *Proceedings of the National Academy of Sciences of the United States of America*, 101(34), 12422-12427.

Hellman, E. W., Takow, E. A., Tchakerian, M. D., & Coulson, R. N. (2011). Geographic Information System Characterization of Four Appellations in West Texas, USA. *Geoscience Canada*, 38(1).

High Plains Underground Water Conservation District No 1, 10- Year Amended Management Plan 2011-2021, 2010. *Available on-line at http://www.hpwd.com/rules-and-management-plan/district-management-plan* [Accessed 12 May 2014].

Hijmans, R. J., Cameron, s. E., Parra, j. L., Jones, P. G., & Jarvis, A. (2005). Very high resolution interpolated climate surfaces for global land areas. *International Journal of Climatology,* 25, 1965-1978.

Hoogenboom, G., J.W. Jones, C.H. Porter, P.W. Wilkens, K.J. Boote, L.A. Hunt, & G.Y.Tsuji (Ed's). (2010). Decision Support System for Agrotechnology Transfer Version 4.5. Volume 1: Overview. University of Hawaii, Honolulu, HI.

Hoogenboom, G., Jones, J. W., Wilkens, P. W., Porter, C. H., Boote, K. J., Hunt, L. A., Singh, U., Lizaso, J. L., White, J. W., Uryasev, O., Royce, F. S., Ogoshi, R., Gijsman, A. J., Tsuji, G. Y., & Koo, J. 2012. Decision Support System for Agrotechnology Transfer (DSSAT) Version 4.5 [CD-ROM]. University of Hawaii, Honolulu, HI.

Howell, T. A. 2003. Irrigation efficiency. In: Stewart, B. A., and Howell, T. A. editors, Encyclopedia of water science. Marcel Dekker, New York. p. 467–472. *Available on-line at http://thinktech.lib.ttu.edu.libezproxy.tamu.edu:2048/ttuir/bitstream/handle/2346/1685/Regional%20Economic%20Impact.pdf?sequence=1* [Accessed on 9th April 2012].

Hunt, L. A., White, J. W., & Hoogenboom, G. (2001). Agronomic data: advances in documentation and protocols for exchange and use. *Agricultural Systems*, 70(2), 477-492.

IBSNAT, International Benchmark Sites Network for Agrotechnology Transfer Project, (1989). Decision Support System for Agrotechnology Transfer Version 21. (DSSAT V2.1), Dept. Agronomy and Soil Sci.; College of Trop. Agric. And Human Resources; University of Hawaii, Honolulu, HI 96822.

Ines, A. V., & Hansen, J. W. (2006). Bias correction of daily GCM rainfall for crop simulation studies. *Agricultural and forest meteorology*, 138(1), 44-53.

IPCC-SRES, Intergovernmental panel on Climate Change- Special Report on Emission Scenarios. (2000). *Available on-line at: http://www.ipcc.ch/pdf/special-reports/spm/sres-en.pdf.*

Jensen, R. (2004). Ogallala Aquifer: Using improved irrigation technology and water conservation to meet future needs. Texas Water Resource Institute. *Available on-line at: http://twri.tamu.edu/newsletters/texaswaterresources/twr-v28n2.pdf* [Accessed 23 February 2012].

Johnson, J. W., Johnson, P. N., Guerrero, B., Weinheimer, J., Amosson, S., Almas, L., Golden, B., & Wheeler-Cook, E. (2011). Groundwater policy research: collaboration with groundwater conservation districts in Texas. *Journal of Agricultural and Applied Economics,* 43(3), 345-356.

Jones, J. W., Hoogenboom, G., Porter, C. H., Boote, K. J., Batchelor, W. D., Hunt, L., & Ritchie, J. T. (2003). The DSSAT cropping system model. *European Journal of Agronomy,* 18(3), 235-265.

Karl, T. R., Melillo, J. M., & Peterson, T. C. (Ed.). (2009). *Global climate change impacts in the United States*. Cambridge University Press, New York.

Kimball, B. A. (1982). Carbon dioxide and agricultural yield: an assemblage on analysis of 430 prior observations. *Agronomy Journal*, 75(5), 779-788.

Lafon, T., Dadson, S., Buys, G., & Prudhomme, C. (2013). Bias correction of daily precipitation simulated by a regional climate model: a comparison of methods. *International Journal of Climatology*, 33(6), 1367-1381.

Lal, H., Hoogenboom, G., Calixte, J. P., Jones, J. W., & Beinroth, F. H. (1993). Using crop simulation models and GIS for regional productivity analysis. *Transactions-American Society of Agricultural Engineers,* 36, 175-175.

Legates, D. R., & McCabe, G. J. (1999). Evaluating the use of "goodness-of-fit" measures in hydrologic and hydroclimatic model validation, *Water Resources Research,* 35(1), 233–241.

Li, H., Sheffield, J., & Wood, E. F. (2010). Bias correction of monthly precipitation and temperature fields from Intergovernmental Panel on Climate Change AR4 models using equidistant quantile matching. *Journal of Geophysical Research: Atmospheres (1984–2012)*, 115(D10).

Mailhot, A., Beauregard, I., Talbot, G., Caya, D., & Biner, S. (2012). Future changes in intense precipitation over Canada assessed from multi-model NARCCAP ensemble simulations. *International Journal of Climatology*, 32(8), 1151-1163.

Maurer, E.P., Adam, J.C., & Wood, A. W. (2008). Climate model based consensus on the hydrologic impacts of climate change to the Rio Lempa basin of Central America. *Hydrology and Earth System Sciences Discussions*, 5(6).

Mearns, L. O., Gutowski, W., Jones, R., Leung, R., McGinnis, S., Nunes, A., & Qian, Y. (2009). A regional climate change assessment program for North America. *Eos, Transactions American Geophysical Union*, 90(36), 311-311.

Mearns, L.O., McGinnis, S., Arritt, R., Biner, S., Duffy, P., Gutowski, W., & Zoellick, C. (2007). The North American Regional Climate Change Assessment Program dataset, *National Center for Atmospheric Research Earth System Grid data portal*, Boulder, CO. Data downloaded 2013-02-21.

Modala, N. R., Ale, S., Rajan, N., Munster, C., DeLaune, P. B., Thorp, K. R., Nair, S., and Barnes, E. (2014). Evaluation of DSSAT-CROPGRO-Cotton model for the Texas Rolling Plains region and simulation of strategies for increasing water and nutrient use efficiency. *Transactions of the ASABE.* (In Review)

Morison, J. I. L. (1993). Response of plants to CO_2 under water limited conditions. Vegetatio, 104(1), 193-209.

Musick, J. T., Pringle, F. B., & Walker, J. D. (1988). Sprinkler and furrow irrigation trends-Texas high plains. *Applied Engineering in Agriculture,* 4(1), 46-52.

Nakicenvoic et al. (2000). Special Report on Emissions Scenarios. A Special Report of Working Group III of the Intergovernmental Panel on Climate Change. Cambridge University Press: Cambridge, 599 pp.

Nielsen-Gammon, J. (2011). The changing climate of Texas. *The impact of global warming on Texas.* University of Texas Press, Austin, 39-68.

Nieswiadomy, M. (1985). The demand for irrigation water in the high plains of Texas, 1957-80. *American Journal of Agricultural Economics,* 67(3), 619-626.

Ortiz, B., Hoogenboom, G., Vellidis, G., Boote, K., Davis, R., & Perry, C. (2009). Adapting the CROPGRO-cotton model to simulate cotton biomass and yield under southern root-knot nematode parasitism. *Transactions of the ASABE,* 52(6), 2129-2140.

Overpeck, J. T., Meehl, G. A., Bony, S., & Easterling, D. R. (2011). Climate data challenges in the 21st century. *Science (Washington)*, 331(6018), 700-702.

Pathak, T., Fraisse, C., Jones, J., Messina, C., & Hoogenboom, G. (2007). Use of global sensitivity analysis for CROPGRO cotton model development. *Transactions of the ASABE,* 50(6), 2295-2302.

Pathak, T. B., Jones, J. W., Fraisse, C. W., Wright, D., & Hoogenboom, G. (2012). Uncertainty analysis and parameter estimation for the CSM-CROPGRO-cotton model. *Agronomy Journal,* 104(5), 1363-1373.

Paz, J. O., Woli, P., Garcia y Garcia, A., & Hoogenboom, G. (2012). Cotton yields as influenced by ENSO at different planting dates and spatial aggregation levels. *Agricultural Systems*, 111, 45-52.

Piani, C., Haerter, J. O., & Coppola, E. (2010). Statistical bias correction for daily precipitation in regional climate models over Europe. *Theoretical and Applied Climatology*, 99(1-2), 187-192.

Porter, D., T. Marek, T. Howell & L. New. (2005). The Texas High Plains Evapotranspiration Network (TXHPET) User Manual. TAMU-TAES, Amarillo Agricultural Research and Extension Center, Amarillo, TX, Publication AREC 05-37.

Priestley, C. H. B., & Taylor, R, J. (1972). On the assessment of surface heat flux and evaporation using large-scale parameters. *Monthly Weather Review,* 100(2), 81-92.

Pryor, S. C., & Barthelmie, R. J. (2013). Assessing the vulnerability of wind energy to climate change and extreme events. *Climatic change*, 121(1), 79-91.

Rajan, N., Maas, S. J., & Kathilankal, J. C. (2010). Estimating crop water use of cotton in the Southern High Plains. *Agronomy Journal,* 102(4), 1641-1651.

Rajan, N., Maas, S. J., & Cui, S. (2013). Extreme drought effects on carbon dynamics of a

semi-arid pasture. *Agronomy Journal*, 105(6), 1749-1760.

Rajan, N., Ale, S., & DeLaune, P. B. (2013). Demonstrating tools for improving on farm irrigation efficiency. Texas Water Development Board. Retrieved from http://www.twdb.state.tx.us/publications/reports/contracted_reports/doc/1103581253.pdf.

Ritchie, J. T. (1981). Water dynamics in the soil-plant-atmosphere system. *Plant and Soil,* 58(1), 81-96.

Ritchie, J., & Otter, S. (1985). Description and performance of CERES-wheat: A user-oriented wheat yield model. *ARS-United States Department of Agriculture, Agricultural Research Service (USA).*

Ritchie, J. T. (1998). Soil water balance and plant water stress. pp. 41-54 in G. Y. Tsuji et al. (Ed.) *Understanding Options for Agricultural Production*, Kluwer Academic Publishers, Great Britian.

Sage, F. R. (1995). Was low atmospheric CO_2 during the Pleistocene a limiting factor for the origin of agriculture? Global Change Biology, 1(2), 93-106.

Schaap, M. G., Leij, F. J., & van Genuchten, M. T. (2001). Rosetta: A computer program for estimating soil hydraulic parameters with hierarchical pedotransfer functions. *Journal of Hydrology,* 251(3), 163-176.

Segarra, E., & Feng, Y. (1994). Irrigation technology adoption in the Texas High Plains. *Texas Journal of Agricultural Natural Resources*, 7(1), 71-83.

Solomon, S. (Ed.). (2007). Climate change 2007-the physical science basis: Working group I contribution to the fourth assessment report of the IPCC (Vol. 4). Cambridge University Press.

Stewart, B. A. (2003). Aquifers, Ogallala. *Encyclopedia of Water Science*, 43-44.

Takle, E. S., Jha, M., Lu, E., Arritt, R. W., & Gutowski, W. J. (2010). Stream flow in the upper Mississippi river basin as simulated by SWAT driven by 20th Century contemporary results of global climate models and NARCCAP regional climate models. *Meteorologische Zeitschrift*, 19(4), 341-346.

Takow, E. A., Hellman, E. W., Birt, A. G., Tchakerian, M. D., & Coulson, R. N. (2013). A Web-based geographic information system application for description of American Viticultural Areas in Texas. *HortTechnology*, 23(2), 165-172.

Tans, P., & Keeling, R. (2011). National Oceanic and Atmospheric Administration/Earth System Research Laboratory. *Available on-line at: ftp://ftp.cmdl.noaa.gov/ccg/co2/*

trends/co2_annmean_mlo.txt.

Teutschbein, C., & Seibert, J. (2010). Regional climate models for hydrological impact studies at the catchment scale: a review of recent modeling strategies. *Geography Compass*, 4(7), 834-860.

Teutschbein, C., & Seibert, J. (2012). Bias correction of regional climate model simulations for hydrological climate-change impact studies: Review and evaluation of different methods. *Journal of Hydrology*, 456, 12-29.

Texas Alliance for water conservation annual report. (2008). *Available on-line at: http://www.depts.ttu.edu/tawc/documents/TAWC_annualreport_2008.pdf*.

Texas Water Development Board. (2007). Water for Texas, pp. 2, 392.

Thom, H. C. S. (1952). Seasonal degree-day statistics for the United States 1. *Monthly Weather Review*, 80(9), 143-147.

Thom, H. C. S. (1958). A note on the gamma distribution. *Monthly Weather Review*, 86(4), 117-122.

Thorp, K., Ale, S., Bange, M., Barnes, E., Hoogenboom, G., Lascano, R., & Rajan, N. (2014). Development and application of process-based simulation models for cotton production: A review of past, present, and future directions. *Journal of Cotton Science,* 18, 10-47.

Tsuji, G. Y., du Toit, A., Jintrawet, A., Jones, J., Bowen, W. T., Ogoshi, R. M., & Uehara, G. (2002). Benefits of models in research and decision support: The IBSNAT experience. *Agricultural System Models in Field Research and Technology Transfer,* 71-89.

USDA 2007 Census of Agriculture for Texas state and county data report. 2009. U.S. Department of Agriculture 1(43A). *Available on-line at: http://www.agcensus.*usda.gov/ Publications/2007/Full_Report/Volume_1,_Chapter_1_State_Level/Texas/txv1a.pdf.

USDA-NASS. (2013). Crop production. 1936-3737. Washington D.C.: USDA National Agricultural Statistics Service. *Retrieved from http://www.nass.usda.gov/Publications/ Todays_Reports/reports/crop1213.pdf.*

USDA-NASS. (2014). Texas cotton production. PR-123-14. Washington D.C.: USDA National Agricultural Statistics Service. *Retrieved from http://www.nass.usda.gov/ Statistics_by_State/Texas/Publications/pr12314.pdf.*

USDA-SCS. (1972). *National Engineering Handbook,* Section 4. Washington, D.C: USDA Soil Conservation Service.

Wang, T., Hamann, A., Spittlehouse, D. L., & Murdock, T. Q. (2012). Climate WNA-High-resolution spatial climate data for Western North America. *Journal of Applied Meteorology & Climatology*, 51(1).

Webb, W. P. (1931). The Great Plains. Ginn and Co., New York, NY.

Weeks, J. B., Gutentag, E. (1984). The High Plains regional aquifer—geohydrology. In: Whetstone (Ed.), Proceedings of the Ogallala Aquifer Symposium II. Water Resources Center. Texas Tech University, Lubbock, Texas.

Weeks, J. B., Sun, R. J., (1986). High plains regional aquifer study, in: Sun, R. J. (Ed.), Regional Aquifer-System Analysis Program of the U.S. Geological Survey of Projects, 1978–1984. U.S. Geological Survey Circular 1002. U.S. Government Printing Office, Washington DC.

Wilby, R. L., & Wigley, T. M. L. (2002). Future changes in the distribution of daily precipitation totals across North America. Geophysical Research Letters, 29(7), 39-1.

Williams, J., Hanks, J., & Ritchie, J. (1991). Runoff and water erosion. *Modeling Plant and Soil Systems,* 439-455.

Willmott, C. J. (1981). On the validation of models. *Physical Geography,* 2(2), 184-194.

Wood, A. W., Leung, L. R., Sridhar, V., & Lettenmaier, D. P. (2004). Hydrologic implications of dynamical and statistical approaches to downscaling climate model outputs. *Climatic change*, 62(1-3), 189-216.

Yates, J., J. Smith, and J. Pate. (2010). Regional economic impact of irrigated versus dryland agriculture in the Texas High Plains. *Available online at: http://thinktech.lib.ttu.edu.libzproxy.tamu.edu:2048/ttuir/bitstream/handle/2346/1685/Regional%20Economic%20Impact.pdf?sequence=1* [Accessed on 9th April 2012].

Yang,Y., Wilson, L. T., & Wang, J. (2010). Development of an automated climatic data scraping, filtering and display system. *Computers and Electronics in Agriculture*, 71(1), 77-87.

Zamora, D. S., Jose, S., Jones, J. W., & Cropper Jr, W. P. (2009). Modeling cotton production response to shading in a pecan alley cropping system using CROPGRO. *Agroforestry Systems,* 76(2), 423-435.

APPENDIX I

MATLAB PROGRAM CREATED FOR BIAS CORRECTION OF RAINFALL DATA

```
function [xval] =GFDL_Precp_indexing(x)
current_dir=pwd;
combined_dir=[current_dir '\Combined_data\'];
cd(combined_dir);
data1 = xlsread(x);
cd ..;
current_dir=pwd;
final_dir=[current_dir '\Final_output\'];
if ~isdir(final_dir)
    mkdir(final_dir)
end
outfile=[final_dir x(1:length(x)-5) '_final_future.xlsx'];
outfile_2=[final_dir x(1:length(x)-5) '_final_historic.xlsx'];
outfile_mean=[final_dir x(1:length(x)-5) '_monthlymean.xlsx'];
outfile_stats_fut=[final_dir x(1:length(x)-5) '_stats_future.xlsx'];
outfile_stats_hist=[final_dir x(1:length(x)-5) '_stats_historic.xlsx'];

%%%%%%%%%%%%%%%%%%%%%%%%%%%%%%%%%%%%%%%%%%%%%%%%%%%%%%%%%%%%%%%%
%%%%%%%%%%%
count=1;
for i=1:length(data1)-1
    data(count,:)=data1(i,:);
    %     if((rem(data1(i,3),4)==0) && (data1(i,1)==2) && (data1(i,2)==28))
    %         count=count+1;
    %         data(count,:)=(data1(i,:)+data1(i+1,:))/2;
    %         data(count,1)=2;
    %         data(count,2)=29;
    %     end
    count=count+1;
end

d=isnan(data);
data(d)=0;
mySize = size(data);
nmonths = 12;
col1=6;
col2=9;
col3=15;
precp_obsdata=cell(1,nmonths);
precp_simdata=cell(1,nmonths);
precp_simcorrecteddata=data(:,col2);
precp_simcorrectedthresholddata=data(:,col2);
precp_simoriginaldata=data(:,col2);
precp_simindexdata=cell(1,nmonths);
temp_arr=[];

precp_futureoriginaldata = data(:,col3);
```

```
precp_futurecorrecteddata = data(:,col3);
precp_futurecorrectedthresholddata=data(:,col3);
precp_futuredata=cell(1,nmonths);
precp_futureindexdata=cell(1,nmonths);
%%%%%%%%%%%%To count the number of events in each month %%%%%%%%%%%%%%
for j=1:nmonths
   for i = 1 : mySize(1,1)
      if(data(i,1) == j && data(i,col1)>0)
         temp_arr  = [temp_arr ;data(i,col1)];
      end
   end
   precp_obsdata{1,j}=temp_arr;
   temp_arr=[];
end
%%%%%%%%%%%%%%%%%%%%%%%%%%%%%%%%%%%%%%%%%%%%%%%%%%%%%%%%%%%%
%%%%%%%%%%%%%%%%%
%%%%%%%%%%% To find the thresholds of each month %%%%%%%%%%%%%%%%%%%%%
for j=1:nmonths
   thresh=0.01;
   count2=0;
   count2prev=length(precp_obsdata{1,j});
   while(1)
      for i = 1 : mySize(1,1)
         if(data(i,1) == j && data(i,col2)>thresh)
            count2 = count2+1;
         end
      end
      if(count2==length(precp_obsdata{1,j}))
         threshold(j)=thresh;
         break;
      elseif( (count2prev > length(precp_obsdata{1,j})) && (count2 < length(precp_obsdata{1,j})))
         disp(['Countprev is ', num2str(count2prev), ' and required is ',num2str(length(precp_obsdata{1,j})),
...
            ' count is ',num2str(count2),' for month ',num2str(j), ' from file ' , x ])
         %           error('Couldnt find equal number of events. Increase resolution');
         threshold(j)=thresh;
         break;
      else
         count2prev=count2;
         count2=0;
         thresh=thresh+0.0001;
      end
   end
end
%%%%%%%%%%%%%%%%%%%%%%%%%%%%%%%%%%%%%%%%%%%%%%%%%%%%%%%%%%%%
%%%%%%%%%%%%%%%%%

%%%%%%%%%%%%%Indexing of
data%%%%%%%%%%%%%%%%%%%%%%%%%%%%%%%
temp_arr=[];temp_arr2=[];
indexdata_arr=[];
indexfuturedata=[];
```

```
for j=1:nmonths
   for i = 1 : mySize(1,1)
      if(data(i,1) == j && data(i,col2)>threshold(j))
         temp_arr =[temp_arr ; data(i,col2)];
         indexdata_arr=[indexdata_arr ; i];
      end
      if(data(i,1) == j && data(i,col2)<=threshold(j))
         precp_simcorrectedthresholddata(i)=0;
      end

      if(data(i,1) == j && data(i,col3)>threshold(j))
         temp_arr2 =[temp_arr2 ; data(i,col3)];
         indexfuturedata=[indexfuturedata ; i];
      end
      if(data(i,1) == j && data(i,col3)<=threshold(j))
         precp_futurecorrectedthresholddata(i)=0;
      end
   end
   precp_simdata{1,j}=temp_arr;
   precp_simindexdata{1,j}=indexdata_arr;
   temp_arr=[];
   indexdata_arr=[];

   precp_futuredata{1,j}=temp_arr2;
   precp_futureindexdata{1,j}=indexfuturedata;
   temp_arr2=[];
   indexfuturedata=[];
end
%%%%%%%%%%%%%%%%%%%%%%%%%%%%%%%%%%%%%%%%%%%%%%%%%%%%%%%%%%%%
%%%%%%%%%%
precp_simoriginalthresholddata=precp_simcorrectedthresholddata;
precp_futureoriginalthresholddata=precp_futurecorrectedthresholddata;

precp_obs=cell(1,nmonths);
phat_obs=cell(1,nmonths);
y_obs=cell(1,nmonths);

precp_sim=cell(1,nmonths);
precp_simindex=cell(1,nmonths);
phat_sim=cell(1,nmonths);
y_sim=cell(1,nmonths);
corrected_data=cell(1,nmonths);

precp_future=cell(1,nmonths);
precp_futureindex=cell(1,nmonths);
phat_future=cell(1,nmonths);
y_future=cell(1,nmonths);
future_corrected_data=cell(1,nmonths);

for j=1:nmonths
   precp_obs{1,j}=sort(precp_obsdata{1,j});
```

```
    phat_obs{1,j} = gamfit(precp_obs{1,j});
    y_obs{1,j}=gamcdf (precp_obs{1,j},phat_obs{1,j}(1),phat_obs{1,j}(2));
    subplot(4,3,j);
    plot(precp_obs{1,j},y_obs{1,j},'--bo','MarkerSize',2)
    xlabel('Daily Precipitation (mm/d)');
    ylabel('Cummulative Probability');
    title(j);
    hold on;

    [precp_sim{1,j}, precp_simindex{1,j}]=sort(precp_simdata{1,j});
    phat_sim{1,j} = gamfit(precp_sim{1,j});
    y_sim{1,j}=gamcdf (precp_sim{1,j},phat_sim{1,j}(1),phat_sim{1,j}(2));
    plot(precp_sim{1,j},y_sim{1,j},'-.r*','MarkerSize',2);
    legend('Obs','Sim',4);
    legend boxoff
    outfigfile1=[final_dir x(1:length(x)-5) '_precipcdf_fig.jpg'];
    saveas(gcf,outfigfile1);

    [precp_future{1,j}, precp_futureindex{1,j}]=sort(precp_futuredata{1,j});
    phat_future{1,j} = gamfit(precp_future{1,j});
    y_future{1,j}=gamcdf (precp_future{1,j},phat_future{1,j}(1),phat_future{1,j}(2));
end
figure;
simdata1=[];
futuredata1=[];
for j=1:nmonths
    corrected_data{1,j} = gaminv(y_sim{1,j},phat_obs{1,j}(1),phat_obs{1,j}(2));
    future_corrected_data{1,j} = ...

gaminv(y_future{1,j},(phat_future{1,j}(1)*(phat_obs{1,j}(1)/phat_sim{1,j}(1))),(phat_future{1,j}(2)*(ph
at_obs{1,j}(2)/phat_sim{1,j}(2))));
    %       subplot(4,3,j);
    %       plot(corrected_data{1,j},future_corrected_data{1,j},'.');
    %       xlabel('Bias Corrected Precipitation (mm/d)');
    %       ylabel('Future Corrected Precipitation (mm/d)');
    %       title(j);
    %       outfigfile2=[final_dir x(1:length(x)-5) '_precipcorrected_fig.jpg'];
    %       saveas(gcf,outfigfile2);
    simdata1=[simdata1 sum(corrected_data{1,j})/30];
    futuredata1=[futuredata1 sum(future_corrected_data{1,j})/30];

end
% xlswrite(outfile_mean, {'Month';}, 'Sheet1', 'A1')
% xlswrite(outfile_mean, data(:,1), 'Sheet1', 'A2')
xlswrite(outfile_mean, {'Bias corrected monthly mean historic values';}, 'Sheet1', 'B1')
xlswrite(outfile_mean, simdata1, 'Sheet1', 'B2')
xlswrite(outfile_mean, {'Bias corrected monthly mean future values';}, 'Sheet1', 'C1')
xlswrite(outfile_mean, futuredata1, 'Sheet1', 'B3')
plot(simdata1,'--bo','LineWidth',2)
hold on;
plot(futuredata1,'--ro','LineWidth',2)
ylim([0 160])
```

```
xlim([1 12])
xlabel('Months');
ylabel('Mean Monthly Precipitation (mm)');
legend('1971-2000','2041-2070',4);
hold off;
outfigfile=[final_dir x(1:length(x)-5) '_precip_fig.jpg'];
saveas(gcf,outfigfile);

%%%%%%%%%%%Replacing the data in the original order %%%%%%%%%%%%%%%
for j=1:nmonths
   for k =1:length(corrected_data{1,j})
      precp_simcorrecteddata(precp_simindexdata{1,j}(precp_simindex{1,j}(k)))=corrected_data{1,j}(k);

precp_simcorrectedthresholddata(precp_simindexdata{1,j}(precp_simindex{1,j}(k)))=corrected_data{1,j}
(k);
   end
   for k =1:length(future_corrected_data{1,j})

precp_futurecorrecteddata(precp_futureindexdata{1,j}(precp_futureindex{1,j}(k)))=future_corrected_data
{1,j}(k);

precp_futurecorrectedthresholddata(precp_futureindexdata{1,j}(precp_futureindex{1,j}(k)))=future_corre
cted_data{1,j}(k);
   end
end
% phat_corr=cell(1,nmonths);
% y_corr=cell(1,nmonths);
% for j=1:nmonths
%     phat_corr{1,j} = gamfit(corrected_data{1,j});
%     y_corr{1,j}=gamcdf (corrected_data{1,j},phat_corr{1,j}(1),phat_corr{1,j}(2));
% end
%
% temp=[];
% for j=1:nmonths
%     temp= [temp; phat_obs{1,j} phat_sim{1,j} phat_corr{1,j}];
% end
% xlswrite(outfile, {'simoriginaldata','simcorrecteddata';}, 'Sheet1', 'L1')
% xlswrite(outfile, precp_simoriginaldata, 'Sheet1', 'L2')
% xlswrite(outfile, precp_simcorrecteddata, 'Sheet1', 'M2')
temp1=[];
temp2=[];
Precp_min_fut=[];
Precp_max_fut=[];
Precp_mean_fut=[];
Precp_median_fut=[];
for abc=1:mySize(1,1)-1
   current_year=data(abc,12);
   current_month=data(abc,10);
   next_year=data(abc+1,12);
   next_month=data(abc+1,10);
   if ((current_year == next_year) && (current_month == next_month))
      temp1 = [temp1 precp_futurecorrectedthresholddata(abc,1)];
```

```
      if(abc == (mySize(1,1)-1))
         temp1 = [temp1 precp_futurecorrectedthresholddata(abc+1,1)];
      end
   else
      temp2=temp1(find(temp1));
      if isempty(temp2)
         Precp_min_fut=[Precp_min_fut; 0];
      else
         Precp_min_fut=[Precp_min_fut; min(temp2)];
      end
      Precp_max_fut=[Precp_max_fut; max(temp1)];
      Precp_mean_fut=[Precp_mean_fut; mean(temp2)];
      Precp_median_fut=[Precp_median_fut; median(temp2)];
      temp1=[];
   end
end

temp1=[];
temp2=[];
Precp_min_hist=[];
Precp_max_hist=[];
Precp_mean_hist=[];
Precp_median_hist=[];
for abc=1:mySize(1,1)-1
   current_year=data(abc,3);
   current_month=data(abc,1);
   next_year=data(abc+1,3);
   next_month=data(abc+1,1);
   if ((current_year == next_year) && (current_month == next_month))
      temp1 = [temp1 precp_simcorrectedthresholddata(abc,1)];
      if(abc == (mySize(1,1)-1))
         temp1 = [temp1 precp_simcorrectedthresholddata(abc+1,1)];
      end
   else
      temp2=temp1(find(temp1));
      if isempty(temp2)
         Precp_min_hist=[Precp_min_hist; 0];
      else
         Precp_min_hist=[Precp_min_hist; min(temp2)];
      end
      Precp_max_hist=[Precp_max_hist; max(temp1)];
      Precp_mean_hist=[Precp_mean_hist; mean(temp2)];
      Precp_median_hist=[Precp_median_hist; median(temp2)];
      temp1=[];
   end
end

xlswrite(outfile, {'Precipfuturecorrecteddata(mm)';}, 'Sheet1', 'D1')
%xlswrite(outfile, precp_futureoriginaldata, 'Sheet1', 'N2')
xlswrite(outfile, precp_futurecorrectedthresholddata, 'Sheet1', 'D2')
%xlswrite(outfile, precp_futurecorrectedthresholddata, 'Sheet1', 'G2')
```

```
xlswrite(outfile_2, {'PrecipHistoriccorrecteddata(mm)';}, 'Sheet1', 'D1')
xlswrite(outfile_2, precp_simcorrectedthresholddata, 'Sheet1', 'D2')

xlswrite(outfile_stats_fut, {'Precp_Min','Precp_Max','Precp_Mean','Precp_Median';}, 'Sheet1', 'C1')
xlswrite(outfile_stats_fut, Precp_min_fut, 'Sheet1', 'C2')
xlswrite(outfile_stats_fut, Precp_max_fut, 'Sheet1', 'D2')
xlswrite(outfile_stats_fut, Precp_mean_fut, 'Sheet1', 'E2')
xlswrite(outfile_stats_fut, Precp_median_fut, 'Sheet1', 'F2')

xlswrite(outfile_stats_hist, {'Precp_Min','Precp_Max','Precp_Mean','Precp_Median';}, 'Sheet1', 'C1')
xlswrite(outfile_stats_hist, Precp_min_hist, 'Sheet1', 'C2')
xlswrite(outfile_stats_hist, Precp_max_hist, 'Sheet1', 'D2')
xlswrite(outfile_stats_hist, Precp_mean_hist, 'Sheet1', 'E2')
xlswrite(outfile_stats_hist, Precp_median_hist, 'Sheet1', 'F2')

%%%%%%%%%%%%%%%%%%%%%%%%%%%%%%%%%%%%%%%%%%%%%%%%%%%%%%%%
%%%%%%%%%%%%

xval = 0;
```

MATLAB PROGRAM FOR BIAS CORRECTION OF TEMPERATURE (MINIMUM AND MAXIMUM)

```
function [xval] =GFDL_Temp_indexing(x)
current_dir=pwd;
combined_dir=[current_dir '\Combined_data\'];
cd(combined_dir);
data1 = xlsread(x);
count=1;
cd ..;
current_dir=pwd;
final_dir=[current_dir '\Final_output\'];
if ~isdir(final_dir)
   mkdir(final_dir)
end
outfile=[final_dir x(1:length(x)-5) '_final_future.xlsx'];
outfile_2=[final_dir x(1:length(x)-5) '_final_historic.xlsx'];
outfile_mean=[final_dir x(1:length(x)-5) '_monthlymean.xlsx'];
outfile_stats_fut=[final_dir x(1:length(x)-5) '_stats_future.xlsx'];
outfile_stats_hist=[final_dir x(1:length(x)-5) '_stats_historic.xlsx'];

for i=1:length(data1)-1
   data(count,:)=data1(i,:);
   %    if((rem(data1(i,3),4)==0) && (data1(i,1)==2) && (data1(i,2)==28))
   %       count=count+1;
   %       data(count,:)=(data1(i,:)+data1(i+1,:))/2;
   %       data(count,1)=2;
   %       data(count,2)=29;
   %    end
   count=count+1;
```

```
end
d=isnan(data);
data(d)=0;
mySize = size(data);
nmonths = 12;
%%%%%%%%%%%%%%****************************************%%%%%%%
%%%%%%%%%%
col1=7;                    %%%%%%%%%%Historic Max
col2=13;                    %%%%%%%%%%Future Max
maxtemp_obsdata=cell(1,nmonths);
maxtemp_simdata=cell(1,nmonths);
maxtemp_simoriginaldata=data(:,col1);
maxtemp_simcorrecteddata=data(:,col1);
maxtemp_simindexdata=cell(1,nmonths);
temp_arr=[];
maxtemp_futureoriginaldata = data(:,col2);
maxtemp_futurecorrecteddata = data(:,col2);
maxtemp_futuredata=cell(1,nmonths);
maxtemp_futureindexdata=cell(1,nmonths);
for j=1:nmonths
    for i = 1 : mySize(1,1)
        if(data(i,1) == j)
            temp_arr  = [temp_arr ;data(i,4)];  %%%%%%%%%%Observed Max
        end
    end
    maxtemp_obsdata{1,j}=temp_arr;
    temp_arr=[];
end
%%%%%%%%%%%%Indexing of
data%%%%%%%%%%%%%%%%%%%%%%%%%%
temp_arr=[];temp_arr2=[];
indexdata_arr=[];
indexfuturedata=[];
for j=1:nmonths
    for i = 1 : mySize(1,1)
        if(data(i,1) == j)
            temp_arr =[temp_arr ; data(i,col1)];
            indexdata_arr=[indexdata_arr ; i];
        end
        if(data(i,1) == j)
            temp_arr2 =[temp_arr2 ; data(i,col2)];
            indexfuturedata=[indexfuturedata ; i];
        end
    end
    maxtemp_simdata{1,j}=temp_arr;
    maxtemp_simindexdata{1,j}=indexdata_arr;
    temp_arr=[];
    indexdata_arr=[];

    maxtemp_futuredata{1,j}=temp_arr2;
    maxtemp_futureindexdata{1,j}=indexfuturedata;
    temp_arr2=[];
```

```
    indexfuturedata=[];
end
%%%%%%%%%%%%%%%%%%%%%%%%%%%%%%%%%%%%%%%%%%%%%%%%%%%%%%%%%
%%%%%%%%%%%
maxtemp_obs=cell(1,nmonths);
mu_obs=cell(1,nmonths);
sigma_obs=cell(1,nmonths);
y_obs=cell(1,nmonths);

maxtemp_sim=cell(1,nmonths);
mu_sim=cell(1,nmonths);
sigma_sim=cell(1,nmonths);
y_sim=cell(1,nmonths);
corrected_data=cell(1,nmonths);
maxtemp_simindex=cell(1,nmonths);

maxtemp_future=cell(1,nmonths);
mu_future=cell(1,nmonths);
sigma_future=cell(1,nmonths);
y_future=cell(1,nmonths);
future_corrected_data=cell(1,nmonths);
maxtemp_futureindex=cell(1,nmonths);

for j=1:nmonths
    maxtemp_obs{1,j}=sort(maxtemp_obsdata{1,j});
    [mu_obs{1,j},sigma_obs{i,j}] = normfit(maxtemp_obs{1,j});
    y_obs{1,j}=normcdf (maxtemp_obs{1,j},mu_obs{1,j},sigma_obs{i,j});
    %     subplot(4,3,j);
    %     plot(maxtemp_obs{1,j},y_obs{1,j},'-b')
    %     xlabel('Daily Max Temperature (C)');
    %     ylabel('Cummulative Probability');
    %     title(j);
    %     hold on;
    [maxtemp_sim{1,j}, maxtemp_simindex{1,j}]=sort(maxtemp_simdata{1,j});
    maxtemp_sim{1,j}=sort(maxtemp_simdata{1,j});
    [mu_sim{1,j},sigma_sim{i,j}] = normfit(maxtemp_sim{1,j});
    y_sim{1,j}=normcdf (maxtemp_sim{1,j},mu_sim{1,j},sigma_sim{i,j});
    %     plot(maxtemp_sim{1,j},y_sim{1,j},'-r');
    %     legend('Obs','Sim',4);
    %     legend boxoff
    [maxtemp_future{1,j}, maxtemp_futureindex{1,j}]=sort(maxtemp_futuredata{1,j});
    maxtemp_future{1,j}=sort(maxtemp_futuredata{1,j});
    [mu_future{1,j},sigma_future{i,j}] = normfit(maxtemp_future{1,j});
    y_future{1,j}=normcdf (maxtemp_future{1,j},mu_future{1,j},sigma_future{i,j});
end

simdata1=[];
futuredata1=[];
for j=1:nmonths
    corrected_data{1,j} = norminv(y_sim{1,j},mu_obs{1,j},sigma_obs{i,j});
    future_corrected_data{1,j} = ...
```

```
      norminv(y_future{1,j},mu_future{1,j}+(mu_obs{1,j}-
mu_sim{1,j}),sigma_future{i,j}*(sigma_obs{i,j}/sigma_sim{i,j}));
   %        subplot(4,3,j);
   %        plot(corrected_data{1,j},'b');
   %        hold on;
   %        plot(future_corrected_data{1,j},'r');
   %        title(j);
   simdata1=[simdata1 mean(corrected_data{1,j})];
   futuredata1=[futuredata1 mean(future_corrected_data{1,j})];
end
%xlswrite(outfile_mean, {'Bias corrected monthly mean historic values';}, 'Sheet1', 'B1')
xlswrite(outfile_mean, simdata1, 'Sheet1', 'B5')
%xlswrite(outfile_mean, {'Bias corrected monthly mean future values';}, 'Sheet1', 'C1')
xlswrite(outfile_mean, futuredata1, 'Sheet1', 'B6')
figure;
plot(simdata1,'--bo','LineWidth',2)
hold on;
plot(futuredata1,'--ro','LineWidth',2)
xlim([1 12])
xlabel('Months');
ylabel('GFDL Mean Max Temperature (C)');
legend('1971-2000','2041-2070',4);
outfigfile=[final_dir x(1:length(x)-5) '_MaxTemp_fig.jpg'];
saveas(gcf,outfigfile);
mu_corr=cell(1,nmonths);
sigma_corr=cell(1,nmonths);
y_corr=cell(1,nmonths);
%%%%%%%%%%%%Replacing the data in the original order %%%%%%%%%%%%%%%
for j=1:nmonths
   for k =1:length(corrected_data{1,j})

maxtemp_simcorrecteddata(maxtemp_simindexdata{1,j}(maxtemp_simindex{1,j}(k)))=corrected_data{1,
j}(k);
   end
   for k =1:length(future_corrected_data{1,j})

maxtemp_futurecorrecteddata(maxtemp_futureindexdata{1,j}(maxtemp_futureindex{1,j}(k)))=future_cor
rected_data{1,j}(k);
   end
end


% for j=1:nmonths
%    [mu_corr{1,j},sigma_corr{1,j}] = normfit(corrected_data{1,j});
%    y_corr{1,j}=norminv (corrected_data{1,j},mu_corr{1,j},sigma_corr{1,j});
% end
%
% temp=[];
% for j=1:nmonths
%    temp= [temp;mu_obs{1,j} sigma_obs{i,j} mu_sim{1,j} sigma_sim{i,j} mu_corr{1,j}
sigma_corr{1,j} ];
% end
temp1=[];
```

```
month_fut=[];
year_fut=[];
Maxtemp_min_fut=[];
Maxtemp_max_fut=[];
Maxtemp_mean_fut=[];
Maxtemp_median_fut=[];
for abc=1:mySize(1,1)-1
   current_year=data(abc,12);
   current_month=data(abc,10);
   next_year=data(abc+1,12);
   next_month=data(abc+1,10);
   if ((current_year == next_year) && (current_month == next_month))
      temp1 = [temp1 maxtemp_futurecorrecteddata(abc,1)];
      if(abc == (mySize(1,1)-1))
         temp1 = [temp1 maxtemp_futurecorrecteddata(abc+1,1)];
      end
   else
      month_fut=[month_fut; current_month ];
      year_fut=[year_fut; current_year];
      Maxtemp_min_fut=[Maxtemp_min_fut; min(temp1)];
      Maxtemp_max_fut=[Maxtemp_max_fut; max(temp1)];
      Maxtemp_mean_fut=[Maxtemp_mean_fut; mean(temp1)];
      Maxtemp_median_fut=[Maxtemp_median_fut; median(temp1)];
      temp1=[];
   end
end

temp1=[];
month_hist=[];
year_hist=[];
Maxtemp_min_hist=[];
Maxtemp_max_hist=[];
Maxtemp_mean_hist=[];
Maxtemp_median_hist=[];
for abc=1:mySize(1,1)-1
   current_year=data(abc,3);
   current_month=data(abc,1);
   next_year=data(abc+1,3);
   next_month=data(abc+1,1);
   if ((current_year == next_year) && (current_month == next_month))
      temp1 = [temp1 maxtemp_simcorrecteddata(abc,1)];
      if(abc == (mySize(1,1)-1))
         temp1 = [temp1 maxtemp_simcorrecteddata(abc+1,1)];
      end
   else
      month_hist=[month_hist; current_month ];
      year_hist=[year_hist; current_year];
      Maxtemp_min_hist=[Maxtemp_min_hist; min(temp1)];
      Maxtemp_max_hist=[Maxtemp_max_hist; max(temp1)];
      Maxtemp_mean_hist=[Maxtemp_mean_hist; mean(temp1)];
      Maxtemp_median_hist=[Maxtemp_median_hist; median(temp1)];
      temp1=[];
```

```
   end
end


xlswrite(outfile, {'Month','Day','Year';}, 'Sheet1', 'A1')
xlswrite(outfile, data(:,10), 'Sheet1', 'A2')
xlswrite(outfile, data(:,11), 'Sheet1', 'B2')
xlswrite(outfile, data(:,12), 'Sheet1', 'C2')
xlswrite(outfile, {'MaxTempfuturecorrecteddata (c)'}, 'Sheet1', 'E1')
% xlswrite(outfile, maxtemp_simoriginaldata, 'Sheet1', 'D2')
% xlswrite(outfile, maxtemp_simcorrecteddata, 'Sheet1', 'E2')
% xlswrite(outfile, maxtemp_futureoriginaldata, 'Sheet1', 'F2')
xlswrite(outfile, maxtemp_futurecorrecteddata, 'Sheet1', 'E2')

xlswrite(outfile_2, {'Month','Day','Year';}, 'Sheet1', 'A1')
xlswrite(outfile_2, data(:,1), 'Sheet1', 'A2')
xlswrite(outfile_2, data(:,2), 'Sheet1', 'B2')
xlswrite(outfile_2, data(:,3), 'Sheet1', 'C2')
xlswrite(outfile_2, {'MaxTempHistoriccorrecteddata (c)'}, 'Sheet1', 'E1')
% xlswrite(outfile, maxtemp_simoriginaldata, 'Sheet1', 'D2')
% xlswrite(outfile, maxtemp_simcorrecteddata, 'Sheet1', 'E2')
% xlswrite(outfile, maxtemp_futureoriginaldata, 'Sheet1', 'F2')
xlswrite(outfile_2, maxtemp_simcorrecteddata, 'Sheet1', 'E2')

xlswrite(outfile_stats_fut, {'Month','Year';}, 'Sheet1', 'A1')
xlswrite(outfile_stats_fut, {'Maxtemp_Min','Maxtemp_Max','Maxtemp_Mean','Maxtemp_Median';},
'Sheet1', 'G1')
xlswrite(outfile_stats_fut, month_fut, 'Sheet1', 'A2')
xlswrite(outfile_stats_fut, year_fut, 'Sheet1', 'B2')
xlswrite(outfile_stats_fut, Maxtemp_min_fut, 'Sheet1', 'G2')
xlswrite(outfile_stats_fut, Maxtemp_max_fut, 'Sheet1', 'H2')
xlswrite(outfile_stats_fut, Maxtemp_mean_fut, 'Sheet1', 'I2')
xlswrite(outfile_stats_fut, Maxtemp_median_fut, 'Sheet1', 'J2')

xlswrite(outfile_stats_hist, {'Month','Year';}, 'Sheet1', 'A1')
xlswrite(outfile_stats_hist, {'Maxtemp_Min','Maxtemp_Max','Maxtemp_Mean','Maxtemp_Median';},
'Sheet1', 'G1')
xlswrite(outfile_stats_hist, month_hist, 'Sheet1', 'A2')
xlswrite(outfile_stats_hist, year_hist, 'Sheet1', 'B2')
xlswrite(outfile_stats_hist, Maxtemp_min_hist, 'Sheet1', 'G2')
xlswrite(outfile_stats_hist, Maxtemp_max_hist, 'Sheet1', 'H2')
xlswrite(outfile_stats_hist, Maxtemp_mean_hist, 'Sheet1', 'I2')
xlswrite(outfile_stats_hist, Maxtemp_median_hist, 'Sheet1', 'J2')

clearvars -global -except data mySize nmonths
%%%%%%%%%%%%%%%%%%%%**********************************************%%%%%%%
%%%%%%%%%%%%%
%%%%%%%%%%%%%%%%%%%%**********************************************%%%%%%%
%%%%%%%%%%%%%
col1=8;                 %%%%%%%%%%%%Historic Min
col2=14;                %%%%%%%%%%%%Future Min
```

```
mintemp_obsdata=cell(1,nmonths);
mintemp_simdata=cell(1,nmonths);
mintemp_simoriginaldata=data(:,col1);
mintemp_simcorrecteddata=data(:,col1);
mintemp_simindexdata=cell(1,nmonths);
temp_arr=[];
mintemp_futureoriginaldata = data(:,col2);
mintemp_futurecorrecteddata = data(:,col2);
mintemp_futuredata=cell(1,nmonths);
mintemp_futureindexdata=cell(1,nmonths);
for j=1:nmonths
    for i = 1 : mySize(1,1)
        if(data(i,1) == j)
            temp_arr  = [temp_arr ;data(i,5)];   %%%%%%%%%%%Observed Min
        end
    end
    mintemp_obsdata{1,j}=temp_arr;
    temp_arr=[];
end
%%%%%%%%%%%%%Indexing of
data%%%%%%%%%%%%%%%%%%%%%%%%%%%%%
temp_arr=[];temp_arr2=[];
indexdata_arr=[];
indexfuturedata=[];
for j=1:nmonths
    for i = 1 : mySize(1,1)
        if(data(i,1) == j)
            temp_arr =[temp_arr ; data(i,col1)];
            indexdata_arr=[indexdata_arr ; i];
        end
        if(data(i,1) == j)
            temp_arr2 =[temp_arr2 ; data(i,col2)];
            indexfuturedata=[indexfuturedata ; i];
        end
    end
    mintemp_simdata{1,j}=temp_arr;
    mintemp_simindexdata{1,j}=indexdata_arr;
    temp_arr=[];
    indexdata_arr=[];

    mintemp_futuredata{1,j}=temp_arr2;
    mintemp_futureindexdata{1,j}=indexfuturedata;
    temp_arr2=[];
    indexfuturedata=[];
end
%%%%%%%%%%%%%%%%%%%%%%%%%%%%%%%%%%%%%%%%%%%%%%%%%%%
%%%%%%%%%%%
mintemp_obs=cell(1,nmonths);
mu_obs=cell(1,nmonths);
sigma_obs=cell(1,nmonths);
y_obs=cell(1,nmonths);
```

```
mintemp_sim=cell(1,nmonths);
mu_sim=cell(1,nmonths);
sigma_sim=cell(1,nmonths);
y_sim=cell(1,nmonths);
corrected_data=cell(1,nmonths);
mintemp_simindex=cell(1,nmonths);

mintemp_future=cell(1,nmonths);
mu_future=cell(1,nmonths);
sigma_future=cell(1,nmonths);
y_future=cell(1,nmonths);
future_corrected_data=cell(1,nmonths);
mintemp_futureindex=cell(1,nmonths);

for j=1:nmonths
   mintemp_obs{1,j}=sort(mintemp_obsdata{1,j});
   [mu_obs{1,j},sigma_obs{i,j}] = normfit(mintemp_obs{1,j});
   y_obs{1,j}=normcdf (mintemp_obs{1,j},mu_obs{1,j},sigma_obs{i,j});
   %     subplot(4,3,j);
   %     plot(mintemp_obs{1,j},y_obs{1,j},'-b')
   %     xlabel('Daily min Temperature (C)');
   %     ylabel('Cummulative Probability');
   %     title(j);
   %     hold on;
   [mintemp_sim{1,j}, mintemp_simindex{1,j}]=sort(mintemp_simdata{1,j});
   mintemp_sim{1,j}=sort(mintemp_simdata{1,j});
   [mu_sim{1,j},sigma_sim{i,j}] = normfit(mintemp_sim{1,j});
   y_sim{1,j}=normcdf (mintemp_sim{1,j},mu_sim{1,j},sigma_sim{i,j});
   %     plot(maxtemp_sim{1,j},y_sim{1,j},'-r');
   %     legend('Obs','Sim',4);
   %     legend boxoff
   [mintemp_future{1,j}, mintemp_futureindex{1,j}]=sort(mintemp_futuredata{1,j});
   mintemp_future{1,j}=sort(mintemp_futuredata{1,j});
   [mu_future{1,j},sigma_future{i,j}] = normfit(mintemp_future{1,j});
   y_future{1,j}=normcdf (mintemp_future{1,j},mu_future{1,j},sigma_future{i,j});
end
simdata1=[];
futuredata1=[];
for j=1:nmonths
   corrected_data{1,j} = norminv(y_sim{1,j},mu_obs{1,j},sigma_obs{i,j});
   future_corrected_data{1,j} = ...
      norminv(y_future{1,j},mu_future{1,j}+(mu_obs{1,j}-
mu_sim{1,j}),sigma_future{i,j}*(sigma_obs{i,j}/sigma_sim{i,j}));
   %        subplot(4,3,j);
   %        plot(corrected_data{1,j},'b');
   %        hold on;
   %        plot(future_corrected_data{1,j},'r');
   %        title(j);
   simdata1=[simdata1 mean(corrected_data{1,j})];
   futuredata1=[futuredata1 mean(future_corrected_data{1,j})];
end
%xlswrite(outfile_mean, {'Bias corrected monthly mean historic values';}, 'Sheet1', 'B1')
```

```
xlswrite(outfile_mean, simdata1, 'Sheet1', 'B8')
%xlswrite(outfile_mean, {'Bias corrected monthly mean future values';}, 'Sheet1', 'C1')
xlswrite(outfile_mean, futuredata1, 'Sheet1', 'B9')
figure;
plot(simdata1,'--bo','LineWidth',2)
hold on;
plot(futuredata1,'--ro','LineWidth',2)
xlim([1 12])
xlabel('Months');
ylabel('GFDL Mean Min Temperature (C)');
legend('1971-2000','2041-2070',4);
hold off;
outfigfile=[final_dir x(1:length(x)-5) '_MinTemp_fig.jpg'];
saveas(gcf,outfigfile);
mu_corr=cell(1,nmonths);
sigma_corr=cell(1,nmonths);
y_corr=cell(1,nmonths);
%%%%%%%%%%%Replacing the data in the original order %%%%%%%%%%%%%%%
for j=1:nmonths
   for k =1:length(corrected_data{1,j})

mintemp_simcorrecteddata(mintemp_simindexdata{1,j}(mintemp_simindex{1,j}(k)))=corrected_data{1,j
}(k);
   end
   for k =1:length(future_corrected_data{1,j})

mintemp_futurecorrecteddata(mintemp_futureindexdata{1,j}(mintemp_futureindex{1,j}(k)))=future_corre
cted_data{1,j}(k);
   end
end


% for j=1:nmonths
%     [mu_corr{1,j},sigma_corr{1,j}] = normfit(corrected_data{1,j});
%     y_corr{1,j}=norminv (corrected_data{1,j},mu_corr{1,j},sigma_corr{1,j});
% end
%
% temp=[];
% for j=1:nmonths
%     temp= [temp;mu_obs{1,j} sigma_obs{i,j} mu_sim{1,j} sigma_sim{i,j} mu_corr{1,j}
sigma_corr{1,j} ];
% end
temp1=[];
Mintemp_min_fut=[];
Mintemp_max_fut=[];
Mintemp_mean_fut=[];
Mintemp_median_fut=[];
for abc=1:mySize(1,1)-1
   current_year=data(abc,12);
   current_month=data(abc,10);
   next_year=data(abc+1,12);
   next_month=data(abc+1,10);
   if ((current_year == next_year) && (current_month == next_month))
```

```
      temp1 = [temp1 mintemp_futurecorrecteddata(abc,1)];
      if(abc == (mySize(1,1)-1))
         temp1 = [temp1 mintemp_futurecorrecteddata(abc+1,1)];
      end
   else
      Mintemp_min_fut=[Mintemp_min_fut; min(temp1)];
      Mintemp_max_fut=[Mintemp_max_fut; max(temp1)];
      Mintemp_mean_fut=[Mintemp_mean_fut; mean(temp1)];
      Mintemp_median_fut=[Mintemp_median_fut; median(temp1)];
      temp1=[];
   end
end

temp1=[];
Mintemp_min_hist=[];
Mintemp_max_hist=[];
Mintemp_mean_hist=[];
Mintemp_median_hist=[];
for abc=1:mySize(1,1)-1
   current_year=data(abc,3);
   current_month=data(abc,1);
   next_year=data(abc+1,3);
   next_month=data(abc+1,1);
   if ((current_year == next_year) && (current_month == next_month))
      temp1 = [temp1 mintemp_simcorrecteddata(abc,1)];
      if(abc == (mySize(1,1)-1))
         temp1 = [temp1 mintemp_simcorrecteddata(abc+1,1)];
      end
   else
      Mintemp_min_hist=[Mintemp_min_hist; min(temp1)];
      Mintemp_max_hist=[Mintemp_max_hist; max(temp1)];
      Mintemp_mean_hist=[Mintemp_mean_hist; mean(temp1)];
      Mintemp_median_hist=[Mintemp_median_hist; median(temp1)];
      temp1=[];
   end
end

xlswrite(outfile, {'Minfuturecorrecteddata (c)';}, 'Sheet1', 'F1')
xlswrite(outfile, mintemp_futurecorrecteddata, 'Sheet1', 'F2')

xlswrite(outfile_2, {'MinTempHistoriccorrecteddata (c)';}, 'Sheet1', 'F1')
xlswrite(outfile_2, mintemp_simcorrecteddata, 'Sheet1', 'F2')

xlswrite(outfile_stats_fut, {'Mintemp_Min','Mintemp_Max','Mintemp_Mean','Mintemp_Median';},
'Sheet1', 'K1')
xlswrite(outfile_stats_fut, Mintemp_min_fut, 'Sheet1', 'K2')
xlswrite(outfile_stats_fut, Mintemp_max_fut, 'Sheet1', 'L2')
xlswrite(outfile_stats_fut, Mintemp_mean_fut, 'Sheet1', 'M2')
xlswrite(outfile_stats_fut, Mintemp_median_fut, 'Sheet1', 'N2')

xlswrite(outfile_stats_hist, {'Mintemp_Min','Mintemp_Max','Mintemp_Mean','Mintemp_Median';},
'Sheet1', 'K1')
```

```
xlswrite(outfile_stats_hist, Mintemp_min_hist, 'Sheet1', 'K2')
xlswrite(outfile_stats_hist, Mintemp_max_hist, 'Sheet1', 'L2')
xlswrite(outfile_stats_hist, Mintemp_mean_hist, 'Sheet1', 'M2')
xlswrite(outfile_stats_hist, Mintemp_median_hist, 'Sheet1', 'N2')

clearvars -global -except data mySize nmonths
%%%%%%%%%%%%%%%%%%**********************************************%%%%%%%%
%%%%%%%%%%%%

xval = 0;
```